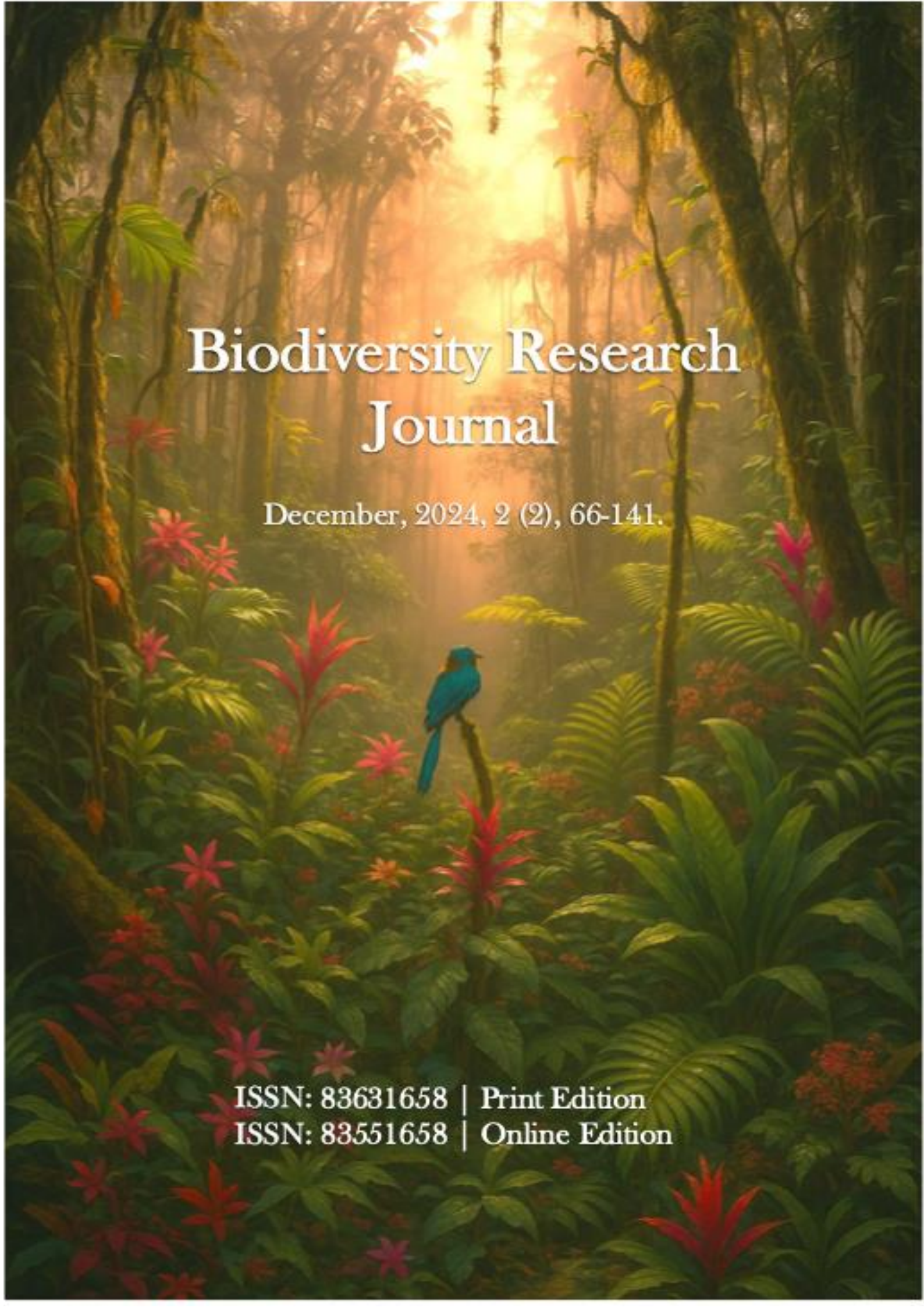

Biodiversity Research Journal

December, 2024, 2 (2), 66-141.

ISSN: 83631658 | Print Edition
ISSN: 83551658 | Online Edition

Biodiversity Research Journal

Referred Scientific Journal

By College of Science, Princess Nourah bint Abdulrahman University,

Riyadh, Saudi Arabia

Volume 2, Issue 2, December 2024

December, 2024

Table of Contents

Journal Description

The "Biodiversity Research Journal" was established in 2021, and it is the first peer-reviewed scientific journal (biannual) published by the College of Science at the Princess Nourah bi Abdulrahman University. The journal aims to publish all types of scientific research in different fiel of biodiversity and ecology in the English Language. The journal avails free and open access to all published research. All articles are always published online to ensure their distribution ar availability to the academic community and researchers.

Procedures for receiving and arbitrating research

The researchers submits their manuscript by email and fills in the relevant forms on the journal's website. A cover letter addressed to the Editor-in-Chief, requesting publication in the journal, mus be included.

- The researcher shall provide a written declaration that the manuscript has not been previous published and is not under consideration for publication in any other journal.
- The editorial secretary receives the manuscripts and assigns them numbers based on the order arrival.
- The researcher is notified upon receipt of the manuscript.
- Manuscripts are reviewed by the Editorial Board to determine their suitability for peer review. deemed unsuitable, the researcher will be informed, and a rejection letter will be sent.
- Manuscripts and studies submitted for publication are reviewed by at least two referees.
- If there is a discrepancy between the reviewers' opinions, a third referee is assigned upon the recommendation of the Editor-in-Chief, after considering the comments.
- The researcher will be notified by the review outcome and will be asked to make necessary revisior
- Revised manuscripts are resubmitted to the journal's email.
- If the manuscript is accepted for publication, a notification of acceptance will be sent to tl researcher. If rejected, a rejection letter will be sent along with reviewers' comments.

Contact Us

The Biodiversity Research Journal, College of Science, Princess Nourah Bint Abdulrahman Universit King Khalid International Airport Road, Post Box 8428, Code 11671, Riyadh, Saudi Arabia.
Email: cs-bio-brj@pnu.edu.sa

Editorial Board

Advisory Board

Head Advisory Board
Prof. Ahmed M. Saleh Professor of plant Quality and physiology, Taibah University, Kingdom of Saudi Arabia.
Members
Prof. Wafa Abdullah Al-Megrin Professor of Parasitology, Department of Biology, College of Science, Princess Nourah bint Abdulrahman University, Riyadh, Kingdom of Saudi Arabia.
Prof. Sami Alyahya Professor of Molecular Microbiology, King Abdulaziz city for science and Technology, Riyadh, Kingdom of Saudi Arabia.
Prof. Osama B Mohammed Professor of Molecular Parasitology, College of Science, King Saud University, Riyadh, Saudi Arabia
Prof. Elke Pawelzik Professor of Quality of Plant Products, Göttingen University, Germany
Prof. Stephen Compton Professor of Ecology and Entomology, School of Biology, University of Leeds, Leeds, UK
Prof. Ahmed Esmat Abdel Moneim Professor of Ecology and Physiology, Helwan University, Egypt
Prof. Mansour El-Matbouli Professor of Fish Medicine, University of Veterinary Medicine, Vienna
Prof. Hamada Abd Elgawad Professor of plant physiology, Beni-Suef University, Beni Suef, Egypt
Prof. Ahmed Abd El Wahed Professor of Microbiology, Institute of Animal Hygiene and Veterinary Public Health, Leipzig University, Germany

Journal Editorial

Prof. Wafa Abdullah Al-Megrin, Editor-in-Chief. Professor of Parasitology, Department of Biology, College of Science, Princess Nourah bint Abdulrahman University, Riyadh, Kingdom of Saudi Arabia.

Praise be to Allah, the Lord of all worlds, and blessings and peace upon the noblest of prophets and messengers, our Prophet Mohammed.

The Biodiversity Research Journal is pleased to present to our esteemed readers the second issue of the second volume. This issue contains five distinguished and diverse scientific research from different biodiversity aspects.

The editorial board is committed to achieving scientific quality in every piece of academic output it publishes, reinforcing creative research movement in the fields of biodiversity, staying up-to-date with innovations, and encouraging global researchers to contribute their academic work to the journal.

We extend our gratitude and appreciation to everyone who contributed and assisted in producing this issue.

GREEN FABRICATION OF SILVER AND MANGANESE OXIDE NANOPARTICLES USING *Leucophyllum frutescens* LEAF EXTRACT: CHARACTERIZATION AND ANTIBACTERIAL ACTIVITY

Author name and information

Sarah Abdullah AL Masoud[1], Sarah Ibrahim Alnasser[1], Amjad Saad Alotaibi[1], Hessa O. Aldraiwiesh[1], Dhuha Alsuwaid[2], Kholoud M. Baeshen[3], Reham M. Aldahasi[1,2], Afrah E. Mohammed[1,2*]

[1]Department of Biology, College of Sciences, Princess Nourah bint Abdulrahman University, Riyadh P.O. Box 84428, Riyadh,11671, Saudi Arabia.
[2]Microbiology and Immunology Unit, Research Department, Natural and Health Sciences Research Center, Princess Nourah bint Abdulrahman University, P.O. Box 84428, Riyadh 11671, Saudi Arabia.
[3]Research Department, Natural and Health Sciences Research Center, Princess Nourah bint Abdulrahman University, Riyadh, Saudi Arabia.

***Correspondence**: AFAMohammed@pnu.edu.sa

Keywords

Silver; manganese; nanoparticles; antibacterial; *Escherichia coli; Klebsiella pneumoniae*.

ABSTRACT

Nanotechnology is increasingly adopting green synthesis techniques, prioritizing non-toxic reaction components and mild reaction conditions to promote sustainable and environmentally friendly solutions. As a reliable alternative to conventional chemical methods, natural sources have been explored as cost-effective and eco-friendly reducing and capping agents for nanomaterial fabrication. This study explores the green synthesis of silver (AgNPs) and manganese oxide (MnONPs) nanoparticles using *Leucophyllum frutescens* leaf extract as an eco-friendly approach. Their antibacterial effect has been evaluated. UV-Vis spectroscopy confirmed nanoparticle formation, with AgNPs exhibiting an absorption peak at 439.32 nm and MnONPs at 304.25 nm. FTIR analysis identified functional groups at 1637 cm^{-1} and 3344 cm^{-1}, suggesting their role in nanoparticle stabilization. Zeta potential analysis indicated that AgNPs (128 nm) and MnONPs (151.2 nm) carried a negative charge. Antimicrobial testing against *Staphylococcus aureus*, *Klebsiella pneumoniae*, and *Escherichia coli* demonstrated that AgNPs (1mg/mL) exhibited superior significant antibacterial activity against *K. pneumoniae*. These findings highlight the potential of *L. frutescens*-derived nanoparticles as effective antimicrobial agents, suggesting further investigation at higher concentrations for biomedical and environmental applications.

INTRODUCTION

The urgent global health crisis of antibiotic resistance necessitates the development of novel antimicrobial therapies. Nanotechnology provides a promising approach, with metallic nanoparticles (NPs) exhibiting unique properties that overcome bacterial resistance mechanisms.

These properties include the ability to circumvent drug resistance, inhibit biofilm formation, and disrupt bacterial cell walls, making them ideal candidates for antimicrobial applications (Ozdal & Gurkok, 2022; Behzad et al., 2021). Nanotechnology's precise control over materials at the nanoscale (1-100 nm) (Chenthamara et al., 2019) integrates physics, chemistry, and biology (Malik et al., 2023). The high surface-to-volume ratio of NPs enhances catalytic activity and efficiency, minimizing waste generation (Nasrollahzadeh et al., 2019). This versatility extends to various applications, including wastewater treatment and antibacterial agents (Slavin et al., 2017). Expanding biotechnological and microbiological applications are driven by NPs' biocompatibility, anti-inflammatory and antibacterial effects, efficient drug delivery, and tumor-targeting capabilities (Slavin et al., 2017). Metallic NPs are especially valuable in biomedical applications, effectively combating bacterial infections by disrupting essential bacterial structures and facilitating penetration of cell walls (Ozdal & Gurkok, 2022).

Although nanoparticles can be synthesized via biological, physical, and chemical routes, the latter two often incur high costs and environmental burdens (Khan et al., 2022). This has fueled the rise of green nanotechnology, which employs environmentally benign processes using biological sources such as viruses, bacteria, fungi, algae, and plants (Saratale et al., 2018; Pandit et al., 2022). Green synthesis offers significant advantages: lower costs, reduced hazardous chemical use, and the production of non-toxic, biocompatible nanoparticles ideal for biomedical applications (Singh et al., 2021).

Leucophyllum frutescens (Berl.), a drought-resistant Scrophulariaceae shrub, is a particularly promising plant for nanoparticle synthesis. It demonstrated strong antibacterial activity, attributed to leubethanol (a diterpenoid effective against multidrug-resistant tuberculosis) and other components like anthocyanins, carotenoids, and phenolics (Molina-Salinas et al., 2011; Jaramillo-Morales et al., 2023), along with its ability to facilitate the green synthesis of antimicrobial nanoparticles (Van Tien et al., 2020), making it ideal for this application. The phytochemical composition of *L. frutescens* encompasses various compounds, including flavonol glycosides, triterpenoids, cycloartane glycosides, flavonoids, canavanine, pinitol, and γ-aminobutyric acid (GABA). These bioactive constituents are believed to contribute significantly to the plant's pharmacological properties and may also play a role in the synthesis of nanoparticles (Mutukwa, Taziwa & Khotseng, 2022).

Silver nanoparticles (AgNPs) are potent antibacterial agents effective against Gram-positive and Gram-negative bacteria, including drug-resistant strains, by disrupting cell walls and modulating cellular signaling (Arya et al., 2011; Bruna et al., 2021). AgNP synthesis from plant extracts, such as those from *Zingiber officinale*, *Thymus vulgaris*, and *Cinnamomum zeylanicum*,
demonstrates strong antimicrobial and antibiofilm activity (Al Shahwany et al., 2016), as does synthesis from *Bougainvillea glabra* extract, showing greater efficacy against *Staphylococcus aureus* than *Escherichia coli* (Momeni et al., 2021). Manganese nanoparticles (MnNPs) also possess antimicrobial, antioxidant, anticancer, and drug-delivery properties (Haque et al., 2021; Van Tien et al., 2020; Joshi et al., 2020), making them suitable for various biological applications. This study investigates the green synthesis of AgNPs and MnONPs using *L. frutescens* leaf extract, followed by characterization and evaluation of their antibacterial activity against *Escherichia coli*, *Staphylococcus aureus*, and *Klebsiella pneumoniae*.

MATERIALS AND METHODS

Materials:

Leaves of *Leucophyllum frutescens* were collected from the nursery of the Royal Commission of Riyadh City, Riyadh, Saudi Arabia, in March 2023 and were authenticated at Princess Nourah Bint Abdulrahman University. Silver nitrate and manganese sulfate were brought from the university's Department of Biology.

Preparation of Plant Aqueous Extract

To prepare the plant extract, 2 g of powdered *L. frutescens* leaves were mixed with 100 ml of distilled water. This mixture was then placed in a water bath at 80°C for 15 minutes. Afterward, the extract was filtered through filter paper with a pore diameter of 20 mm.

Preparation of Silver Nanoparticles

To synthesize silver nanoparticles, 90 ml of 1 mM aqueous silver nitrate was combined with 10 ml of the *L. frutescens* extract (1:9 ratio) in an Erlenmeyer flask. The mixture progressively became brown after it had been heated to 80°C for 25 minutes in a water bath. Following this, the mixture was centrifuged at 5500 rpm for 40 minutes. The supernatant was carefully discarded, and the pellet was washed with distilled water under consistent conditions. Finally, the pellet was air-dried at room temperature.

Preparation of Manganese Oxide Nanoparticles

To synthesize manganese oxide nanoparticles, 45 ml of a 1 mM manganese sulfate solution was combined with 45 ml of the extract in a 1:1 ratio. The mixture was then heated in a water bath at 80°C for 25 minutes, deepening the manganese color. Subsequently, it was centrifuged at 5500 rpm for 40 minutes. The supernatant was removed, and the resulting pellet was thoroughly washed with distilled water under consistent conditions before being air-dried at room temperature.

Characteristics of Nanoparticles:

The characteristics of the synthesized nanoparticles were analyzed using various spectroscopic techniques. Ultraviolet-visible spectroscopy (UV-Vis) was conducted with an Evolution 201 UV-visible spectrophotometer (Thermo Fisher Scientific, Waltham, MA, USA) to monitor the formation of nanoparticles, analyzing the reaction mixture over a wavelength range of 200–500 nm. Fourier-Transform Infrared Spectroscopy (FTIR) was utilized to identify the functional groups responsible for the reduction and stabilization of the nanoparticles. This analysis used an FTIR spectrometer (SPECTRUM100; Perkin-Elmer, Waltham, MA, USA) with a scanning range of 500–4,000 cm^{-1}. Additionally, Dynamic Light Scattering (DLS) and Zeta Potential analysis were carried out using a Zetasizer (NANO ZSP; Malvern Instruments Ltd., Serial Number: MAL1118778, ver 7.11, Malvern, UK) to determine the hydrodynamic size distribution, polydispersity index (PDI), and surface charge (zeta potential) of the nanoparticles, providing valuable insights into their stability and dispersibility.

Assessment of the Antibacterial Properties of Nanoparticles (NPs):

The biosynthesized AgNPs and MnONPs were evaluated for their antibacterial activity against two multidrug-resistant Gram-negative bacterial strains, *Klebsiella pneumoniae* and *Escherichia coli*, and one Gram-positive strain, *Staphylococcus aureus*. The microbial strains were sourced from the Bio-house Medical Lab in Riyadh, Saudi Arabia. The antibacterial assay was performed using the agar well-diffusion method. Bacterial cultures were inoculated onto nutrient agar plates through the direct colony suspension method, and wells were created for nanoparticle application. Each type of nanoparticle, AgNPs, and MnONPs, was applied at a concentration of 1 mg/mL for 30 minutes under aseptic conditions before being incubated at 37°C for 24 hours. After incubation, the diameter of the inhibition zone surrounding each well was measured in millimeters to assess the antibacterial efficacy of the nanoparticles.

Statistical Analysis

All data were represented as mean and standard deviations. One-way analysis of variance (ANOVA) was calculated by Graph-bad Prism 9.1 software (Inc., La Jolla, CA, USA), and the statistical significance level was set at $p \leq 0.05$. Spectra for FTIR and UV-Vis were generated using OriginPro® 2023b.

RESULTS AND DISCUSSION

Ultraviolet-visible spectroscopy UV

The UV measurements were conducted between the wavelength range of 200 and 500 nm. As illustrated in Figure 1, the recorded results for AgNPs and MnONPs were 439.316 nm and 304.251 nm, respectively.

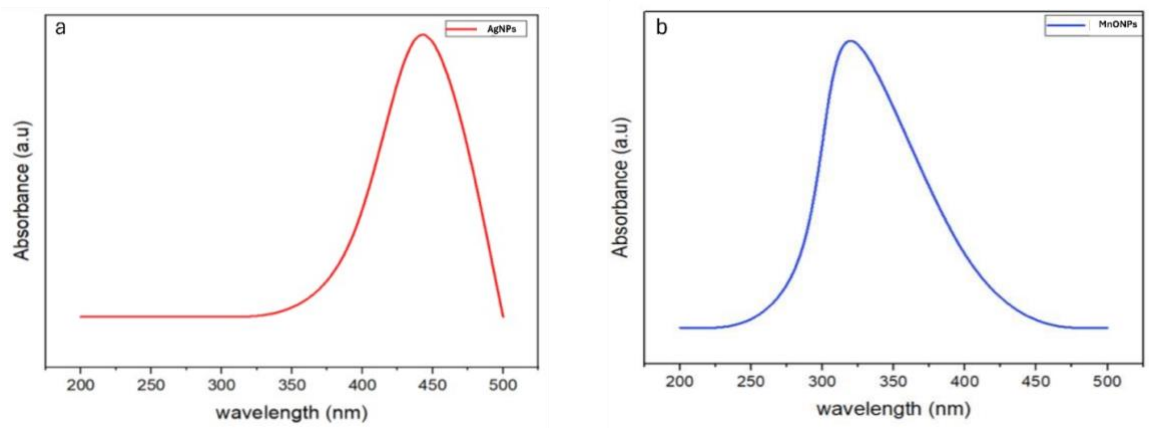

Figure 1. UV-vis spectra showing absorbance peaks of AgNPs (a) and MnONPs(b) prepared by *L. frutescens* leaf extract.

A similar range of observations was noted in the current study, emphasizing the role of the plant extract in nanoparticle (NP) formation. Specifically, silver nanoparticles were synthesized using an extract from Arbutus unedo leaves at two different concentrations, demonstrating varying UV-Vis absorption spectra (Skandalis et al., 2017). Additionally, silver nanoparticles synthesized from

Phlomis leaf extract exhibited a strong, broad peak around 440 nm in the UV-Vis spectra, indicating the formation of AgNPs (Allafchian et al., 2016). AgNPs were also produced from the leaves of *Chromolaena odorata*, showing a maximum absorption at 464.5 nm (Hashim & John, 2023). A previous study synthesized manganese oxide nanoparticles from green tea extract, revealing a peak at 410 nm (Saod et al., 2022). Furthermore, MnO NPs were synthesized from *Dittrichia graveolens* extract, displaying maximum absorption peaks at 284 nm and 325 nm (Souri et al., 2018). Manganese nanoparticles produced using lemon extract showed a maximum absorption peak of 360 nm (Jayandran et al., 2015).

Fourier-transform infrared spectroscopy FTIR

FTIR analysis, an essential analytical technique for distinguishing between organic and inorganic materials, played a crucial role in identifying the biomolecules involved in the synthesis of nanoparticles (NPs) (Mohammed & Al-Megrin, 2021). FTIR analyses were performed on both the L. frutescens leaf extract and the nanoparticles, as illustrated in Figure 2. The FTIR spectrum of the L. frutescens leaf extract exhibited significant peaks at 1637 cm^{-1} and 3344 cm^{-1}. According to previous studies, the FTIR peak at 1637 cm^{-1} corresponds to the carbonyl stretch of amides (Chung et al., 2016; Kong & Yu, 2007). Our observation at 1637 cm^{-1} can also be attributed to olefinic (alkene), primary amino, secondary amino, and carbonyl compounds (Nandiyanto et al., 2019). The FTIR peak at 3344 cm^{-1} is associated with hydroxyl groups and both primary and secondary amid groups (-NH stretch) (Nandiyanto et al., 2019; Li et al., 2013). Functional groups such as the carbonyl stretch of amides, which may relate to proteins, are thought to facilitate the capping of nanoparticles (Chung et al., 2016). Alkene functional groups also contribute to the synthesis and stability of nanoparticles (Batool et al., 2021). Additionally, the hydroxyl and amino groups present in proteins have been recognized for their dual roles in the reduction and stabilization of metal nanoparticles (Rostamizadeh et al., 2020).

Dynamic light scattering (DLS) and zeta potential:

The size distribution of the nanoparticles reveals average sizes of 128 nm for silver AgNPs and 151.2 nm for MnONPs, as shown in Figure 3. The polydispersity indices (PDI) suggest good quality and monodispersity of the nanoparticles at values of 0.1599 for AgNPs and 0.2912 for MnONPs. Elamawi et al., (2018) reported that the PDI scale range at zero denotes a monodispersed sample and that at 1 indicates polydispersity.

A low-quality sample, characterized by a wide size distribution and a potential for larger particles or aggregates, typically has a PDI value closer to one. For accurate measurements and high-quality colloidal suspensions, the preferred PDI range is between 0.1 and 0.5 (Hebeish et al., 2014). The current fabricated NPs had fewer polydispersed particles since the PDI was below 0.3 (Filippov et al., 2023). Additionally, zeta potential analysis determines the surface charge of nanoparticles in colloidal solutions (Joudeh & Linke, 2022). The zeta potential measurements yielded values of -20.2 mV for AgNPs and -18.65 mV for MnONPs, as illustrated in Figure 4.

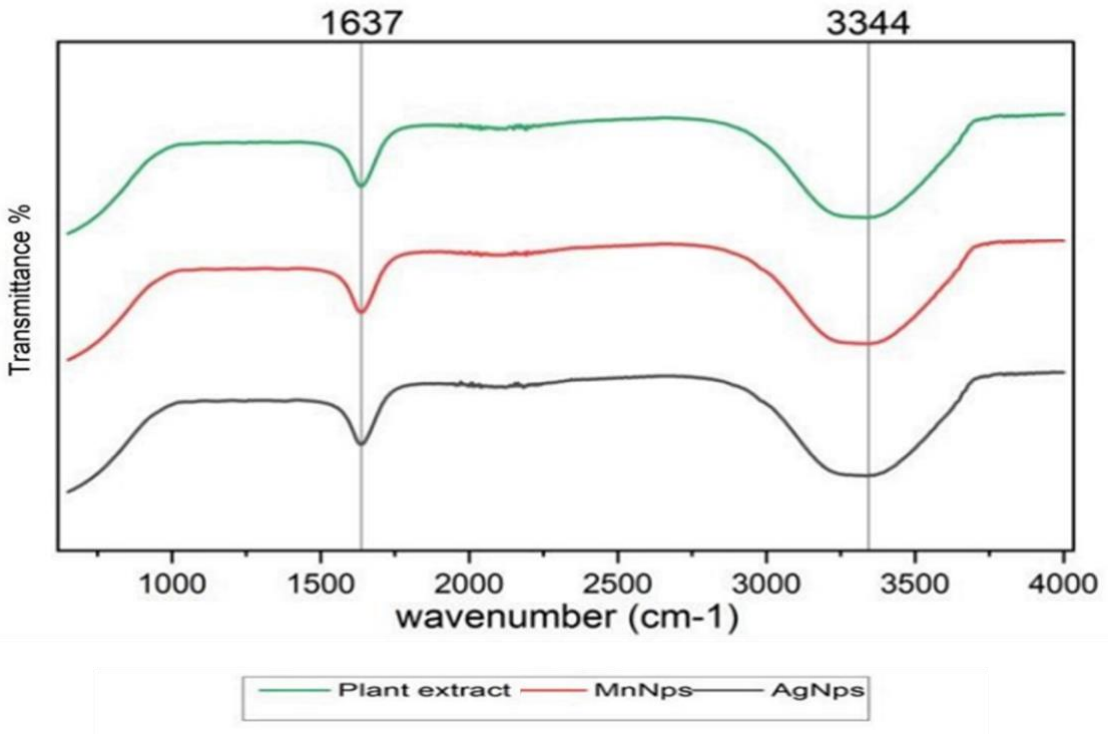

Figure 2. The FTIR spectra of *L. frutescens* leaf extra, phyto-fabricated nanoparticles

The high negative zeta potential enhances the stability of the formulation by promoting repulsion among the particles (Subba Rao et al., 2013). Nanoparticles could be cationic or anionic if their zeta potential is greater than +30 mV or less than -30 mV, respectively (Clogston & Patri, 2011). Numerous studies have shown that biogenic nanoparticles derived from plant materials typically exhibit negative zeta potentials (Mohammed & Al-Megrin, 2021). For instance, AgNPs synthesized using Phyla dulcis plant extract demonstrated an average size of 114.04 nm and a zeta potential of -21.18 mV (Carson et al., 2020). Similarly, AgNPs produced from Maesa calophylla plant extract showed an average size of 122.6 nm with a zeta potential of -26.55 mV (Ahn & Park, 2020).

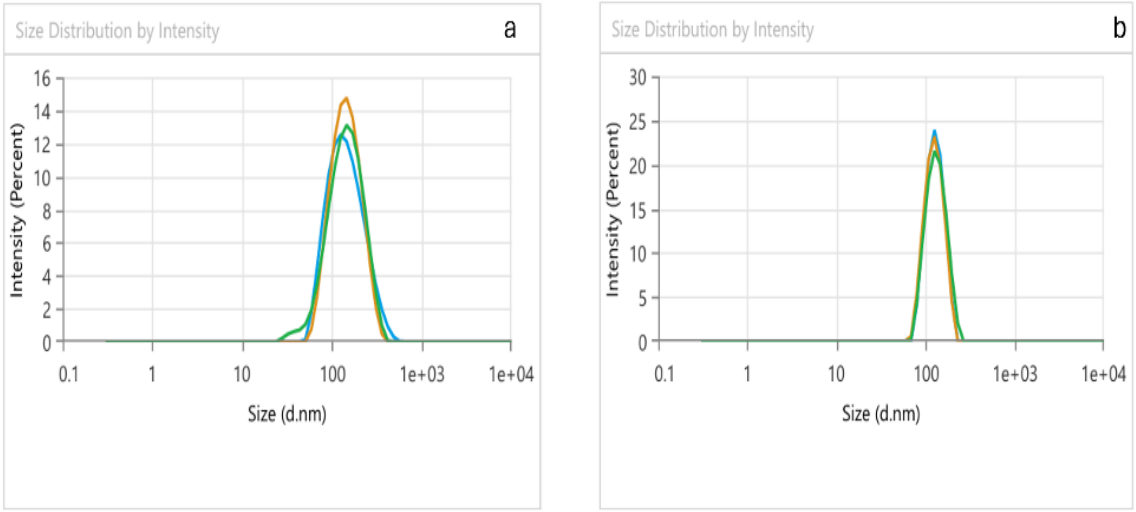

Figure 3. The size distribution of AgNPs (a) and MnONPs (b).

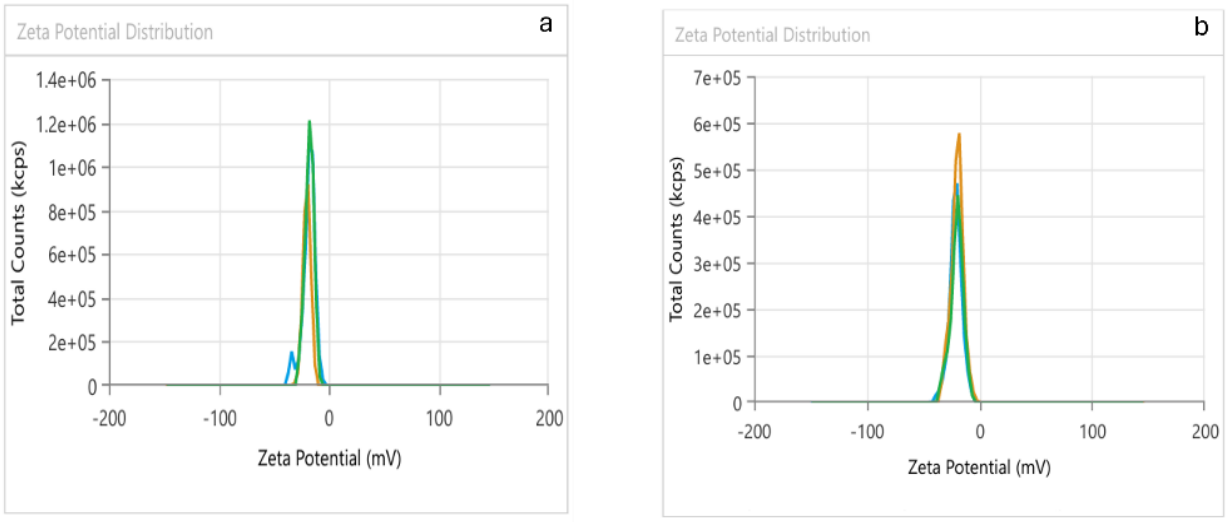

Figure 4. Zeta potential distribution for AgNPs(a) and MnONPs(b)

Antibacterial activity

Table 1 and Figure 5 present the antibacterial activity of a tested agent against three bacterial strains (*Staphylococcus aureus, Escherichia coli,* and *Klebsiella pneumoniae*) by measuring the inhibition zone (mm), which indicates the effectiveness of the antimicrobial treatment. The inhibition zone values are expressed as mean ± standard deviation (SD), showing the average diameter of bacterial growth inhibition with variability across replicates. Among the tested bacteria, *Klebsiella pneumoniae* exhibited significantly the largest inhibition zone suggesting a higher susceptibility to the treatment compared to *Staphylococcus aureus* and *Escherichia coli*. The ANOVA p-value determined whether there is a statistically significant difference in inhibition zones among the bacterial strains, typically with a significance threshold of $p \leq 0.05$. Data suggested that the antibacterial agent demonstrates varying degrees of effectiveness against different bacterial strains, with *Klebsiella pneumoniae* showing the highest susceptibility.

Table 1. Inhibition zone (mean ± SD) of biologically synthesized AgNPs against tested bacteria. Different letters indicate significant variations among tested strains.

Bacteria Strains	Inhibition Zone
Staphylococcus aureus	11.6 ± 1.8 ^{b}
Escherichia coli	11.5 ± 1.1 ^{b}
klebsiella pneumoniae	15.1 ± 1.3 ^{a}
ANOVA (p-value)	0.0009

In a similar study, silver nanoparticles (AgNPs) synthesized from *Salvia spinosa* plant extract grown in vitro exhibited a 12 mm inhibition zone against *E. coli* (Pirtarighat et al., 2019). Likewise, another study reported the synthesis of AgNPs from *Phlomis* leaf extract, demonstrating inhibition zones of 14.7 mm for *Staphylococcus aureus* and 15 mm for *Escherichia coli* (Allafchian et al., 2016), which are comparable to our study's findings.

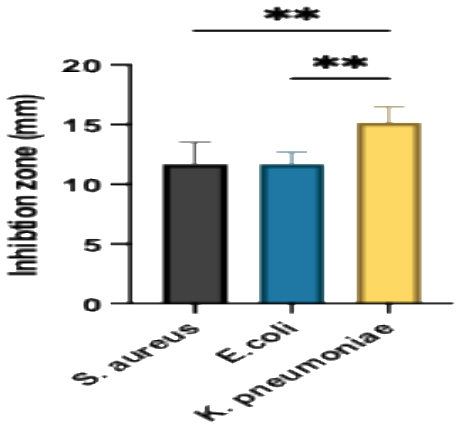

Figure 5: Inhibition zone of biologically synthesized AgNPs against tested bacteria.

CONCLUSION

With the growing challenge of bacterial resistance to conventional antibiotics, nanoparticles have emerged as promising alternatives due to their potent antimicrobial properties. This study explored the biogenic synthesis of silver (AgNPs) and manganese oxide nanoparticles (MnONPs) using *Leucophyllum frutescens* leaf extract, followed by their characterization through UV-Vis spectroscopy, FTIR, and DLS analyses. The synthesized AgNPs exhibiting the most potent inhibition against all tested bacterial strains, particularly *Klebsiella pneumoniae*. These findings highlight the potential of *L. frutescens*-derived nanoparticles as eco-friendly antimicrobial agents. Future research should explore the use of different plant parts, variations in mineral composition, and their influence on nanoparticle synthesis and activity. Additionally, further investigation into the relationship between nanoparticle properties and antimicrobial efficacy will facilitate the development of optimized nanomaterials for biomedical and environmental applications.

ACKNOWLEDGEMENTS

Authors are grateful to Nourah Alshuwayi, Wafa Almadi, Monerah Almusah Department of Biology, Faculty of Science at Princess Nourah bint Abdulrahman University for assisting during

Data availability: Data supporting the findings of this study are available from the corresponding author [A.E. M] upon request.

Conflicts of Interest: The authors declare no conflict of interest.

REFERENCES:

Ahmad, M. M., Kotb, H. M., Mushtaq, S., Waheed-Ur-rehman, M., Maghanga, C. M., & Alam, M. W. (2022). Green Synthesis of Mn + Cu Bimetallic Nanoparticles Using *Vinca rosea* Extract and Their Antioxidant, Antibacterial, and Catalytic Activities. *Crystals*, *12*(1). https://doi.org/10.3390/cryst12010072

Ahn, E. Y., & Park, Y. (2020). Anticancer prospects of silver nanoparticles green synthesized by plant extracts. *Materials Science and Engineering C*, *116*. https://doi.org/10.1016/j.msec.2020.111253

Alherz F.,A., Negm W.,A., Elekhnawy E., ElMasry T.,A., Haggag E.,M., Alqahtani M.,J., Hussein I.,A. (2022). Silver Nanoparticles prepared using *encephalartos laurentianus* de wild leaf extract have inhibitory activity against *Candida albicans* clinical isolates. *Journal of Fungi* 8(10):1005

Al Shahwany, A. W., Tawfeeq, H. K., & Hamed, S. E. (2016). Antibacterial and Antibiofilm Activity of Three Phenolic Plant Extract and Silver Nanoparticles on Staphylococcus aureus and Klebsiella pneumoniae. *Biomedicine and Biotechnology*, *4*(1), 12–18. https://doi.org/10.12691/bb-4-1-3

Alafaleq, N. O., Zughaibi, T. A., Jabir, N. R., Khan, A. U., Khan, M. S., & Tabrez, S. (2023). Biogenic Synthesis of Cu-Mn Bimetallic Nanoparticles Using Pumpkin Seeds Extract and Their Characterization and Anticancer Efficacy. *Nanomaterials*, *13*(7). https://doi.org/10.3390/nano13071201

Alanís-Garza, B., Salazar-Aranda, R., Ramírez-Durón, R., Garza-González, E., & Waksman De Torres, N. (2012). *A New Antimycobacterial Furanolignan from Leucophyllum frutescens*.

Allafchian, A. R., Mirahmadi-Zare, S. Z., Jalali, S. A. H., Hashemi, S. S., & Vahabi, M. R. (2016). Green synthesis of silver nanoparticles using phlomis leaf extract and investigation of their antibacterial activity. *Journal of Nanostructure in Chemistry*, *6*, 129-135.

Arya, V., Komal, R., Kaur, M., & Goyal, A. (2011). Silver nanoparticles as a potent antimicrobial agent: a review. *Pharmacologyonline*, *3*, 118-124.

Batool, F., Iqbal, M. S., Khan, S. U. D., Khan, J., Ahmed, B., & Qadir, M. I. (2021). Biologically synthesized iron nanoparticles (FeNPs) from Phoenix dactylifera have anti-bacterial activities. *Scientific Reports*, *11*(1). https://doi.org/10.1038/s41598-02101374-4

Behzad, F., Naghib, S. M., kouhbanani, M. A. J., Tabatabaei, S. N., Zare, Y., & Rhee, K. Y. (2021). An overview of the plant-mediated green synthesis of noble metal nanoparticles for antibacterial applications. *Journal of Industrial and Engineering Chemistry*, *94*, 92–104. https://doi.org/10.1016/J.JIEC.2020.12.005

Bruna, T., Maldonado-Bravo, F., Jara, P., & Caro, N. (2021). Silver nanoparticles and their antibacterial applications. *International journal of molecular sciences*, *22*(13), 7202. https://doi.org/10.3390/ijms22137202

Carson, L., Bandara, S., Joseph, M., Green, T., Grady, T., Osuji, G., Weerasooriya, A., Ampim, P., & Woldesenbet, S. (2020). Green Synthesis of Silver Nanoparticles with Antimicrobial Properties Using Phyla dulcis Plant Extract. *Foodborne Pathogens and Disease*, *17*(8), 504–511. https://doi.org/10.1089/fpd.2019.2714

Chenthamara, D., Subramaniam, S., Ramakrishnan, S. G., Krishnaswamy, S., Essa, M. M., Lin, F. H., & Qoronfleh, M. W. (2019). Therapeutic efficacy of nanoparticles and routes of administration. *Biomaterials Research*, *23*(1). https://doi.org/10.1186/S40824-019-0166-X/

Chung, I. M., Park, I., Seung-Hyun, K., Thiruvengadam, M., & Rajakumar, G. (2016). Plant-mediated synthesis of silver nanoparticles: their characteristic properties and therapeutic applications. *Nanoscale research letters*, *11*, 1-14. https://doi.org/10.1186/s11671-016-1257-4

Elamawi, R. M., Al-Harbi, R. E., & Hendi, A. A. (2018). Biosynthesis and characterization of silver nanoparticles using Trichoderma longibrachiatum and their effect on phytopathogenic fungi. *Egyptian Journal of Biological Pest Control*, *28*(1). https://doi.org/10.1186/s41938-018-0028-1

Elemike, E. E., Onwudiwe, D. C., Fayemi, O. E., & Botha, T. L. (2019). Green synthesis and electrochemistry of Ag, Au, and Ag–Au bimetallic nanoparticles using golden rod (Solidago

canadensis) leaf extract. *Applied Physics A: Materials Science and Processing*, *125*(1). https://doi.org/10.1007/s00339-018-2348-0

Elemike, E. E., Onwudiwe, D. C., Nundkumar, N., Singh, M., & Iyekowa, O. (2019). Green synthesis of Ag, Au and Ag-Au bimetallic nanoparticles using Stigmaphyllon ovatum leaf extract and their in vitro anticancer potential. *Materials Letters*, *243*, 148–152. https://doi.org/10.1016/j.matlet.2019.02.049

Franci, G., Falanga, A., Galdiero, S., Palomba, L., Rai, M., Morelli, G., & Galdiero, M. (2015). molecules Silver Nanoparticles as Potential Antibacterial Agents. *Molecules*, *20*, 8856–8874. https://doi.org/10.3390/molecules20058856

Gami, B., Bloch, K., Mohammed, S. M., Karmakar, S., Shukla, S., Asok, A., Thongmee, S., & Ghosh, S. (2022). Leucophyllum frutescens mediated synthesis of silver and gold nanoparticles for catalytic dye degradation. *Frontiers in Chemistry*, *10*. https://doi.org/10.3389/fchem.2022.932416

Haque, S., Tripathy, S., & Patra, C. R. (2021). Manganese-based advanced nanoparticles for biomedical applications: future opportunity and challenges. *Nanoscale*, *13*(39), 16405-16426. https://doi.org/10.1039/d1nr04964j

Hashim, S. E., & John, A. P. (2023). Green Synthesis of Silver Nanoparticles Using Leaves of Chromolaena odorata and its Antioxidant Activity. *Journal of Tropical Life Science*, *13*(2), 305–310. https://doi.org/10.11594/jtls.13.02.08

Hebeish, A., El-Rafie, M. H., EL-Sheikh, M. A., & El-Naggar, M. E. (2014). Ultra-Fine Characteristics of Starch Nanoparticles Prepared Using Native Starch with and without Surfactant. *Journal of Inorganic and Organometallic Polymers and Materials*, *24*(3), 515–524. https://doi.org/10.1007/s10904-013-0004-x

Jaramillo-Morales, O. A., Díaz-Cervantes, E., Via, L. D., Garcia-Argaez, A. N., EspinosaJuárez, J. V., Ovando-Zambrano, J. C., Muñoz-Pérez, V. M., Valadez-Vega, C., & Bautista, M. (2023). Hepatoprotective Activity, In Silico Analysis, and Molecular Docking Study of Verbascoside from Leucophyllum frutescens in Rats with Post- Necrotic Liver Damage. *Scientia Pharmaceutica*, *91*(3). https://doi.org/10.3390/scipharm91030040

Jayandran, M., Muhamed Haneefa, M., & Balasubramanian, V. (2015). Green synthesis and characterization of Manganese nanoparticles using natural plant extracts and its evaluation of antimicrobial activity. *Journal of Applied Pharmaceutical Science*, *5*(12), 105–110. https://doi.org/10.7324/JAPS.2015.501218

Joshi, N. C., Siddiqui, F., Salman, M., & Singh, A. (2020). Antibacterial Activity, Characterizations, and Biological Synthesis of Manganese Oxide Nanoparticles using the Extract of Aloe vera. *Asian Pacific Journal of Health Sciences*, *7*(3), 27–29. https://doi.org/10.21276/apjhs.2020.7.3.7

Joudeh, N., & Linke, D. (2022). Nanoparticle classification, physicochemical properties, characterization, and applications: a comprehensive review for biologists. *Journal of Nanobiotechnology*, *20*(1), 262. . https://doi.org/10.1186/s12951-022-01477-8

Khan, F., Shariq, M., Asif, M., Siddiqui, M. A., Malan, P., & Ahmad, F. (2022). Green nanotechnology: plant-mediated nanoparticle synthesis and application. *Nanomaterials*, *12*(4), 673.

Kong, J., & Yu, S. (2007). Fourier transform infrared spectroscopic analysis of protein secondary structures. *Acta Biochimica et Biophysica Sinica*, *39*(8), 549–559. https://doi.org/10.1111/j.1745-7270.2007.00320.x

Li, H., Minor, E. C., & Zigah, P. K. (2013). Diagenetic changes in Lake Superior sediments as seen from FTIR and 2D correlation spectroscopy. *Organic Geochemistry*, *58*, 125–136. https://doi.org/10.1016/j.orggeochem.2013.03.002

Malik, S., Muhammad, K., & Waheed, Y. (2023). Nanotechnology: a revolution in modern industry. *Molecules*, *28*(2), 661. https://doi.org/10.3390/MOLECULES28020661

Mohammed, A. E., & Al-Megrin, W. A. (2021). Biological potential of silver nanoparticles mediated by leucophyllum frutescens and *Russelia equisetiformis* extracts. *Nanomaterials*, *11*(8). https://doi.org/10.3390/nano11082098

Molina-Salinas, G. M., Rivas-Galindo, V. M., Said-Fernández, S., Lankin, D. C., Muñoz, M. A., Joseph-Nathan, P., ... & Waksman, N. (2011). Stereochemical analysis of leubethanol, an anti-TB-active serrulatane, from *Leucophyllum frutescens*. *Journal of natural products*, *74*(9), 1842-1850. https://doi.org/10.1021/np2000667

Momeni, M., Asadi, S., & Shanbedi, M. (2021). Antimicrobial Effect of Silver Nanoparticles Synthesized with *Bougainvillea Glabra* Extract on *Staphylococcus aureus* and *Escherichia Coli*. *Iranian Journal of Chemistry and Chemical Engineering*, *40*(2).

Nandiyanto, A. B. D., Oktiani, R., & Ragadhita, R. (2019). How to read and interpret FTIR spectroscope of organic material. *Indonesian Journal of Science and Technology*, *4*(1), 97–118. https://doi.org/10.17509/ijost.v4i1.15806

Nasrollahzadeh, M., Sajadi, S. M., Sajjadi, M., & Issaabadi, Z. (2019). Applications of nanotechnology in daily life. *Interface science and technology*, *28*, 113-143. https://doi.org/10.1016/B978-0-12-813586-0.00004-3

Ozdal, M., & Gurkok, S. (2022). Recent advances in nanoparticles as antibacterial agent. *ADMET and DMPK*, *10*(2), 115-129. https://doi.org/10.5599/admet.1172

Pandit, C., Roy, A., Ghotekar, S., Khusro, A., Islam, M. N., Emran, T. Bin, Lam, S. E., Khandaker, M. U., & Bradley, D. A. (2022). Biological agents for synthesis of nanoparticles and their applications. *Journal of King Saud University - Science*, *34*(3) https://doi.org/10.1016/j.jksus.2022.101869

Pirtarighat, S., Ghannadnia, M., & Baghshahi, S. (2019). Green synthesis of silver nanoparticles using the plant extract of Salvia spinosa grown in vitro and their antibacterial activity assessment. *Journal of Nanostructure in Chemistry*, *9*(1), 1–9. https://doi.org/10.1007/s40097-018-0291-4

Rostamizadeh, E., Iranbakhsh, A., Majd, A., Arbabian, S., & Mehregan, I. (2020). Green synthesis of Fe2O3 nanoparticles using fruit extract of Cornus mas L. and its growth promoting roles in Barley. *Journal of Nanostructure in Chemistry*, *10*(2), 125–130. https://doi.org/10.1007/s40097-020-00335-z

Saod, W. M., Hamid, L. L., Alaallah, N. J., & Ramizy, A. (2022). Biosynthesis and antibacterial activity of manganese oxide nanoparticles prepared by green tea extract. *Biotechnology Reports*, *34*. https://doi.org/10.1016/j.btre.2022.e00729

Saratale, R. G., Karuppusamy, I., Saratale, G. D., Pugazhendhi, A., Kumar, G., Park, Y., ... & Shin, H. S. (2018). A comprehensive review on green nanomaterials using biological systems: Recent perception and their future applications. *Colloids and Surfaces B: Biointerfaces*, *170*, 20-35. https://doi.org/10.1016/j.colsurfb.2018.05.045

Sim, S., & Wong, N. K. (2021). Nanotechnology and its use in imaging and drug delivery (Review). *Biomedical Reports*, *14*(5). https://doi.org/10.3892/br.2021.1418

Singh, K. R., Nayak, V., & Singh, R. P. (2021). Introduction to bionanomaterials: an overview. *Bionanomaterials: Fundamentals and biomedical applications*, 1-1. https://doi.org/10.1088/978-0-75033767-0ch1

Skandalis, N., Dimopoulou, A., Georgopoulou, A., Gallios, N., Papadopoulos, D., Tsipas, D., ... & Chatzinikolaidou, M. (2017). The effect of silver nanoparticles size, produced using plant extract from *Arbutus unedo*, on their antibacterial efficacy. *Nanomaterials*, *7*(7), 178. https://doi.org/10.3390/nano7070178

Slavin, Y. N., Asnis, J., Häfeli, U. O., & Bach, H. (2017). Metal nanoparticles: understanding the mechanisms behind antibacterial activity. *Journal of Nanobiotechnology*, *15*, 65. https://doi.org/10.1186/s12951-017-0308-z

Souri, M., Hoseinpour, V., Shakeri, A., & Ghaemi, N. (2018). Optimisation of green synthesis of MnO nanoparticles via utilising response surface methodology. *IET Nanobiotechnology*, *12*(6), 822–827. https://doi.org/10.1049/iet-nbt.2017.0145

Subba Rao, Y., Kotakadi, V. S., Prasad, T. N. V. K. V., Reddy, A. V., & Sai Gopal, D. V. R. (2013). Green synthesis and spectral characterization of silver nanoparticles from Lakshmi tulasi (*Ocimum sanctum*) leaf extract. *Spectrochimica Acta - Part A: Molecular and Biomolecular Spectroscopy*, *103*,156–159. https://doi.org/10.1016/j.saa.2012.11.028

Van Tien, H., Tri, N., Anh, N. P., Nhi, D. M., Bich, L. T., Hang, D. N. L., & Van Minh, N. (2020). Characterization and antibacterial activity of silver-manganese bimetallic nanoparticles biofabricated using Arachis pintoi extract. *Int. J. Pharm. Phytopharm. Res. EIJPPR*, *10*, 70-76. https://www.researchgate.net/publication/341554926

Younis, A., Riaz, A., Tariq, U., Nadeem, M., Khan, N. A., Ahsan, M., Adil, W., & Naseem, M. K. (2017). Drought tolerance of *leucophyllum frutescens*: Physiological and morphological studies reveal the potential xerophyte. *Acta Scientiarum Polonorum, Hortorum Cultus*, *16*(6), 89–98. https://doi.org/10.24326/asphc.2017.6.8

EXPLORING ANTIOXIDANT ACTIVITY OF DATE AND Fenugreek ESSENTIAL OILS: INVESTIGATING INDIVIDUAL AND COMBINED EFFECTS USING IN VITRO AND IN SILICO ANALYSIS.

Author name and information

Rasha Saad Suliman[1], Priya Breitener[1], Amal Ahmed Almuflehi[1], Aya Khaldoon Al Zaghir[1], Hiba Elamin Elsadig[1], Sara Faraj Eisa Alfalahi[2], Hussah N Albahlal[2], Sahar S. Alghamdi[2,3*]

[1]Department of Pharmacy, Fatima College of Health Sciences, Abu Dhabi, UAE
[2]Department of Pharmaceutical Sciences, College of Pharmacy, King Saud bin Abdulaziz University for Health Sciences, Saudi Arabia
[3]King Abdullah International Medical Research Center, Riyadh, Saudi Arabia

* Correspondence; ghamdi@ksau-hs.edu.sa

Keywords

Antioxidant; Date oil *(Phoenix dactylifera); Fenugreek* oil *(Trigonella foenum-graecum); In vitro* methods; *In silico* analysis.

ABSTRACT

Antioxidants play a pivotal role in mitigating the damaging effects of oxidative stress, which is a major contributor to the development of various diseases. *Fenugreek* (*Trigonella foenum-graecum*), known for its wide range of therapeutic properties, contains bioactive compounds that have been shown to counteract oxidative stress. Similarly, dates (*Phoenix dactylifera*) are widely used for their nutritional value and health-promoting benefits, particularly in their capacity to protect against chronic diseases. Although the individual antioxidant properties of *Fenugreek* and dates are well-established, their combined effects have yet to be comprehensively explored. This study seeks to address this gap by investigating the antioxidant potential of a *Fenugreek* oil and date oil combination. To test our hypothesis, we employed in vitro and *in silico* methods. Specifically, laboratory experiments were conducted to assess the radical scavenging activity of *Fenugreek* oil, date oil, and their combination (mixture) using the DPPH assay. Concurrently, the antioxidant potential of the mixture was evaluated through *in* silico analysis using the PASS (Prediction of Activity Spectra for Substances) computational tool. Our findings revealed that the combination of *Fenugreek* and date palm oils exhibited a dose-dependent increase in antioxidant activity. In addition, the *in* silico results suggested that *Fenugreek* and date oils exhibit comparable antioxidant activity, with date oil displaying a slightly higher range. Consequently, we hypothesize that the combined oils would retain a similar antioxidant effect, although possibly reduced somewhat compared to their individual effects. In conclusion, and date palm oils independently demonstrate significant antioxidant properties. However, these oils exhibit a marginally reduced overall antioxidant effect when combined, providing new insights into their effects following *in vitro* analysis.

INTRODUCTION

Antioxidants play a key role in protecting human bodies against the harmful effects of oxidative stress, a significant contributor to various diseases, including cancer, cardiovascular disorders, and neurodegenerative conditions (Aziz et al., 2019). *Fenugreek* (*Trigonella foenum-graecum*) and date (*Phoenix dactylifera*), revered for centuries for their culinary and medicinal significance, are now emerging as potent antioxidative stress foods, showcasing their ability to combat free radicals and protect cells from oxidative damage, adding them to the list of promising natural defense sources that combat oxidative damage (Akbari et al., 2019; Al-Shwyeh, 2019). This recent discovery emphasizes the importance of utilizing known and safe edible natural antioxidant stores to improve health and well-being (Almatroodi et al., 2021).

Fenugreek is a versatile herb with a rich history dating back thousands of years. It has been esteemed for its medicinal and therapeutic properties across diverse cultures. Scientific exploration has revealed *fenugreek*'s remarkable ability to combat oxidative stress, a process implicated in numerous chronic diseases ranging from diabetes to cardiovascular disorders. Its antioxidant activity is attributed to many bioactive compounds, including flavonoids, alkaloids, and saponins, which synergize the eradication of the harmful effects of free radicals and mitigate cellular damage (Akbari et al., 2019; Almatroodi et al., 2021)

Dates, the succulent fruits harvested from the date palm tree (*Phoenix dactylifera*), have long been celebrated for their exquisite taste and remarkable health-promoting properties (Alahyane et al., 2019). Revered as a symbol of vitality and longevity in many cultures, dates have earned their place as a nutritional powerhouse enriched with antioxidants. Studies have elucidated significant antioxidant activity in dates, attributable to their diverse bioactive compounds, including phenolic compounds, flavonoids, carotenoids, and tocopherols, exerting a potent scavenging effect against free radicals (Metoui et al., 2018). Furthermore, research suggests that the consumption of dates may confer protection against chronic diseases due to their ability to combat inflammation and oxidative damage at the cellular level (Metoui et al., 2018; Hussain et al., 2020).

The chemical composition varies between the date and *fenugreek* oils. For *fenugreek,* the chemical composition responsible for its antioxidant activity includes phenolic compounds, flavonoids, alkaloids, and saponins. Phenolic compounds, such as coumarins and flavanols, exhibit strong antioxidant properties, scavenging free radicals that prevent cellular oxidative damage. Flavonoids, like quercetin and rutin, contribute to *fenugreek*'s antioxidant capacity by neutralizing reactive oxygen species. Alkaloids, including trigonelline, have been shown to possess antioxidant effects, aiding in the protection against oxidative stress-related ailments. In addition, saponins found in *fenugreek* exhibit antioxidant activity, further enhancing its health-promoting properties. Together, these chemical constituents make *Fenugreek* a valuable natural source of antioxidants, supporting overall well-being and potentially mitigating various chronic diseases (Niknam et al., 2021; Benziane et al., 2019; Kumar et al., 2021). On the other hand, the antioxidant activity of date palms (*Phoenix dactylifera*) is primarily attributed to various chemical groups, including phenolic compounds, flavonoids, carotenoids, and tocopherols. Phenolic compounds, such as caffeic acid and ferulic acid, are known for their potent

antioxidant properties, helping to neutralize free radicals and prevent cellular damage. Flavonoids, such as quercetin and kaempferol, contribute further to the antioxidant capacity of dates by scavenging reactive oxygen species. Carotenoids, like β-carotene and lutein, give dates their vibrant color and possess antioxidant properties that protect against oxidative stress. Additionally, tocopherols, a form of vitamin E, play a vital role in combating free radicals and maintaining cellular health. Together, these chemical groups make dates a potent source of natural antioxidants, promoting overall well-being and potentially reducing the risk of chronic diseases (Metoui et al., 2018; Mohamed et al., 2021; Hussain et al., 2019; Ourradi et al., 2021). Previous studies have individually demonstrated the antioxidant properties of date and *fenugreek* oils. However, there is a lack of research exploring their combined antioxidant activity and understanding the mechanisms underlying any potential effects of their combination. This gap underscores the need for comprehensive investigations into the antioxidant properties of herbal combinations (Al-Shwyeh, 2019; Singh, 2023). The proposed study addresses this gap by comparing both *in vitro* (lab experiments) and *in silico* study data for each oil and their combined effects. This approach will provide a holistic understanding of the antioxidant activity of date and *fenugreek* oils, thereby contributing to the advancement of research and development in the field of antioxidants.

MATERIALS AND METHODS

The study investigates the antioxidant impact of date and *fenugreek* oils separately and in combination via *in silico* and *in vitro* analysis. A DPPH (2,2-diphenyl-1-picrylhydrazyl) assay performed to assess antioxidant activity in vitro, while the PASS online web server was utilized to evaluate antioxidant activity *in silico*, as shown in **Figure 1.**

Sample Collection

The essential oil samples were procured via the online platform of Hemani Herbal, Pakistan, a reputable company specializing in producing and distributing essential oils (https://pk.hemaniherbals.com/). Freshly obtained samples of *fenugreek* essential oil (*Trigonella foenum-graecum L.*) and date oil (*Phoenix dactylifera L.*) were subjected to comprehensive *in vitro* and *in silico* analyses to assess their antioxidant potential and associated bioactive properties.

Preparation of Oil Samples

The oil samples, including fenugreek oil, date oil, and their combination, were mixed with a DPPH solution (reagent) and 99% ethanol (solvent) in test tubes at various oil concentrations (analyte) (20 µl, 40 µl, 60 µl, 80 µl, and 100 µl) as illustrated in **Table 1**.

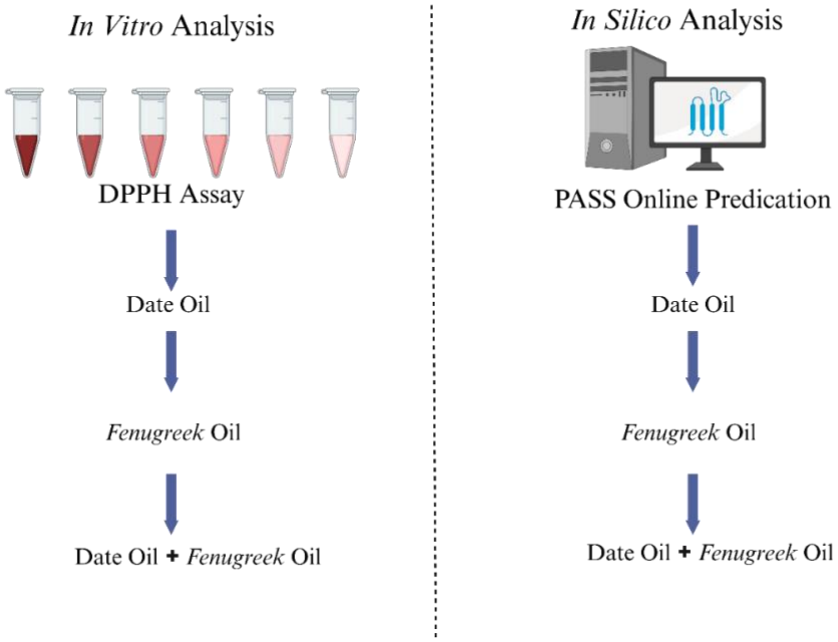

Figure 1. Schematic representation of the study workflow, combining the DPPH assay (left) to assess antioxidant activity and in silico analysis (right) to predict molecular interactions, providing comprehensive insights into the oils' antioxidant properties.

Table 1: The oil samples' concentration, including *fenugreek* and date oils, and their combination.

Oil type	Concentration
Fenugreek oil	0 *µl*, 20 *µl*,40 *µl*,60 *µl*, 80 *µl*, and 100 *µl*
Date oil	0 *µl*, 20 *µl*,40 *µl*,60 *µl*, 80 *µl*, and 100 *µl*
Combination of both oils (1:1)*	0 *µl*, 20 *µl*,40 *µl*,60 *µl*, 80 *µl*, and 100 *µl*

** Note: (1:1) ratio was used in the combination samples because both date and fenugreek oils had almost similar densities. Fenugreek oil = 0.8051g/ml, Date oil = 0.8526g/ml* (Noureddini et al., 2016).

The total volume of each sample was 4 ml, comprising 2.4 ml of DPPH solution and 1.6 ml of ethanol. Notably, the volume of ethanol was adjusted proportionally with the increase in the sample concentration to ensure a consistent total volume of 4 ml in each sample. The samples were vigorously shaken for 10 minutes in each test tube to ensure proper interaction between the oil components and DPPH. Then, the mixtures were allowed to stand for an additional 10 minutes in the dark to facilitate the reaction between the antioxidants in the oil and the DPPH radical. The samples were centrifuged for 5 minutes to separate the water and oil phases. The supernatant layer was carefully collected for further analysis, leaving behind the oil phase. This step helps remove oil components that may cause turbidity and interference during absorbance measurement.

In Vitro Analysis via Determination of DPPH Measuring Radical Scavenging Activity

The baseline correction (control) uses a blank solution comprising 1.6 ml of ethanol solvent and 2.4 ml of DPPH solution. To ensure precise and reliable data acquisition, the absorbance measurements were recorded at a wavelength of 517 nm using a UV-1900i spectrophotometer. The antioxidant

activity of the oil samples is evaluated by quantifying the reduction in absorbance compared to the blank solution, employing established computational methods to obtain accurate results. Additionally, each step in the experiment was performed in triplicate to ensure consistency in the results.

Measurement of Absorbance at 517nm

Absorbance was measured at 517 nm for all 18 samples (comprising six distinct samples, each analyzed in triplicate). This precise wavelength is selected due to its alignment with the peak absorption of the DPPH radical, thereby ensuring optimal sensitivity and accuracy in detecting radical concentration. The continuous monitoring of absorbance at 517 nm enables the quantitative evaluation of the samples' capacity to neutralize DPPH radicals, serving as a robust and reliable measure of their antioxidant activity under controlled experimental conditions.

Antioxidant Activity Calculation

The absorbance was measured at a wavelength of 517 nm, and the antioxidant activity, expressed as the percentage of DPPH radical scavenging activity, was determined using the following equation:

$$DPPH\ Radical\ Scavenging\ Activity\ (\%) = \frac{(A_{control} - A_{sample}) \times 100}{A_{control}}$$

In this formula, $A_{control}$ represents the absorbance of the DPPH solution in ethanol without the oil sample. A_{sample} corresponds to the absorbance of the mixture containing the oil sample at various concentrations, including ethanol and DPPH solution.

The reaction mechanism involves the interaction of the DPPH radical with antioxidant compounds capable of donating hydrogen atoms, leading to the reduction of DPPH as represented by the equation:

$$DPPH^* + RH \rightarrow DPPH_2 + R^*$$

This reduction is accompanied by a colorimetric change from deep violet to light yellow, indicative of the neutralization of DPPH radicals. The degree of this color change, a quantitative measure of antioxidant activity, was recorded at 517 nm using a UV-visible spectrophotometer.

Data Analysis

The absorbance values for each sample and concentration were recorded using a UV-visible spectrophotometer. Subsequently, the antioxidant activity of each sample concentration was calculated using the formula for DPPH radical scavenging activity shown in section 2.3.2. Statistical analysis was performed to evaluate the antioxidant efficacy of *fenugreek* oil, date oil, and their combinations at various concentrations. The analysis included determining the half-maximal inhibitory concentration (IC_{50}) value, representing the concentration required to inhibit 50% DPPH radicals. Thus, the IC50 value provides a quantitative measure of antioxidant potency.

Determination of IC_{50}

The IC_{50} was determined through graphical analysis. A scatter plot was constructed, with percentage inhibition plotted on the y-axis and sample concentrations (mg/mL) on the x-axis, reflecting a linear relationship. The IC_{50} value was calculated using the equation of the simple linear regression line *(y=mx+c)*, where y represents percentage inhibition, x denotes the sample concentration, and m and c are the slope and intercept, respectively.

In Silico Prediction Using PASS Online

The antioxidant potential of the mixture was assessed using the computer-based tool PASS (Prediction of Activity Spectra for Substances) (http://www.pharmaexpert.ru/passonline/). The software utilizes structure-activity relationships to forecast the biological actions of chemical structures, including phytochemicals, by comparing them to a known chemical entity (Jamkhande et al., 2016). The system forecasts the desired pharmacological outcome and the molecular mechanisms of action and undesired side effects such as mutagenicity, carcinogenicity, teratogenicity, and embryotoxicity. The system compares the structure with a training set comprising over 205,000 chemicals, which display more than 3750 different types of biological activity. The activity is quantified using P_a (probable activity) and P_i (probable inactivity). Only substances with a P_a value greater than P_i were examined for a specific pharmacological activity. Additionally, computational simulations were employed to model and analyze the properties of *fenugreek*, date, and their combined oil samples. Moderately active (scoring between 0.50 and 0.00) or inactive (scoring less than 0.50) against the examined targets. (https://www.molinspiration.com/cgi-bin/properties) (Kulkarni et al., 2022).

RESULTS

In Vitro Analysis

IC_{50} values serve as crucial indicators of potency, elucidating the concentration at which oils exert their inhibitory effect on DPPH radicals. A potent effect is interpreted as having lower IC_{50} values, indicating higher antioxidant activity. The antioxidant activities of *fenugreek* oil, date palm oil, and their combination were evaluated using the DPPH scavenging assay. Investigating the antioxidant activities of *fenugreek* oil, date palm oil, and their combination, **Table 2** presents the inhibition percentage of DPPH radicals at various concentrations for each oil, with samples 1 to 5 representing increasing concentrations.

Fenugreek oil demonstrated a dose-dependent increase in antioxidant activity, reaching 83.31% inhibition at 20.15 mg/ml. Similarly, date palm oil exhibited a dose-dependent increase in antioxidant activity, with 85.93% inhibition at 21.01 mg/ml. The combination of *fenugreek* and date palm oils reached 88% at 22.16 mg/ml, showing a dose-dependent increase in antioxidant activity, as depicted in **Table 2**. This correlation highlights the trend of increasing antioxidant activity with higher oil concentrations.

Table 2: Percentage inhibition of DPPH radicals by *fenugreek* oil, date palm oil, and their combination at various concentrations.

	***Fenugreek* Oil**		**Date Palm Oil**		***Fenugreek* and Date Palm Oils Combination**	
Sample	**Conc (mg/ml)**	**Inhibition (%)**	**Conc (mg/ml)**	**Inhibition (%)**	**Conc (mg/ml)**	**Inhibition (%)**
1	*4.03*	*21.41802*	*4.20*	*24.29629*	*4.43*	*11.68224*
2	*8.06*	*45.64254*	*8.40*	*56.74074*	*8.86*	*24.61059*
3	*12.09*	*59.82275*	*12.60*	*60.59259*	*13.30*	*48.28660*
4	*16.12*	*82.27474*	*16.81*	*69.48148*	*17.73*	*57.00935*
5	*20.15*	*83.30871*	*21.01*	*85.92592*	*22.16*	*88.00623*

The antioxidant activities of *fenugreek* oil, date palm oil, and their combination were evaluated using the DPPH scavenging assay, and the IC_{50} values are illustrated in **Figure 2**.

Fenugreek oil exhibited notable antioxidant activity with an IC_{50} value of 9.9513 mg/ml. This potency can be attributed to its composition, particularly palmitic acid and phytol, as detected by GC-MS analysis (Akbari et al., 2019). The observed IC_{50} value indicates a significant ability of *fenugreek* oil to scavenge free radicals, potentially offering protective effects against oxidative stress. Similarly, date palm oil exhibited a potent antioxidant activity with an IC_{50} value of 9.70 mg/ml, highlighting its rich antioxidant content, likely including compounds such as gallic, protocatechuic, p-coumaric, and ferulic acid (Harkat et al., 2022).

These antioxidants are crucial in neutralizing free radicals and mitigating oxidative damage. Date palm oil's effectiveness in the DPPH scavenging assay suggests its potential utility as a natural antioxidant source for various applications. Surprisingly, the combination of *fenugreek* and date palm oils resulted in an IC50 value of 14.28 mg/ml, indicating a lower antioxidant activity than the individual oils. This unexpected outcome suggests the combination may not have yielded a synergistic effect in this assay. The lack of synergistic effect could be due to various factors, such as the specific ratios of the oils in combination or potential interactions between their components. Further investigations are required to understand the mechanisms underlying the interaction of these oils and their impact on antioxidant activity. These findings raise intriguing questions regarding the optimal blending ratios for synergistic antioxidant effects.

In Silico Analysis:

Molecular Target Predictions Using Molinspiration:

Molinspiration Cheminformatics tools* were used to predict the molecular targets for the identified metabolites, which provide an estimated bioactivity score for metabolites against a variety of biological targets such as G protein-coupled receptors (GPCR), ion channels, nuclear receptors, kinases, Protein-disulfide reductase (glutathione) inhibitor, proteases, and enzymes. The bioactivity score value categorizes substances as active (if the anticipated score equals or exceeds 0.00), *fenugreek*

Oil Identified compounds. The chemical structures of the previously identified active ingredients from *fenugreek* and date oils are shown in **Figures 3** and **4**. Additionally, the percentages of the active ingredients from the *fenugreek* and date oils are shown in **Tables 3** and **4**.

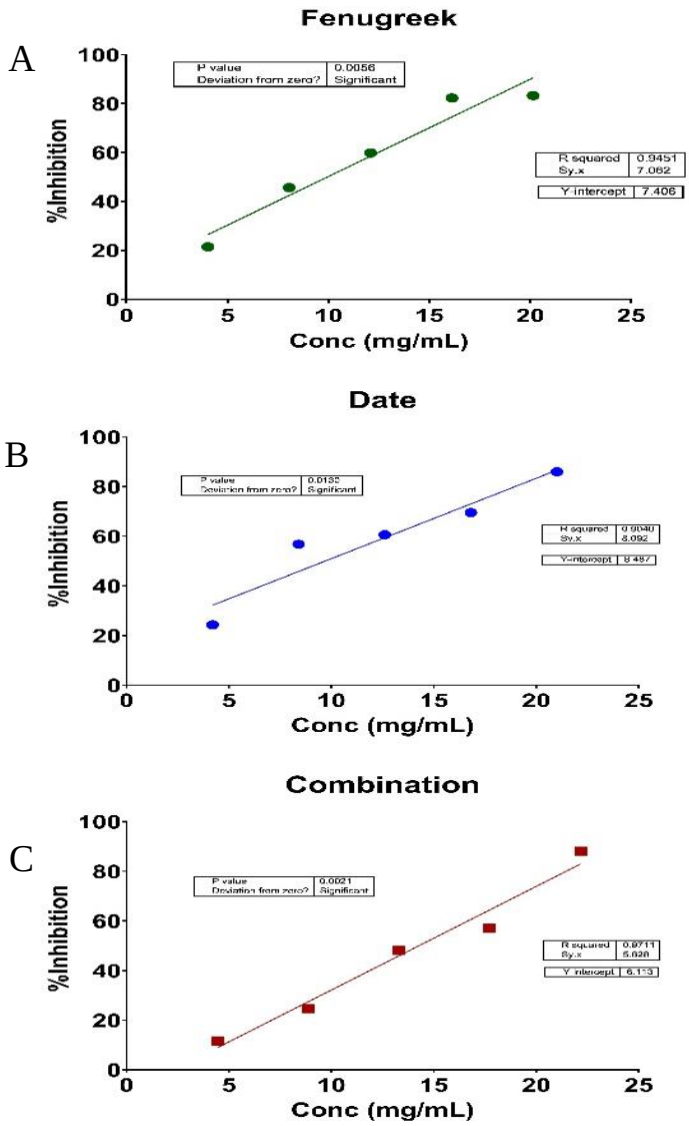

Figure 2: A, B, and C illustrate the correlation between concentration and inhibition percentages of DPPH radicals.

Computational Investigations Using PASS Online:

The eight major phytoconstituents in *fenugreek* are linoleic acid, linolenic acid, oleic acid, neryl acetate, camphor, β-Pinene, β-caryophyllene, and 2,5-dimethyl pyrazine. Moreover, the nine major phytoconstituents in date are lauric acid, myristic acid, palmitic acid, palmitoleic acid, oleic acid, linoleic acid, linolenic acid, tocopherols, and phytosterols, were investigated for evaluating the antioxidant activity by using PASS online program.

Table 3: The percentages of the previously identified active ingredients from *fenugreek* oil.

Compound	Compound Conc (%)	Reference
Linoleic acid	42.80%	
Linolenic acid	26.15%	
Oleic acid	14.40%	(Kulkarni et al., 2022)
Neryl acetate	17.3%	
Camphor	16.3%	
β-Pinene	15.05%	
β-caryophyllene	14.63%	
2,5-dimethyl pyrazine	6.14%	

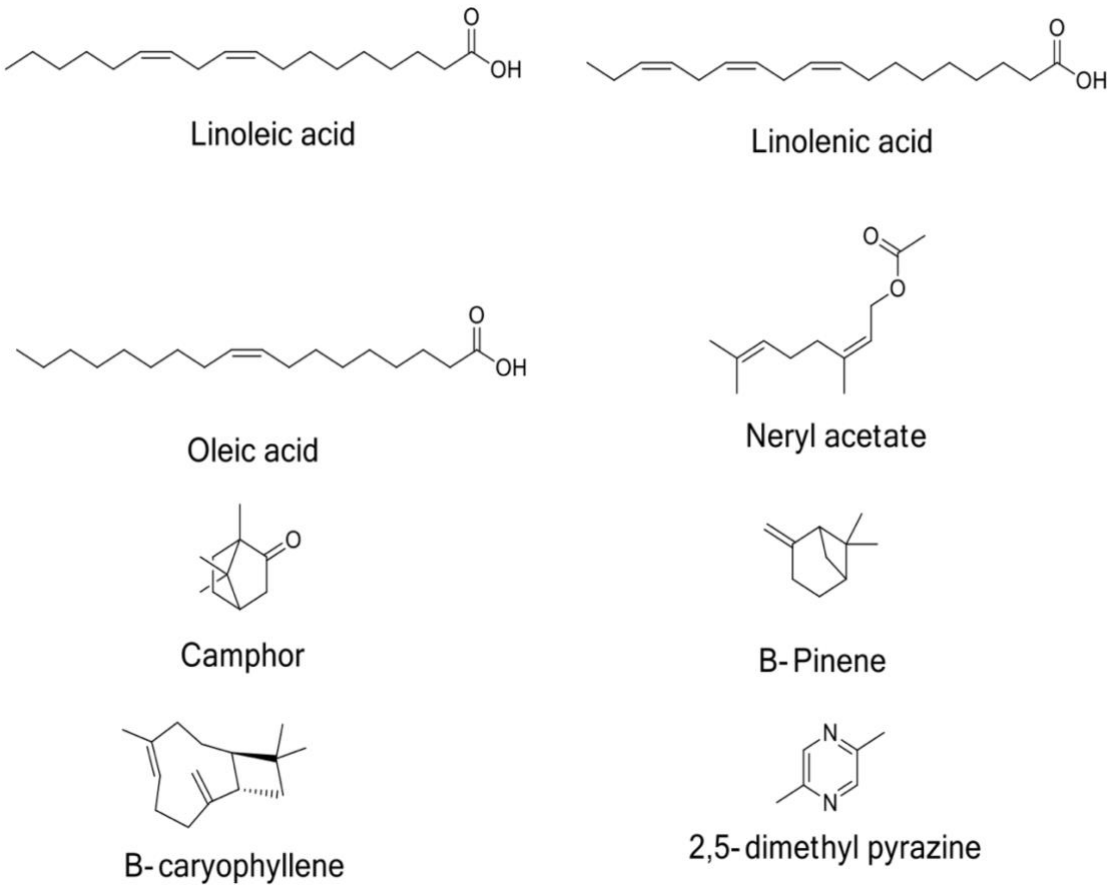

Figure 3: The chemical structures of the previously identified active ingredients from *fenugreek* oil.

Table 4: The percentages of the previously identified active ingredients from date oil.

Compound	Compound Conc (%)	Reference
Lauric acid	17.8%	(Visuvanathan et al., 2022)
Myristic acid	ND	
Palmitic acid	ND	
Palmitoleic acid	ND	
Oleic acid	ND	
Linoleic acid	15%	
Linolenic acid	8%	
Tocopherols	ND	
Phytosterols	ND	

*ND: Not determined

The PASS Online web server was employed to forecast the antioxidant potential of the seven *tentatively identified fenugreek* and date oil metabolites. As indicated in Table 5 for fenugreek oil and Table 6 for date oil, the compounds with the highest P_a and lowest P_i values are more likely to experimentally have the highest antioxidant activity.

Table 5: The prediction of antioxidant activity of identified metabolites from *fenugreek* oil.

Biological Activities for *Fenugreek* Metabolites	Antioxidant activity (Protein-disulfide reductase (glutathione) inhibitor)	
	P_a	P_i
Linoleic acid	0.831	0.007
Linolenic acid	0.775	0.012
Oleic acid	0.853	0.005
Neryl acetate	0.865	0.005
Camphor	0.622	0.060
β-Pinene	0.471	0.082
β-caryophyllene	0.358	0.160
2,5-dimethyl Pyrazine	0.549	0.052

P_a: Probability of being active. P_i: Probability of being inactive

For *fenugreek* oil, neryl acetate possesses the highest antioxidant activity, with a P_a value of 0.865, followed by oleic acid, with a P_a value of 0.853. The remaining metabolites showed lower Pa values, which suggests lower antioxidant activity.

Table 6: The prediction of antioxidant activity of identified metabolites date oil.

Biological Activities for Date Metabolites	Antioxidant activity (Protein-disulfide reductase (glutathione) inhibitor)	
	P_a	P_i
Lauric acid	0.884	0.004
Myristic acid	0.884	0.004
Palmitic acids	0.884	0.004
Palmitoleic cid	0.853	0.005
Oleic acids	0.853	0.005
Linoleic acid	0.831	0.007
Linolenic acid	0.775	0.012
Tocopherols	0.294	0.235
Phytosterols	0.796	0.010

P_a: Probability of being active. P_i: Probability of being inactive

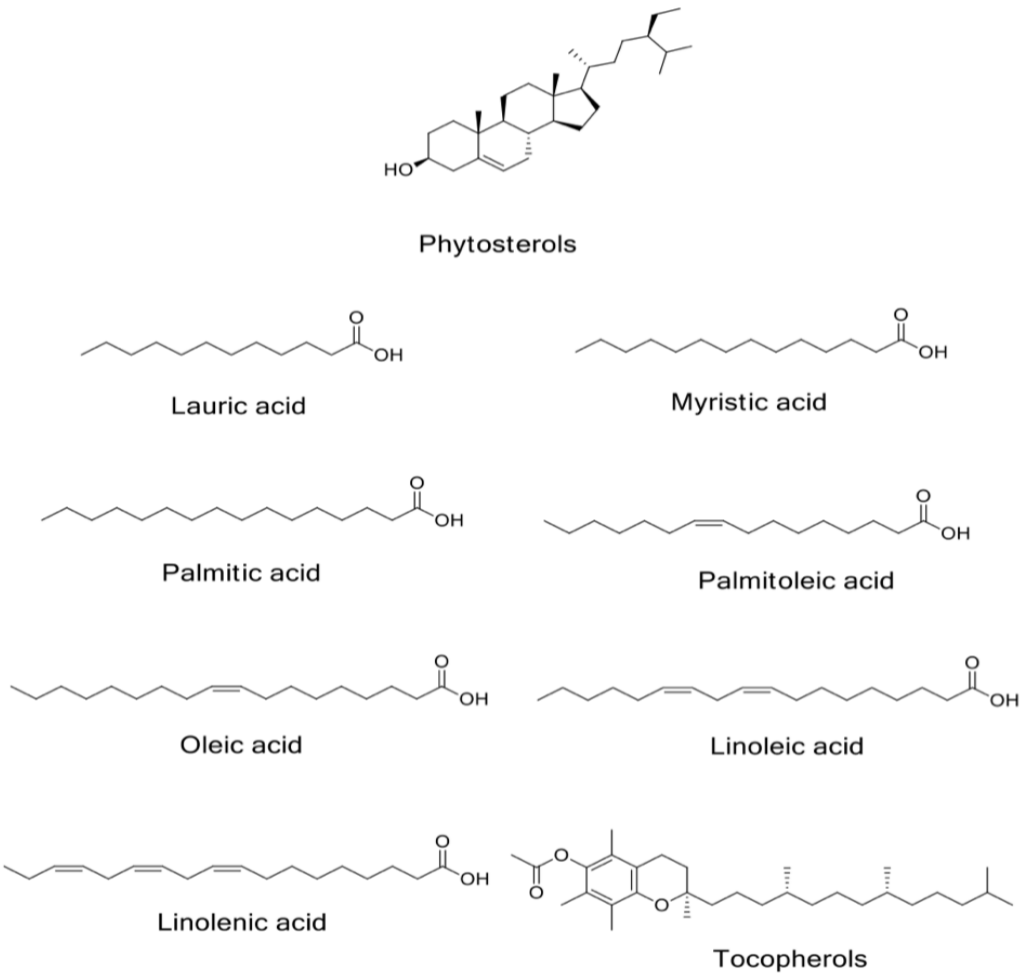

Figure 4: The chemical structures of the previously identified active ingredients from date oil.

On the other hand, β-caryophyllene possesses the lowest antioxidant activity, with a P_a value of 0.358. As for the date oil, lauric acid, myristic acid, and palmitic acids have the highest antioxidant activity with a P_a value of 0.884, followed by palmitoleic acid and oleic acid with a P_a value of 0.853. The remaining metabolites showed lower Pa values, which suggests lower antioxidant activity. On the other hand, Tocopherols possess the lowest antioxidant activity with a P_a value of 0.294. Therefore, date oil and *fenugreek* oil have almost the same range of antioxidant activity. However, date oil may demonstrate a slightly higher range. As such, the combined oils should possess nearly a similar range of activity.

DISCUSSION

Integrating the outcomes of both the DPPH experiment and the *in silico* analysis provides crucial insights into the antioxidant properties of *fenugreek* oil and date palm oil, both individually and in combination. The DPPH analysis demonstrates the impressive antioxidant activity of *fenugreek* oil, as evidenced by its notable IC50 value of 9.95 mg/ml. This potency aligns with previous research attributing *fenugreek* oil's efficacy to its composition, notably enriched with palmitic acid and phytol, as detected through GC-MS analysis (Akbari et al., 2019). Similarly, date palm oil emerges as a potent antioxidant, boasting an IC50 value of 9.70 mg/ml. Its richness in antioxidants such as gallic, protocatechuic, p-coumaric, and ferulic acid (Mrabet et al., 2020) highlights its efficacy in neutralizing free radicals and mitigating oxidative stress.

Moreover, the *in vitro* results from the DPPH assay validate the *in silico* predictions, suggesting that date palm oil may possess a slightly higher range of antioxidant activity than *fenugreek* oil. However, both oils demonstrate comparable levels of antioxidant potential when mixed. Notably, while showing promise, the combination of *fenugreek* and date palm oils presents a surprising revelation. Despite both oils' strong individual antioxidant activities, their combined potency falls short of expectations, as indicated by an IC_{50} value of 14.2804 mg/ml. This unexpected outcome suggests a potential lack of synergistic effects in this assay, raising questions regarding the optimal mixing ratios for maximizing antioxidant effects. When assessing the antioxidant potential of natural oils, such as those derived from *fenugreek* and dates, using computational models, notable discrepancies between predicted and experimental findings emerge. The predicted antioxidant activities of various metabolites from *fenugreek* and date oils provide intriguing insights, particularly concerning tocopherols. For instance, tocopherols in date oil are predicted to exhibit low antioxidant activity, with a P_a of 0.294 and a P_i of 0.235 (Table 6). This suggests that, when modeled computationally, tocopherols may not significantly contribute to antioxidant activity. Similarly, other metabolites, such as β-caryophyllene in fenugreek oil, are also predicted to show reduced activity, with a P_a of 0.358 (Table 5).

However, computational predictions often fail to align with the results observed in experimental settings. Despite the low predicted antioxidant activity of tocopherols, these compounds are widely recognized for their potent antioxidant properties, particularly their role as lipid-soluble antioxidants that neutralize free radicals and protect cellular membranes from oxidative damage (Traber & Stevens, 2011; DellaPenna & Mullet, 2016). The discrepancy between computational models and experimental outcomes may stem from the inherent complexity of *in vitro* conditions,

which predictive algorithms cannot fully encapsulate. Tocopherols may exhibit synergistic interactions with other bioactive compounds in *fenugreek* and date oils, enhancing their overall antioxidant capacity (DellaPenna & Mullet, 2016; Al-Dosary & Al-Mashhadi, 2020). This concern extends to other metabolites, such as linoleic and oleic acids, which are predicted to possess moderate to high antioxidant activity in both *fenugreek* and date oils (Tables 5 and 6). However, their effectiveness may vary under *in vivo* conditions. These discrepancies underscore the importance of not relying solely on computational predictions and emphasize the need for experimental validation to accurately characterize the antioxidant properties of natural plant oils (Ahmed & Farooq, 2021). While both *fenugreek* and date oils have individually demonstrated considerable antioxidant activity, there remains a notable gap in the literature concerning the combined antioxidant effects of these two oils. Previous research has predominantly concentrated on the individual properties of these oils, with limited attention given to their potential synergistic effects when used together. The present study aims to address this gap by investigating the combined antioxidant activity of *fenugreek* and date oils through both *in vitro* and *in silico* methods. This dual approach will provide a more nuanced understanding of how the metabolites in these oils may interact and synergistically enhance their antioxidant effects, thereby offering valuable insights into potential natural therapeutic strategies for combating oxidative stress and related diseases (Ahmed & Farooq, 2021).

Further investigation is needed into the specific mechanisms underlying these oils' antioxidant properties. For instance, a deeper analysis of the molecular interactions between the bioactive compounds in *fenugreek* and date palm oils could shed light on their combined antioxidant effects. Additionally, investigating the influence of factors such as extraction methods and environmental conditions on the antioxidant activity of the oils may provide valuable insights into optimizing their efficacy. These findings emphasize the complexity of interactions among compounds within the oils and the importance of optimizing their ratios to achieve desired antioxidant effects. A significant variable in determining the antioxidant activity of oils is the ratio in which they are mixed. According to studies, mixing oils in particular ratios can have synergistic effects, meaning that the total antioxidant activity of the mixture is higher than that of the separate oils. On the other hand, some ratios can cause antagonistic interactions, which would reduce the antioxidant capability overall. For example, studies showed that altering the blending ratios can improve the antioxidant qualities of oil mixtures by increasing their stability and oxidative resistance (Mollica et al., 2020). Careful testing with various mixing ratios is necessary to find combinations that optimize antioxidant activity. By exploring the details of these interactions, researchers can unlock promising avenues for using *fenugreek* and date palm oils in various industries, including pharmaceuticals, cosmetics, and food.

CONCLUSION

Fenugreek and date palm oils individually demonstrate substantial antioxidant activity, as determined from the *in vitro* DPPH experiment and the in-silico analysis. However, when combined, these oils exhibit a reduced antioxidant effect. The in-silico analysis suggests that date palm oil may possess a slightly higher antioxidant activity than *Fenugreek* oil. However, both oils demonstrate similar levels of antioxidant potential when mixed. These results highlight the necessity of comprehending the interplay of compounds within the oils and optimizing their mixed ratios to achieve the desired antioxidant effects. Further investigation into the specific mechanisms governing

the antioxidant activities of these oils is essential, offering promising avenues for their utilization in pharmaceuticals, cosmetics, and food industries.

Data availability: Data supporting the findings of this study are available from the corresponding author upon request.

Conflicts of Interest: The authors declare no conflict of interest.

REFERENCES:

Ahmed, M.S. and Farooq, U. (2021) 'Combined antioxidant activity of fenugreek and date oils: A computational and experimental approach', *Journal of Natural Products*, 84(5), pp. 1323–1331.

Akbari, S. et al. (2019) 'Extraction, characterization and antioxidant activity of fenugreek (*trigonella-foenum graecum*) seed oil', *Materials Science for Energy Technologies*, 2(2), pp. 349–355. doi:10.1016/j.mset.2018.12.001.

Al-Dosary, A.A. and Al-Mashhadi, A. (2020) 'Antioxidant activity of date palm fruit: Implications for chronic disease prevention', *Food & Function*, 11(7), pp. 5062–5072.

Al-Shwyeh, H. (2019) 'Date palm (phoenix dactylifera L.) fruit as potential antioxidant and antimicrobial agents', Journal of Pharmacy And Bioallied Sciences, 11(1), p. 1. doi:10.4103/jpbs.jpbs_168_18.

Alahyane, A. et al. (2019) 'Bioactive compounds and antioxidant activity of seventeen Moroccan date varieties and clones (Phoenix dactylifera L.)', *South African Journal of Botany*, 121, pp. 402–409. doi:10.1016/j.sajb.2018.12.004.

Almatroodi, S.A. et al. (2021) 'Fenugreek (Trigonella foenum-graecum) and its active compounds: A review of its effects on human health through modulating biological activities', *Pharmacognosy Journal*, 13(3), pp. 813–821. doi:10.5530/pj.2021.13.103.

Aziz, M.A., Diab, A.S. and Mohammed, A.A. (2019) Antioxidant categories and mode of action, IntechOpen. Available at: https://www.intechopen.com/chapters/65225 (Accessed: 15 March 2025).

Benziane, M.N. et al. (2019) 'Phytochemistry, HPLC profile and antioxidant activity of aqueous extracts of fenugreek (trigonella foenum graecum L.) seeds grown in arid zones of Algeria', *Acta Scientifica Naturalis*, 6(2), pp. 71–87. doi:10.2478/asn-2019-0020.

DellaPenna, D. and Mullet, J.E. (2016) 'Synergistic effects of tocopherols in antioxidative defense', *Plant Physiology*, 170(2), pp. 736–746.

Harkat, H. et al. (2022) 'Assessment of biochemical composition and antioxidant properties of Algerian date palm (Phoenix dactylifera L.) seed oil', *Plants*, 11(3), p. 381. doi:10.3390/plants11030381.

Hussain, M.I., Farooq, M. and Syed, Q.A. (2020) 'Nutritional and biological characteristics of the date palm fruit (Phoenix dactylifera L.) – A Review', *Food Bioscience*, 34, p. 100509. doi:10.1016/j.fbio.2019.100509.

Hussain, M.I., Semreen, M.H., Shanableh, A., Khattak, M.N.K., Saadoun, I., Ahmady, I.M. et al. (2019) 'Phenolic composition and antimicrobial activity of different Emirati date (*Phoenix dactylifera* L.) pits: A comparative study', *Plants*, 8(11), p. 497.

Jamkhande, P.G., Pathan, S.K. and Wadher, S.J. (2016) 'In silico pass analysis and determination of antimycobacterial, antifungal, and antioxidant efficacies of maslinic acid in an extract rich in

pentacyclic triterpenoids', *International Journal of Mycobacteriology*, 5(4), pp. 417–425. doi:10.1016/j.ijmyco.2016.06.020.

Kulkarni, A.M. et al. (2022) 'Computational simulations highlight the IL2RA binding potential of polyphenol stilbenes from fenugreek', *Molecules*, 27(4), p. 1215. doi:10.3390/molecules27041215.

Kumar, N., Ahmad, A., Singh, S., Pant, D., Prasad, A. and Rastogi, S. (2021) 'Phytochemical analysis and antioxidant activity of Trigonella foenum-graecum seeds', *Journal of Pharmacognosy and Phytochemistry*, 10(1), pp. 23–26.

Metoui, M. et al. (2018) 'Chemical composition, antioxidant and antibacterial activity of Tunisian date palm seed', *Polish Journal of Environmental Studies*, 28(1), pp. 267–274. doi:10.15244/pjoes/84918.

Mohamed, H.I., El-Beltagi, H.S., Jain, S.M. and Al-Khayri, J.M. (2021) 'Date palm (Phoenix dactylifera L.) secondary metabolites: Bioactivity and pharmaceutical potential', in Phytomedicine. Elsevier, p. 483.

Mollica, F. et al. (2020) 'Effect of antioxidants on high-temperature stability of renewable bio-oils revealed by an innovative method for the determination of kinetic parameters of oxidative reactions', *Antioxidants*, 9(5), p. 399. doi:10.3390/antiox9050399.

Mrabet, A. et al. (2020) 'Date seeds: A promising source of oil with functional properties', *Foods*, 9(6), p. 787. doi:10.3390/foods9060787.

Niknam, R., Kiani, H., Mousavi, Z.E. and Mousavi, M. (2021) 'Extraction, detection, and characterization of various chemical components of Trigonella foenum-graecum L. (fenugreek) known as a valuable seed in agriculture', in Fenugreek: *Biology and Applications*, pp. 189–217.

Noureddini, H., Teoh, B.C. and Clements, L.D. (2016) Densities of vegetable oils and fatty acids - journal of the American Oil Chemists' society, SpringerLink. Available at: https://link.springer.com/article/10.1007/BF02637677 (Accessed: 15 March 2025).

Ourradi, H. et al. (2021) 'Proximate composition of polyphenolic, phytochemical, antioxidant activity content and lipid profiles of date palm seeds oils (Phoenix dactylifera L.)', *Journal of Agriculture and Food Research*, 6, p. 100217. doi:10.1016/j.jafr.2021.100217.

Singh, U. (2023) 'Amazing health benefit of fenugreek (trigonella foenum-Graecum Linn.)', *International Journal of Environment and Health Sciences*, 4(2). doi:10.47062/1190.0402.03.

Traber, M. G., & Stevens, J. F. (2011). Vitamin E: The antioxidant activity of tocopherols and tocotrienols. *Food & Function*, 2(1), 47-60.

Visuvanathan, T. et al. (2022) 'Revisiting trigonella foenum-Graecum L.: Pharmacology and therapeutic potentialities', *Plants*, 11(11), p. 1450. doi:10.3390/plants11111450.

HOW DOES SEASONALITY AND ENVIRONMENTAL PARAMETERS INFLUENCE MEIOFAUNAL COMMUNITIES ASSOCIATED WITH *Cystoseira* sp. MACROALGAE ON ROCKY SUBSTRATES OF RIMEL, BIZERTE (TUNISIA)?

Author name and information

Amel Hannachi[1], Mohamed Allouche*[1,2], Badreddine Sellami[3], Ahmed Nasri[1], Silvia Bianchelli[4], Hamouda Beyrem[1], Fehmi Boufahja[5], Roberto Danovaro[4,6], Ezzeddine Mahmoudi[1]

[1]University of Carthage. Faculty of Sciences of Bizerte. LR01ES14 Laboratory of Environment Biomonitoring, Coastal Ecology and Ecotoxicology Unit, Zarzouna 7021, Tunisia.
[2]University of Jendouba. Higher Institute of Biotechnology of Beja. Biology Department, 9000, BP: 382, Tunisia
[3]Institut National des Sciences et Technologies de la Mer, 28 rue de 2 mars 1934, 2025 Salammbô, Tunisia
[4]Department of Life and Environmental Science, Polytechnic University of Marche, Via Brecce Bianche, 60131 Ancona, Italy
[5]Imam Mohammad Ibn Saud Islamic University (IMSIU). College of Science. Biology Department, Riyadh, 11623, Saudi Arabia.
[6]Stazione Zoologica Anton Dohrn, Villa Comunale, 80121 Naples, Italy

* **Correspondence**: Mohamed.allouche@fsb.ucar.tn

Keywords

Meiofaunal taxa; Meiofaunal abundance; physicochemical parameters; seasonal variation; rocky substrates; Rimel cost; Tunisia.

ABSTRACT

The current study investigated the seasonal variations of meiofauna communities (i.e., nematodes, copepods, oligochaetes, polychaetes, and larvae of crustaceans, respectively) associated with *Cystoseira* sp. macroalgae on the rocky substrates of Rimel, Bizerte (Tunisia). Sampling campaigns took place monthly for a full year and environmental parameters, such as temperature, pH, dissolved oxygen, and suspended matter were measured *in situ*. The results underscore the significance of several abiotic factors in shaping meiofaunal communities over time. Copepods showed a positive correlation with pH ($r = 0.592$, $p = 0.0426$), which achieved a peak in abundance in alkaline conditions. The nematodes were highly abundant during early summer, but declined during high summer temperatures, highlighting their sensitivity to thermal stress. The larvae of crustaceans, in contrast, preferred the more stable winter conditions, reaching maximum abundance in February. Multivariate analyses showed distinct communities in time (ANOSIM (Analysis of Similarities), $R = 0.745$, $p = 0.001$) and seasonal clustering, with spring months characterized by more homogenous conditions as opposed to summer-autumn months. The findings of the current survey underscore the complex interplay between meiofauna and environmental factors, offering valuable insights into the ecological functionality of rocky intertidal habitats. Future studies should explore the role of additional factors, such as organic matter quality and trophic interactions in shaping meiofauna dynamics dwelling on rocky substrate.

INTRODUCTION

Meiofauna is a size-based artificial group, defined by organisms that pass through a 1 mm mesh sieve but are retained by a 40 μm mesh sieve. It includes small benthic invertebrates such as nematodes, copepods, oligochaetes, and polychaetes (Semprucci & Balsamo, 2012; Carriço et al., 2013). These taxa play crucial roles in ecosystem functioning and serve as bioindicators of environmental changes. Nematodes dominate meiofaunal communities and indicate sediment contamination, organic matter levels, and trophic interactions (Santos et al., 2018). Copepods contribute to sediment oxygenation and are highly sensitive to pollutants, making them reliable indicators of water quality and bioaccumulation (Hussain et al., 2020). Oligochaetes thrive in organically enriched and hypoxic environments, serving as markers of eutrophication and pollution from sewage or industrial discharge (Chapman et al., 1982). Polychaetes play a key role in sediment mixing and nutrient cycling, with species composition changes reflecting sediment disturbances and chemical contamination (Hutchings, 1998 ; Mandario et al., 2019). However, most studies with a focus on meiofauna took place on soft substrates, such as sandy or muddy sediments; studies focused on hard substrate dwelling meiofauna are few (Danovaro & Fraschetti., 2002).

Meiofaunal communities dwelling on rocky substrates exhibit distinct characteristics shaped by key factors, such as algal cover, substrate structural complexity, and hydrodynamic conditions (Coull et al., 1983; Danovaro et al., 2000). Compared to soft substrates meiofauna, which are normally dominated by nematodes, rocky substrates support often more evenly distributed communities, but dominated by copepods and amphipods, due to their affinity for micro-refuges offered by macroalgae and fissures (Beckley 1982; Coull et al., 1983; Danovaro & Fraschetti, 2002). These microhabitats host also various species of macroalgae, such as *Cystoseira* sp., a genus of brown macroalgae that plays a crucial ecological role in coastal marine ecosystems, particularly along the rocky shores of the Mediterranean Sea. *Cystoseira* sp. supports diverse meiofauna communities due its remarkable structural complexity, fostering greater abundance and diversity of these organisms (Ape et al., 2018a; Ape et al., 2020). This genus follows a seasonal life cycle characterized by fluctuations in growth and reproductive stages throughout the year. Its presence and morphology vary seasonally, reflecting distinct developmental phases rather than a constant form throughout the year (Sales & Ballesteros, 2012).

Despite their ecological importance, long-term data linking meiofauna and environmental key-factors that drive their existence remain scarce. The current study aimed to fill this knowledge gap based on a 12-month survey of the abundance and composition of meiofauna communities that inhabits the rocky substrates of Rimel, Bizerte (Tunisia). Furthermore, the current study also explored the preferences of meiofauna with macroalgal cover, particularly the complex species of the genus *Cystoseira* sp.

MATERIALS AND METHODS

Collection site and environmental parameters

Meiofauna samples were collected monthly, from March 2021 to February 2022, from *Cystoseira* sp. algae located on the rocky shoreline of the Rimel site (37°15'10.4"N 9°56'39.4"E) in Bizerte, Tunisia (Figure 1). The Rimel coast faces multiple environmental challenges, including pollution from petroleum, microplastics, and metals (Boufahja et al., 2012 ; Martins et al., 2015 ; Abidli et al., 2019), making it an ideal site for year-round biomonitoring and assessing the impact of these pollutants on marine meiofauna.

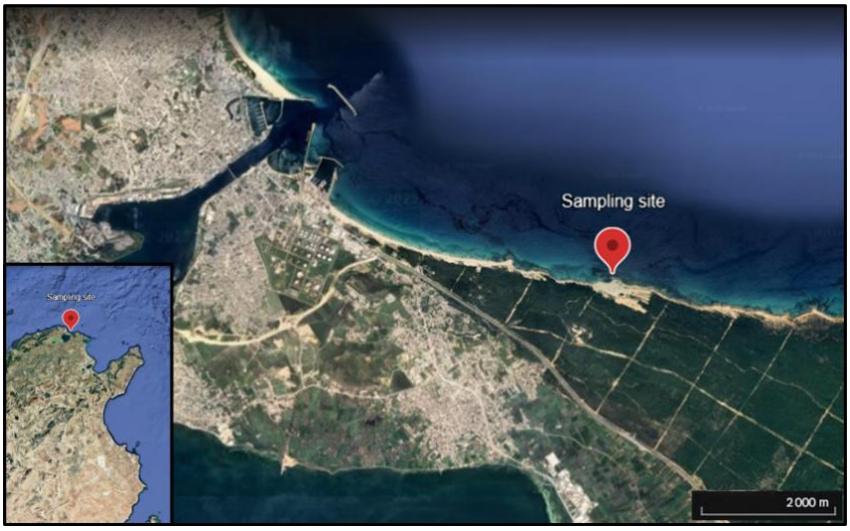

Figure 1. Location of the Sampling Site on the Rocky Shoreline of Rimel, Bizerte (37°15'10.4"N, 9°56'39.4"E), Tunisia.

Dissolved oxygen at water-sediment interface was measured with and oximeter (WTW OXI 330/SET, WTW, Weilheim, Germany). The water temperature and salinity were recorded with a thermosalinometer (WTW LF 196, Weilheim, Germany), and pH with a pH meter (WTW pH 330/SET-1, Germany).

Meiofauna sampling and taxonomic analysis

Meiofauna sampling on rocky substrates associated with various *Cystoseira* species was done with a modified manual hand corer, according to Beckley and McLachlan (1979). The hand corer, with an inner diameter of 8.5 cm, had one open end fitted with a flexible rubber ring (1 cm thick) to adapt to rough surfaces, whereas the other end was sealed with a securely attached plastic bag. During sampling, at 50 cm depth (up to 1 m depth), where these species form dense populations on hard substrata in the upper sublittoral zone (Bellissimo et al., 2014), with the collection bag securely positioned upwards.

A lateral window, located 2 cm above the corer opening, allowed the insertion of a spatula to scrape the rock surface, effectively dislodging debris, whereas simultaneously guiding meiofauna

and associated particles into the collection bag. Once the sampling was complete, the bag was carefully sealed to ensure watertightness.
In the laboratory, meiofauna were separated from macrobenthos and macroalgae by sieving through 1-mm mesh size sieve and retaining it on a second sieve of 40-µm mesh size (Danovaro et al., 2002). The collected specimens were fixed in 4% unbuffered formaldehyde solution and stained with Rose Bengal (0.2 $g.L^{-1}$) to facilitate counting. Meiofauna was individually counted on Delfus plate with a gridded bottom (200 squares of 5 mm^2) under a dissecting microscope (Model WildHeerbrugg M5A), at 50× magnification (Elarbaoui et al., 2015).

Statistical analysis

In order to perform the statistical analyses, the data were first tested for normality (i.e. Kolmogorov-Smirnov test) and equality of variance (i.e. Bartlett test) (Clarke, 1993 ; Clarke and Gorley, 2001). The software GraphPad Prism 8 was used to analyze the monthly monitoring data (Cass, 2000). One-way analysis of variance (ANOVA) and Tukey's HSD (Honestly Significant Difference) test were applied to raw data in order to test for the significant differences ($p < 0.05$) between compartments. Densities of different taxa were compared, and Pearson's correlation coefficient (r) was calculated to illustrate relationships between biotic and abiotic variables, providing a clear visualization of interdependencies. Primer v.5 software was employed to perform non-metric multidimensional scaling (nMDS) ordination based on square root-transformed densities of meiofaunal taxa, using Bray-Curtis similarity indices (Bray & Curtis, 1957). Additionally, the ANOSIM (Analysis of Similarities) analysis was applied to determine significant differences among compartments, followed by SIMPER (Similarity Percentage) analysis (Clarke, 1993) was conducted with the same software to assess the contribution of individual taxa to the average dissimilarity among sampling months.

RESULTS

Physico-chemical parameters

In the current study, the water temperature gradually increased from March (16.2 °C), reaching a peak in August (29.3 °C) before gradually decreasing to a minimum in February (14.3 °C). Salinity fluctuated monthly, ranging from 35.8 PSU in January to 38 PSU in August. Dissolved oxygen remained relatively stable throughout the year, in average 10 $mg.L^{-1}$, except in May, when it peaked at 12.46 mg. L^{-1}. pH also varied in time, with a maximum of 8.67 in May and a minimum of 8.17 in June. Finally, suspended particulate matter (SPM) ranged from a maximum of 28.2 mg. L^{-1} in May to a minimum of 19 mg. L^{-1} in September (Table 1).

Pearson's correlation analysis did not reveal any significant relationship among environmental parameters and meiofauna abundance. However, a significant positive correlation was observed between pH and copepod abundance ($r = 0.592$, $p < 0.05$), explaining 35% of the variance ($R^2 = 0.3504$). The 95% confidence interval for the correlation coefficient ranged from 0.02733 to 0.8702, indicating moderate to strong correlations among variables.

Table1. Monthly variation of physicochemical parameters. SPM: suspended particulate matter

Month	Temperature (°C)	Salinity (PSU)	Dissolved oxygen (mg. L^{-1})	pH	SPM (mg. L^{-1})
March	16.2	37.7	9.85	8.25	18.9
April	21.4	36	10.23	8.49	32.5
May	26.6	37.2	12.46	8.67	28.2
June	27.6	37.7	10.2	8.17	22.78
July	29.3	38	9.6	8.36	21.79
August	26.3	37.33	10.05	8.38	19
September	23.1	37.7	9.51	8.24	26.5
October	21.6	36.8	10.05	8.35	27.8
November	18.2	36.6	10.01	8.24	29.7
December	15.2	35.8	9.95	8.31	27.3
January	14.3	36.1	10.1	8.24	24.27
February	15.4	36.9	10.4	8.26	23

Meiofaunal abundance

Nematodes

The nematode abundance fluctuated significantly over the monitoring period, peaking in June (414.66 ± 86.18 ind. per $10cm^2$) and dropping sharply in July (85.33 ± 8.73 ind. per $10cm^2$). One-way ANOVA confirmed significant variations among sampling months (Levene's test: F = 22.62, p = 0.05 and Tukey-HSD post-hoc tests, $p < 0.05$). The most notable differences were observed between March *vs.* April, May *vs.* June, June *vs.* July, and December *vs.* January (Figure 2).

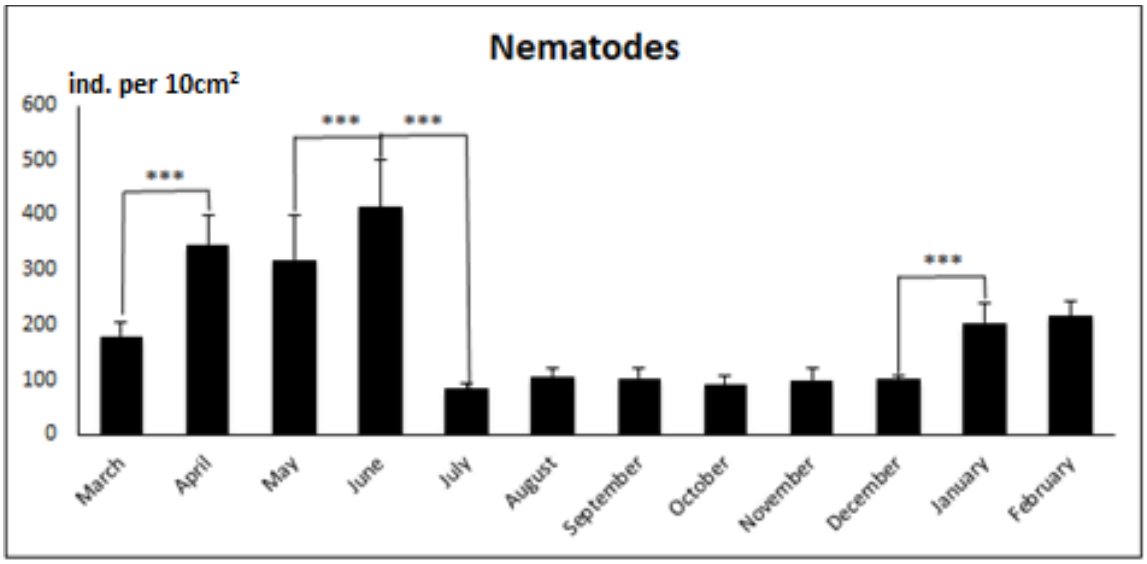

Figure 2. Monthly distribution of nematode density. Significant differences ($p < 0.05$) according to Tukey's HSD test are indicated by *** = $p < 0.001$.

Copepods

The copepods exhibited marked seasonal dynamics, reaching maximum abundance in April (325 ± 47.31 ind. per 10cm²) and minimum in December (82 ± 16.52 ind. per 10cm²). One-way ANOVA revealed significant differences among sampling months (Levene's test: F = 14.082, p = 0.05). Significant variations were noted between March *vs.* April, April *vs.* May, May *vs.* June, and June *vs.* July (Tukey-HSD post-hoc tests, $p < 0.05$, see Figure 3).

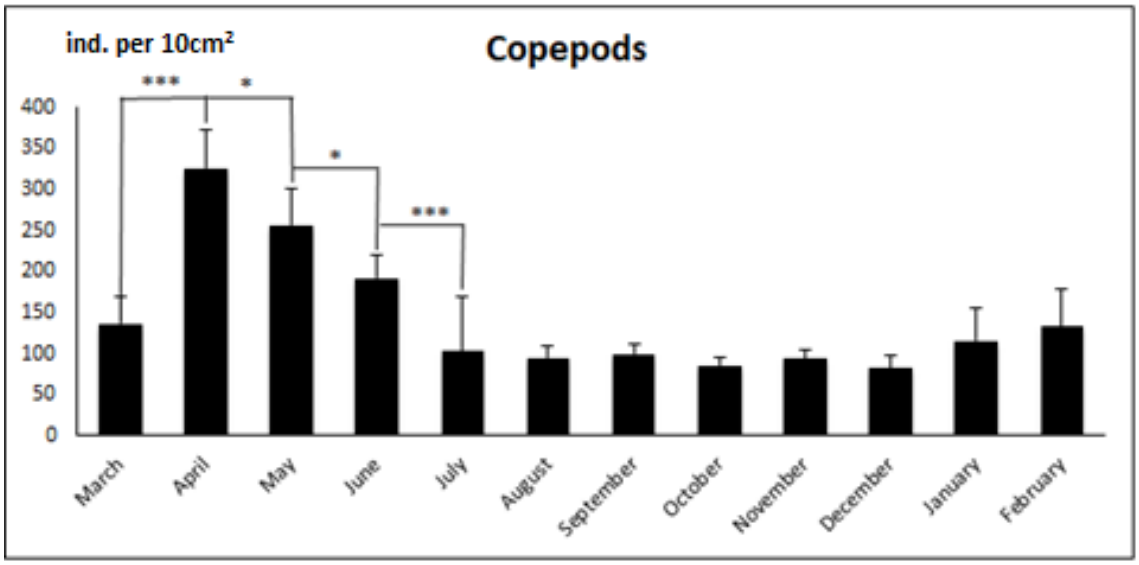

Figure 3. Monthly distribution of copepods density. Significant differences ($p < 0.05$) according to Tukey's HSD test are indicated by * = $p < 0.05$; *** = $p < 0.001$.

Polychaetes

The polychaetes reached maximum abundance in January (57.66 ± 3.06 ind. per 10cm2) and minimum during the summer (12.66 ± 2.08 ind. per 10cm²). One-way ANOVA (Levene's test: F = 8.71, p = 0.05) confirmed significant monthly variations, with a single notable difference observed between June *vs*. July, according to the Tukey-HSD test ($p < 0.05$) (Figure 4).

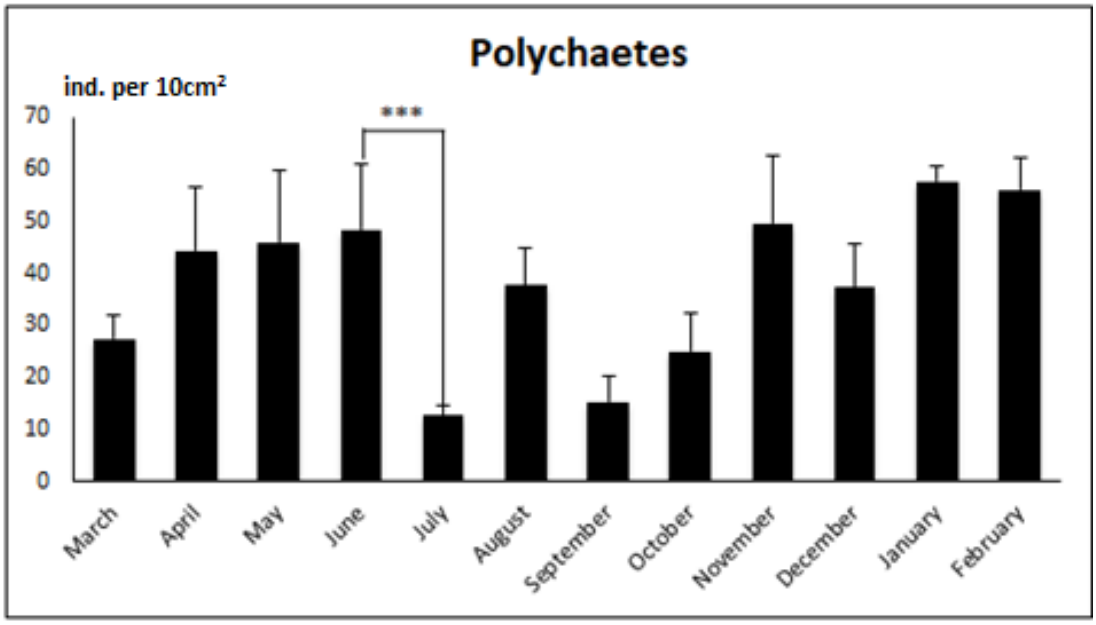

Figure 4. Monthly distribution of polychaetes density. Significant differences ($p < 0.05$) according to Tukey's HSD test are indicated by *** = $p < 0.001$.

Oligochaetes

The oligochaete abundance varied significantly over a full year, reaching a peak in April (13.66 ± 6.11 ind. per 10cm²) and minimum values in September, October, and December (2.66 ± 1.52 to 2.66 ± 0.57 ind. per 10cm², respectively). One-way ANOVA test identified significant differences (Levene's test: $F = 4.06$, $p = 0.05$) over the sampling period, with significant differences between March *vs.* April, as indicated by the Tukey-HSD test ($p < 0.05$) (Figure 5).

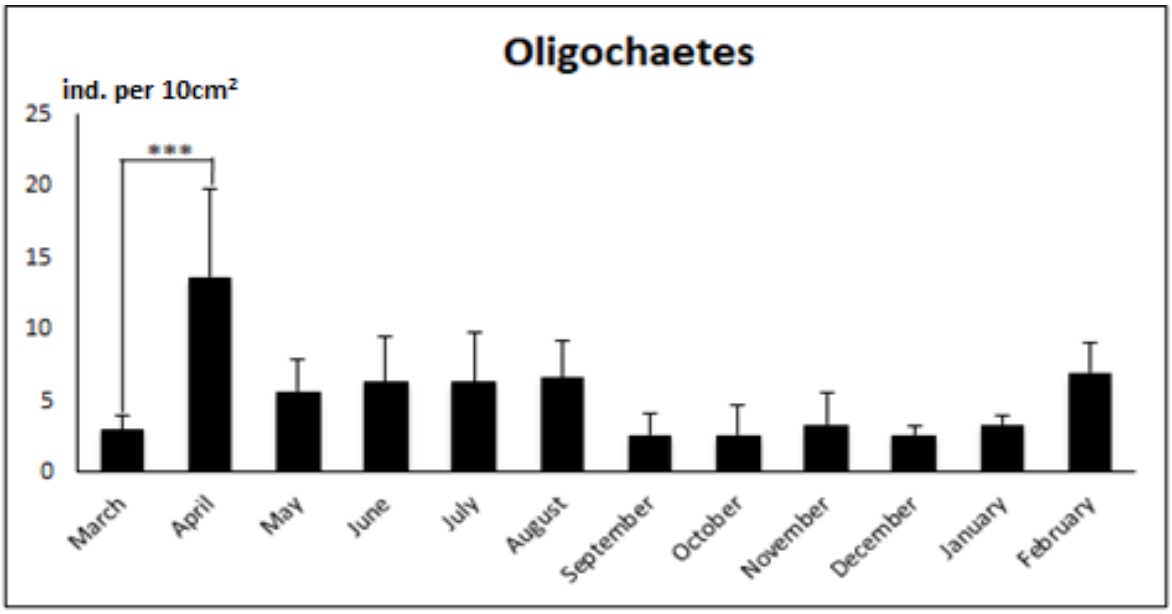

Figure 5. Monthly distribution of oligochaetes density. Significant differences ($p < 0.05$) according to Tukey's HSD test are indicated by *** = $p < 0.001$.

Crustacean Larvae

The larvae of crustaceans displayed seasonal preference for the winter season, with a peak in density in February (43.66 ± 5.03 ind. per 10cm^2) and minimum values recorded in September (10.66 ± 2.08 ind. per 10cm^2). One-way ANOVA indicated significant differences (Levene's test: $F = 11.94$, $p = 0.05$), supported by the Tukey-HSD post-hoc test ($p < 0.05$). The most significant differences were observed between March *vs*. April, June *vs.* July, and December *vs*. January (Figure 6).

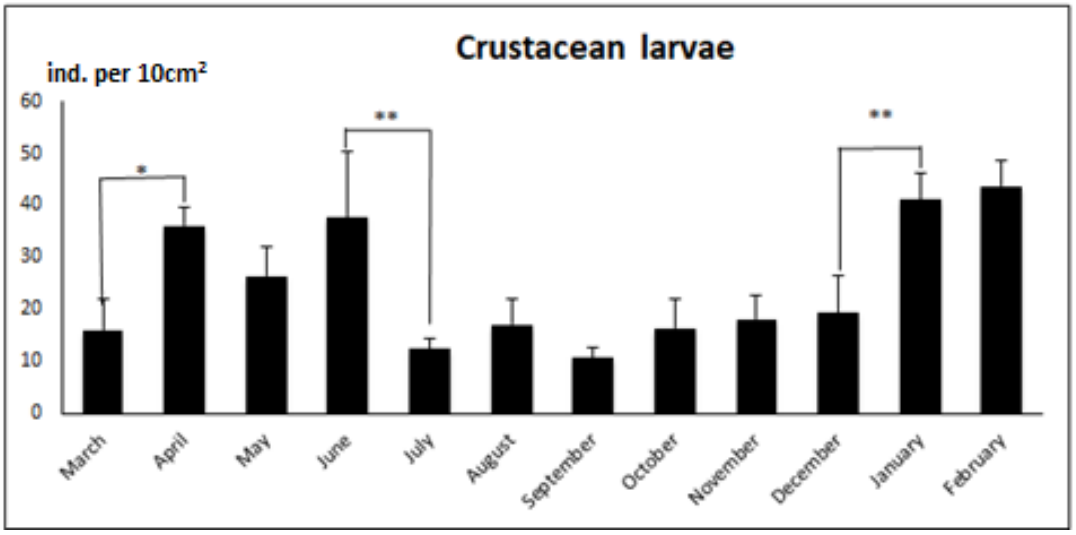

Figure 6. Monthly distribution of crustacean larvae density. Significant differences ($p < 0.05$) according to Tukey's HSD test are indicated by * = $p < 0.05$; ** = $p < 0.01$.

Multivariate Analysis

ANOSIM analysis revealed significant differences within meiofauna communities in time (global $R = 0.745$, $p = 0.001$), indicating important seasonal variations in density. High R values between distant months, such as March *vs*. June (i.e. $R = 0.926$), reflected the impact of seasonal variations on the community structure. However, closely spaced periods, such as April *vs*. May (i.e. $R = 0.037$), exhibited less marked differences, suggesting similar environmental conditions with low impact on the meiofauna assemblages. The nMDS ordination results highlighted an important effect of season variation on meiofauna distribution, with a stress value of 0.07, which indicates good representation quality (Figure 7). Samples from spring months (i.e. April to June) clustered on the left side of the graph, reflecting relatively homogeneous meiofaunal composition during this period. In contrast, summer, autumn, and winter months (i.e. June to December) were scattered towards the right side of the ordination panel, indicating greater heterogeneity, which was likely driven by increased environmental variability. Finally, the samples from January, February, and March were mostly clustered in the center on the graph, suggesting relatively homogeneous meiofauna communities in these months (Figure 6).

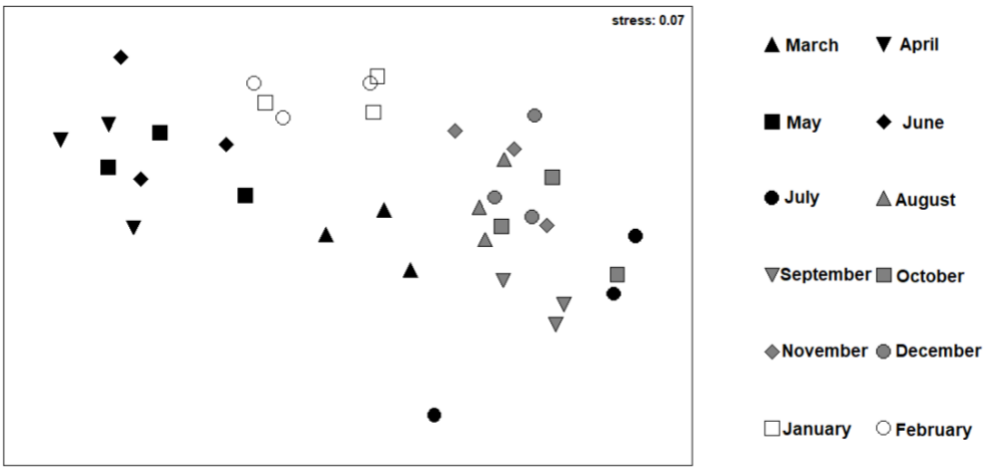

Figure 7. Non-metric multidimensional scaling (nMDS) 2D plot based on Monthly Distribution of meiofauna density

DISCUSSION

The current study was, to the best of our knowledge, the first to explore seasonal changes in meiofaunal communities associated with *Cystoseira* sp. macroalgae on rocky substrates in Tunisia. Using a combined approach of statistical analyses, physicochemical measurements, and multidimensional ordination, this research highlighted the temporal dynamics of these meiofaunal communities. Previous studies examining the physicochemical parameters of water and sediments in the Rimel area revealed that while certain regions exhibited relatively high concentrations of toxic metals, the overall environmental conditions remained favorable, supporting diverse marine communities and high biodiversity (Boufahja et al., 2010 ; Martins et al., 2015 ; Abidli et al., 2019).

The physicochemical parameters showed pronounced seasonal variations, which likely influenced the distribution of meiofaunal communities. Water temperature increased from March (16.2 °C) to a peak in August (29.3 °C) before declining in December (15.2 °C). In this context, nematode density peaked in June (414.66 ± 86.18 ind. per $10cm^2$) during a period of high temperatures, followed by a sharp decline in July (85.33 ± 8.73 ind. per $10cm^2$). This pattern suggests increased sensitivity to summer conditions and aligns with previous findings by Ape et al. (2018b), who reported that higher temperatures were associated with lower meiofaunal densities in intertidal zones.

pH levels ranged from 8.17 to 8.67, while suspended particulate matter fluctuated between 18.9 $mg.L^{-1}$ and 32.5 $mg.L^{-1}$. These environmental parameters likely influenced copepod density, which reached its highest density (325 ± 47.31 ind. per $10cm^2$) during periods of elevated pH and suspended matter levels. A significant positive correlation between pH and copepod density ($r = 0.592$, $p = 0.0426$) suggests that these microcrustaceans thrive in slightly alkaline conditions. This result partially contrasts with the findings of Lee et al. (2017), who demonstrated that a decrease in pH negatively affects the density and species richness of meiofaunal communities. The results of this study indicate that the effects of pH may vary depending on specific thresholds, taxa of interest, and interactions with other abiotic factors. Our findings highlight a distinct response of

copepods to pH variations, suggesting both adaptability and potential benefits in alkaline conditions.

The density of oligochaetes and polychaetes remained relatively low throughout the year, with modest peaks in April and January, respectively. These fluctuations may be attributed to variations in trophic resource availability or changes in salinity (Amei et al., 2021; Sowa & Krodkiewska, 2020; Warwick & Clarke, 1994; Bagheri & McLusky, 1982). Crustacean larvae displayed a strong preference for winter conditions, peaking in February (43.66 ± 5.03 ind. per $10cm^2$). This period was characterized by low temperatures (14.3 °C) and stable dissolved oxygen concentrations, averaging 10 $mg.L^{-1}$. These findings align with previous observations by Cronin et al. (2017), who reported that seasonal occurrences of planktonic larvae from benthic taxa were closely correlated with winter seabed and surface water temperatures. This synchronization suggests an adaptive response of larvae to seasonal environmental variations, enhancing their survival and development in stable, cold environments.

The ANOSIM analysis revealed significant differences between sampling months (global $R = 0.745$, $p = 0.001$), particularly between March and June ($R = 0.926$). These findings are further supported by the nMDS ordination (stress = 0.07), which shows that spring months (April to June) clustered together due to homogeneous conditions, whereas summer and autumn samples were more dispersed, reflecting increased environmental heterogeneity. These observations are supported by studies suggesting that spring months provide more homogeneous environmental conditions, leading to higher meiofaunal abundance. In contrast, summer and autumn months exhibit greater environmental heterogeneity, influenced by factors such as organic matter, salinity, pollution, and temperature, which drive variations in meiofaunal diversity and community structure (Stein & Kreft, 2015; Stark et al., 2020; Ghosh & Mandal, 2021).

These observations indicate, first, the good condition of the *Cystoseira* sp. cover, whose decline has been associated with a significant reduction in meiofaunal biodiversity (Bianchelli & Danovaro, 2020). Second, the findings further support the notion that the impact of environmental parameters on meiofauna is complex and taxon-specific, as evidenced by previous studies (França et al., 2024; Baldrighi et al., 2019; Kim et al., 2019). This highlights the necessity of a nuanced approach to accurately assess meiofaunal community dynamics and their responses to environmental fluctuations. Additionally, factors such as organic matter availability and trophic interactions may also play important roles in shaping meiofaunal distribution, although they were not explicitly examined in this study. These results underscore the importance of an integrative approach, combining statistical and multivariate analyses, to better understand the complex interactions driving seasonal variations in meiofaunal density and community structure. Future research should further investigate these mechanisms, particularly the effects of organic matter quality and trophic interactions on meiofaunal dynamics.

CONCLUSIONS

The current study explored the seasonal variations of meiofauna communities dwelling on rocky substrates in Tunisia and revealed marked temporal structuring, dictated by key abiotic factors, such as temperature, pH, dissolved oxygen and suspended matter. The results showed that

nematodes and copepods, the dominant meiofauna groups, were extremely variable in density over a year. The nematodes reached maximum in density in June, followed by significant drop in July, reflecting potential sensitivity to high summer temperatures. The copepods, in turn, showed positive correlations with pH, reaching maximum density during times of slightly alkaline conditions, which contrasts with generally reported trends in literature. Multivariate analysis also highlighted significant distinctions in variation among sampling months, as well as the importance of seasonal factors in structuring meiofauna communities.

ACKNOWLEDGMENTS

This study was supported by the European Union's EASME (Executive Agency for Small and Medium Enterprise) and EMFF (European Maritime and Fisheries fund) as part of the project AFRIMED, "Algal Forest Restoration in the Mediterranean Sea" (under grant agreement no. 789059), http://afrimed-project.eu/. This study was also supported by a funding of the University of Carthage, Faculty of Science of Bizerte.

Data availability: Data supporting the findings of this study are available from the corresponding author upon request.

Conflicts of Interest: The authors declare no conflict of interest.

REFERENCES

Abidli S., Lahbib Y., Menif T. (2019). Microplastics in commercial molluscs from the lagoon of Bizerte (Northern Tunisia). *Marine Pollution Bulletin, 142*, 243-252. https://doi.org/10.1016/J.MARPOLBUL.2019.03.048

Amei K., Dobashi R., Jimi N., Kitamura M., Yamaguchi A. (2021). Vertical changes in abundance, biomass, and community structure of pelagic polychaetes down to 1000 m depths at Station K2 in the western subarctic Pacific Ocean covering the four seasons and day–night. *Journal of Plankton Research*, 43, 442-457. https://doi.org/10.1093/plankt/fbab031

Ape F., Gristina M., Chemello R., Sarà G., Mirto S. (2020). Meiofaunal community along vermetid reefs: The role of macroalgae in influencing distribution. *Coral Reefs*, 37, 875–889.

Ape F., Gristina M., Chemello R., Sarà G., Mirto S. (2018a). Meiofauna associated with vermetid reefs: the role of macroalgae in increasing habitat size and complexity. *Coral Reefs*, 37, 875-889. https://doi.org/10.1007/s00338-018-1714-x

Ape F., Sarà G., Airoldi L., Mancuso F., Mirto S. (2018b). Influence of environmental factors and biogenic habitats on intertidal meiofauna. *Hydrobiologia*, 807, 349-366. https://doi.org/10.1007/s10750-017-3410-1

Bagheri E., Mclusky D. (1982). Population dynamics of oligochaetes and small polychaetes in the polluted Forth Estuary ecosystem. Netherlands Journal of Sea Research, 16, 55-66. https://doi.org/10.1016/0077-7579(82)90017-5

Baldrighi, E., Semprucci, F., Franzo, A., Cvitković, I., Bogner, D., Despalatović, M., Berto, D., Formalewicz, M., Scarpato, A., Frapiccini, E., Marini, M., Grego, M. (2019). Meiofaunal communities in four Adriatic ports: Baseline data for risk assessment in ballast water

management.. *Marine pollution bulletin*, 171-184. https://doi.org/10.1016/j.marpolbul.2018.06.056.

Beckley L. E. (1982). Studies on the littoral seaweed epifauna of St. Croix Island. III. Gelidium pristoides (Rhodophyta) and its epifauna. *South African Journal of Zoology*, 17, 3–10.

Beckley L. E., McLachlan A. (1979). Studies on the littoral seaweed epifauna of St. Croix Island. I. Physical and biological features of the littoral zone. *South African Journal of Zoology*, 14, 175–182.

Bellissimo G., Rull Lluch J., Tomasello A., Calvo S. (2014). The community of Cystoseira brachycarpa J. Agardh emend. Giaccone (Fucales, Phaeophyceae) in a shallow hydrothermal vent area of the Aeolian Islands (Tyrrhenian Sea, Italy). *Plant Biosystems-An International* Journal Dealing with all Aspects of Plant Biology, 148, 21-26.

Bianchelli S., Danovaro R. (2020). Impairment of microbial and meiofaunal ecosystem functions linked to algal forest loss. *Scientific Reports*, 10. https://doi.org/10.1038/s41598-020-76817-5

Boufahja F., Hedfi A., Amorri J., Aïssa P., Beyrem H., Mahmoudi E. (2010). Évaluation des réponses trophiques des nématodes libres de la baie de Bizerte (Tunisie) au stress pétrolier. *Bulletin de l'Institut Scientifique, Rabat, section Sciences de la Vie*, 32, 55-64.

Boufahja F., Hedfi A., Essid N., Aïssa P., Mahmoudi E., Beyrem H. (2012). An observational study on changes in biometry and generation time of Odontophora villoti (Nematoda, Axonolaimidae) related to petroleum pollution in Bizerte Bay, Tunisia. *Environmental Science and Pollution Research*, 19, 646-655. https://doi.org/10.1007/s11356-011-0609-y

Bray J. R., Curtis J. T. (1957). An ordination of the upland forest communities of southern Wisconsin. *Ecological Monographs*, 27, 325–349.

Cass T. (2000). Easy data analysis. Science, 289, 1158 - 1158. https://doi.org/10.1126/SCIENCE.289.5482.1158A

Carriço R., Zeppilli D., Quillien N., Grall J. (2013). Can meiofauna be a good biological indicator of the impacts of eutrophication caused by green macroalgal blooms? *Anaod-Les Cahiers Naturalistes de l'Observatoire Marin*, 2, 9–16.

Chapman P., Farrell M., Brinkhurst R. (1982). Relative tolerances of selected aquatic oligochaetes to individual pollutants and environmental factors. *Aquatic Toxicology*, 2, 47-67. https://doi.org/10.1016/0166-445X(82)90005-4

Clarke K. R. (1993). Non-parametric multivariate analyses of changes in community structure. *Australian Journal of Ecology*, 18, 117–143.

Clarke K. R., Gorley R. N. (2001). PRIMER V5: User Manual/Tutorial. PRIMER-E, Plymouth, UK, p. 91.

Coull B. C., Creed E. L., Eskin R. A., Montagna P. A., Palmer M. A., Wells J. B. J. (1983). Phytal meiofauna from the rocky intertidal at Murrells Inlet, South Carolina. *Transactions of the American Microscopical Society*, 102, 380–389.

Cronin T., Bok M., Lin C. (2017). Crustacean larvae—vision in the plankton. *Integrative and Comparative Biology*, 57*(5), 1139*-1150. https://doi.org/10.1093/icb/icx007

Danovaro R., Fraschetti S. (2002). Meiofaunal vertical zonation on hard-bottoms: Comparison with soft-bottom meiofauna. *Marine Ecology Progress Series*, 230, 159–169.

Danovaro R., Gambi C., Manini E., Fabiano M. (2000). Meiofauna response to a dynamic river plume front. *Marine Biology*, 137, 359–370.

Elarbaoui S., Richard M., Boufahja F., Mahmoudi E., Thomas-Guyonc H. (2015). Effect of crude oil exposure and dispersant application on meiofauna: *An intertidal mesocosm experiment. Environmental Science: Processes & Impacts*, 17, 997–1004.

França, D., Ingels, J., Stark, J., Da Silva, R., De França, F., Santos, G. (2024). Impact of Different Sources of Anthropogenic Pollution on the Structure and Distribution of Antarctic Marine Meiofauna Communities. *Diversity*, 16(8), 464. https://doi.org/10.3390/d16080464.

Ghosh, M., Mandal, S. (2021). Disentangling the Effect of Seasonal Dynamics on Meiobenthic Community Structure From River Matla of Sundarbans Estuarine System, India. *Frontiers in Marine Science* , 8. https://doi.org/10.3389/fmars.2021.671372.

Hussain M., Laabir M., Yahia M. (2020). A novel index based on planktonic copepod reproductive traits as a tool for marine ecotoxicology studies. *The Science of the Total Environment*, 727, 138621. https://doi.org/10.1016/j.scitotenv.2020.138621

Hutchings P. (1998). Biodiversity and functioning of polychaetes in benthic sediments. *Biodiversity & Conservation*, 7, 1133-1145. https://doi.org/10.1023/A:1008871430178

Kim, H., Song, S., Bae, H., Noh, J., Lee, C., Kwon, B., Lee, J., Ryu, J., Khim, J. (2019). Natural and anthropogenic impacts on long-term meiobenthic communities in two contrasting nearshore habitats. *Environment international*, 134, 105200 . https://doi.org/10.1016/j.envint.2019.105200.

Lee M., Torres R., Manríquez P. (2017). The combined effects of ocean warming and acidification on shallow-water meiofaunal assemblages. *Marine Environmental Research*, 131, 1-9. https://doi.org/10.1016/j.marenvres.2017.09.002

Mandario M., Alava V., Añasco N. (2019). Evaluation of the bioremediation potential of mud polychaete *Marphysa* sp. in aquaculture pond sediments. *Environmental Science and Pollution Research*, *26*, 29810-29821. https://doi.org/10.1007/s11356-019-06092-z

Martins M., Zaaboub N., Aleya L., Frontalini F., Pereira E., Miranda P., Mane M., Rocha F., Laut L., Bour E. (2015). Environmental quality assessment of Bizerte Lagoon (Tunisia) using living foraminifera assemblages and a multiproxy approach. *PLoS ONE*, *10*. https://doi.org/10.1371/journal.pone.0137250

Sales M., Ballesteros E. (2012). Seasonal dynamics and annual production of *Cystoseira crinita* (Fucales: Ochrophyta)-dominated assemblages from the northwestern Mediterranean. *Scientia Marina*, *76*, 391-401. https://doi.org/10.3989/SCIMAR.03465.16D

Santos A., Choueri R., De Figueiredo Eufrasio Pauly G., Abessa D., Gallucci F. (2018). Is the microcosm approach using meiofauna community descriptors a suitable tool for ecotoxicological studies? *Ecotoxicology and Environmental Safety*, *147*, 945-953. https://doi.org/10.1016/j.ecoenv.2017.09.040

Semprucci F., Balsamo M. (2012). Key role of free-living nematodes in the marine ecosystem. In: Boeri F., Jordan A.C. (Eds.), *Nematodes: Morphology*, *Functions and Management Strategies*. NOVA Science Publishers, Inc. Hauppauge, NY, 109-134.

Sowa A., Krodkiewska M. (2020). Impact of secondary salinisation on the structure and diversity of oligochaete communities. *Knowledge & Management of Aquatic Ecosystems*, *421*, 6. https://doi.org/10.1051/kmae/2019049

Stark, J., Mohammad, M., McMinn, A., Ingels, J. (2020). Diversity, Abundance, Spatial Variation, and Human Impacts in Marine Meiobenthic Nematode and Copepod Communities at Casey Station, East Antarctica. *Frontiers in Marine Science*, 7. https://doi.org/10.3389/fmars.2020.00480.

Stein, A., Kreft, H. (2015). Terminology and quantification of environmental heterogeneity in species-richness research. *Biological Reviews*, 90. https://doi.org/10.1111/brv.12135.

Warwick R., Clarke K. (1994). Relearning the ABC: taxonomic changes and abundance/biomass relationships in disturbed benthic communities. *Marine Biology*, *118*, 739-744. https://doi.org/10.1007/BF00347523

Princess Nourah Bint Abdulrahman University
College of Science
جامعة الأميرة نورة بنت عبدالرحمن
كلية العلوم

NATURAL ALLIES: LEVERAGING BIOLOGICAL SYSTEMS FOR CLIMATE CHANGE MITIGATION THROUGH CO_2 REMOVAL

Author name and information

Amr Elkelish

Botany Department, Faculty of Science, Suez Canal University, Egypt

Correspondence: Amr.elkelish@science.suez.edu.eg

Keywords

Carbon Dioxide Removal (CDR); Biological Carbon Sequestration; Photosynthesis; Carbon Capture and Storage (CCS); Bioenergy with Carbon Capture and Storage (BECCS); Algae-based CO_2 Removal

ABSTRACT

This review paper delves into the diverse biological strategies for carbon dioxide removal (BCDR), highlighting their potential to mitigate climate change effectively. Biological systems, ranging from vast forests to microscopic algae, are crucial in capturing atmospheric CO_2 and sequestering it within organic matter or through conversion into bioenergy. The paper begins by discussing the increasing urgency of addressing historical CO_2 accumulations and the complementary role of BCDR to traditional decarbonization efforts. It then explores various biological mechanisms such as photosynthesis and the Calvin-Benson-Bassham cycle, which plants, algae, and microorganisms utilize to convert CO_2 into biomass, thereby contributing to long-term carbon storage. Further sections analyze the role of innovative biological technologies, including genetically engineered microorganisms and hyperaccumulators, in enhancing carbon capture efficiency. The review also addresses the advantages and limitations of these biological strategies, comparing them with mechanical carbon capture technologies. Case studies of successful BCDR projects illustrate the practical implementation and challenges of scaling these approaches. The review concluded that, concerning future directions and policy implications, there is a crucial need for integrated strategies incorporating biological and chemo-physical techniques to mitigate climate change and achieve sustainable carbon reduction. Through a comprehensive analysis of existing and emerging BCDR techniques, this review underscores the importance of biological approaches in the global effort to combat climate change, offering insights into their potential scalability, economic feasibility, and ecological impact. The key finding of the review is that integrating biological carbon dioxide removal (BCDR) strategies with chemo-physical techniques offers a scalable, cost-effective, and sustainable approach to mitigating climate change.

INTRODUCTION

This review aims to evaluate effective biological strategies for carbon dioxide removal (BCDR) and assess their potential capabilities to mitigate carbon dioxide emissions compared with chemical ones, which will mitigate climate change. One effective option to achieve BCDR is through sustainable land use anchored in the United Nations' Agenda 2030, contributing to global food

security, biodiversity protection, climate adaptation, resilience, and mitigation. An extensive biological system, e.g., a forest or an agroforestry system, accumulates more carbon than it annually releases to the atmosphere in carbon dioxide, and it is regularly removed from the system as a raw material or as biomass for energy (National Academies of Sciences 2018). Regrowing biological systems can reduce carbon emissions through biological carbon storage, where chronologically old carbon is injected deep underground in the form of bioenergy with carbon capture and storage (BECCS), also known as bio-CCS. Negative emissions are required because achieving zero emissions does not address the historical carbon dioxide accumulations (Udawatta et al., 2022). The principles of this approach are covered through the expression carbon negative by design as per the circular economy philosophy. Active and passive bioenergy carbon dioxide removal approaches could offer a more flexible, less risky, diverse, and sustainable portfolio to combat climate change (Palmer & Carton, 2021).

The Role of Carbon Dioxide in Climate Change

Climate change has attained critical urgency in the twenty-first century mainly due to increased carbon dioxide (CO_2) emissions, one of the most important greenhouse gases emitted faster than it is removed. Earlier records suggest that atmospheric CO_2 globally averaged about 200 ppm, and the current concentration of CO_2 has exceeded 400 ppm (Nunes, 2023). According to different research organizations, CO_2 is an ideal conserved greenhouse gas as it contributes to around 55% of global warming effects. Though many attempts are being made to slow the increase of carbon dioxide by controlling its release rate, either by extracting naturally or through human influence, little success has been achieved concerning carbon sequestration or elimination. Practical and effective techniques for CO_2 removal are required to protect the climate system (Fawzy et al., 2020). Significant CO_2 emissions occur from fossil fuel burning in power plant industries and bioenergy systems. CO_2 is also emitted from fossil-related events such as agriculture and deforestation. Various countries and regions have agreed to work together to mitigate average temperature levels in response to these issues. Carbon capture and utilization (CCU) and carbon capture and storage (CCS) are widely received for removing or avoiding CO_2 emissions from significant sources of more than 50,000 tons per year, including power plants, industries, and bioenergy systems (Perera, 2018). Historically, geological storage and mineralization have been widely accepted as physical storage technologies to store CO_2 away from the atmosphere for an extended period. However, these approaches have to overcome mechanical issues and depend upon geological availability in the region, as well as the security of the physical store. Biological systems, including trees, plants, and other ecosystems, use photosynthesis to consume CO_2 and produce oxygen, which is also considered an effective mechanism for removing CO_2 from the atmosphere (Omotoso & Omotayo, 2023). Global efforts to mitigate climate change have been shaped by international agreements such as the United Nations Framework Convention on Combating Climate Change (UNFCCC) and the Paris Agreement. These frameworks establish guidelines for reducing greenhouse gas emissions and emphasize the critical role of carbon capture technologies, including biological carbon dioxide removal (BCDR). The Paris Agreement, in particular, sets ambitious targets for limiting the rise of global temperature and encourages the integration of sustainable carbon sequestration methods. By aligning with these international policies, BCDR

strategies can contribute to achieving net-zero emissions while ensuring ecological and economic viability.

Biological Carbon Dioxide Removal Mechanisms

This review will elucidate various mechanisms for biological carbon removal. Diatoms use a unique biological pathway to remove carbon dioxide from the environment, which is also being investigated in research for commercial carbon capture (Sethi et al., 2020). Diatoms, among other biological cellular processes, can remove bioinspired artificial carbon. Thus, exploring and understanding the biological strategies used by diatoms will help further enhance the currently studied carbon dioxide removal techniques. Plants, algae, and cyanobacteria use the Calvin-Benson-Bassham cycle to convert CO_2 and water into glucose (Santos Correa et al., 2022), which are the necessary and valuable building blocks to maximize their energy for growth. The carbon-containing compounds should remain in the plant for effective carbon dioxide removal. In natural systems, algae and plants convert excess sugars to starch, cellulose, or lipids (Daneshvar et al., 2022). Photosynthesis allows converting CO_2 from the atmosphere into new organic matter. It acts as an ocean sink where marine photosynthesis maintains the delicate balance between marine and atmospheric CO_2, lowering the CO_2 concentration in the surrounding water and enhancing the absorption of CO_2 from the atmosphere (Cooley et al., 2023)). Moreover, phytoplankton convert CO_2 to glucose via oxygenic photosynthesis to perform internal processes such as photorespiration, respiration, and various metabolic pathways to sustain life (Elkelish & Abu-Elsaoud, 2024). Removing CO_2 in biological metabolic processes is fundamental to building and maintaining physical structure and reproduction (Yu King Hing et al., 2021).

Photosynthesis and Carbon Sequestration

Photosynthesis is a fundamental biological process that converts light using carbon resources into organic materials in various living systems. The significance of photosynthesis to humanity, however, not only lies in providing food and oxygen for survival and energy for biotic activities but also in the potential of photosynthesis to capture and store CO_2 from the atmosphere, i.e., carbon sequestration (Johnson, 2016). The carbon emitted into the atmosphere, whether of natural or anthropogenic origin, occurs simultaneously, and biochemical activities determine its quantity. However, as a non-conservative element in the atmosphere, CO_2 emission has established global concern for its effects on ecological health, adverse climate conditions, and human survival. With the carbon concentration in the atmosphere continually rising, the effectiveness of photosynthesis in the original CO_2 removal process also becomes a research hotspot with increasing concerns for understanding the biological mechanisms that effectively enhance carbon sequestration (Janssen et al., 2014).

To resolve this problem, fundamental questions must be addressed: how CO_2 is absorbed during biological activities, and how do natural elements continually remove CO_2 from the atmosphere while feeding the Earth's biosphere? (Cooley et al., 2023) Estimating the CO_2 absorption capability and efficiency of the Earth's biosphere thus provides the research of biospheric CO_2 sequestration. Reducing this problem to the simple vision of a carbon reservoir system and an atmospheric

carbon reservoir, the capacity of plant photosynthesis to photosynthetically fix CO_2 would play a role as a much more stocked carbon quantification destination, as one of the most straightforward carbon reservoir units estimated (Wang et al., 2021). That surprising fact also poses another question: how much CO_2 are these reservoir systems expected to absorb or fix during capture?

Algae and Microorganisms as Carbon Dioxide Absorbers

Exploring algae for carbon dioxide removal is an innovative approach aiming to develop a constant supply of feedstock that can be used as biofuels or in industrial feedstock, which is in huge demand. Microorganisms, including algae, photosynthetic bacteria, and cyanobacteria (blue-green algae), can convert solar energy and carbon dioxide into algal biomass and oxygen through photosynthesis. One ton of algae can produce 1.83 tons of oxygen. In addition, a portion of the absorbed carbon is stored inside the algal biomass. Microbial biomass can store about 40% to 50% of the carbon fixed daily. Therefore, both algal and cyanobacterial biomass can be seen as an effective source for carbon dioxide removal by dissociating oxygen and algal biomass. This enables the natural degradation of the biomass into a microbial cell (Ezhumalai et al., 2024).

Cyanobacteria are one of the most significant contributors to carbon dioxide removal from the atmosphere. Cyanobacteria have various forms, are ecologically and biotechnologically significant, and are grouped into three major kinds and biotypes: gas vesicle-associated, heterocystous, and non-heterocystous. Anabaena, Nostoc, Aphanizomenon, and Cylindrospermum are heterocystous species used in agriculture and are essential in soil fertility replenishment through biological nitrogen fixation. The non-heterocystous forms of spirulina have significantly contributed to the food sector to support the supply of natural colorants, vitamins, and minerals. Unicellular and multicellular species such as Chlorella, Spirulina, Euglena, and Ulothrix are only a few examples of photosynthetic microorganisms, mainly algae and adhered microorganisms (Agarwal et al., 2022; Kumar et al., 2010).

Biological Carbon Capture Technologies

Biological processes can be harnessed for carbon dioxide removal, encompassing various species. For example, trees are well-known for facilitating carbon sequestration, a phenomenon that reduces the concentration of carbon dioxide in the atmosphere (Murphy, 2024). Over the years, however, researchers and entrepreneurs have investigated or developed other applications leveraging these biological processes to capture carbon. This can be illustrated with various approaches, such as manipulation, genetic engineering, or the discovery of new enzymes to enhance the capacity of those species that naturally capture carbon (Rodrigues et al., 2023).

One of the earliest and frequently heard-about carbon-capturing entities is single-celled microalgae. These organisms contain specialized genes and biochemical pathways capable of sequestering and storing large amounts of carbon through photosynthesis (Barati et al., 2022). Though sometimes overlooked, certain microalgae species require large amounts of carbon-rich carbon, to which carbon dioxide contributes, to facilitate exponential growth. While microalgae manifest great promise, there are some challenges associated with their use, such as low growth rate and possibly high energy costs for cultivation (Politaeva et al., 2023). Consequently, another popular application has used a similar carbon sequestration pathway in bacteria. Combining

synthetic biology, computational applications, and high-throughput experimentation with biotechnology industry pioneers such as Amyris enabled bacteria to compete as carbon-capturing candidates by providing them with the right carbon-sequestering genes and biochemical pathways (Wongsodiharjo & Masjud, 2024). The advantages of utilizing bacteria and microalgae include, for example, reduced energy requirements for growth and bioconversion. Carbon-capturing microorganisms also have high biological potential as they can prevent environmental degradation while promoting soil fertility. A substantial challenge lies in the development of efficient and robust microbial strains (Li et al., 2023).

Trees and hyperaccumulators naturally remove carbon dioxide from the soil. Hyperaccumulators have high biological potential for soil sequestration and are also used as an effective way to remove heavy metals from the soil (Skuza et al., 2022). For instance, studies suggest that *Vetiveria zizanoides* grown in the land of the breaker of the pharmaceuticals industry are a strong type of phytoextraction plant and are the most efficient accumulator of light and heavy trace metals of all species studied (Rascio & Navari-Izzo, 2011). Selection of tree species may contribute to sequestering carbon beyond that sequestered in wood production and removal from the atmosphere (Siyar et al., 2022). For example, the soil can sequester 3.65-ton CO_2 ha^{-1} yr in poplars and 1.82-ton CO_2 ha−1 yr in intercropped agricultural olive trees. Furthermore, the present review details the currently available biological carbon capture approaches, recent advances, associated challenges, and policy implications (Asare et al., 2023).

Advantages and Limitations of Biological Strategies

Biological strategies are naturally scalable and tunable to reduce CO_2 to a consumable product with minimal waste. The environmental benefits derived from using photosystems are straightforward in reducing anthropogenic carbon dioxide atmospherically, economically, and in terms of existing infrastructure (Turek et al., 2021). The photosynthetic nature tends to grow and repeat existing non-propagative photosystems, facilitating large-scale carbon fixation of small-unit cost. Both land and retort (i.e., without arable land) systems can be used with more than one optimal gas purification strategy, i.e., either 'in liquid' or the form of 'response products.' However, biological systems can be susceptible to location, land, soil type, nutrients, and even climatic conditions. This review evaluates the advantages and limitations of biological implementation for CO_2 capture (Chiellini & Galli, 2002).

Carbon utilization is, therefore, the most attractive, whether by synthetic catalysts or biological techniques. The rate of inorganic carbon sequestration may be limited by the water solubility of irradiated carbon (I) oxides (CO and CO_2) and their protic gas luminescence, which could potentially be harmful to the active sites of enzymes (Lin et al., 2022). Ozonation eliminates volatile organic compounds (VOC) formation during the synthesis of syngas, which is used to produce lower MW alcohol and formalin and as a reaction intermediate for trioxane and other oxygenated products (Shukla et al., 2019). Though chemical strategies for carbon dioxide capture are generally preferred to bioreaction, social, environmental, and economic pressures for further sustainability and new chemical products are driving research in cheap, selective, and biofactor reallocation. Further spontaneous carbon-squandering reactions catalyze several enzymes discussed in the next

section to provide the foundation for this evaluation. The best metabolic habits to improve design are complex metabolic networks/plants adapted to carbon dioxide fixation, sugars, alcohols, and other complex substances in various chemical production scenarios, thereby exploiting C1, C_2, or C_3 assimilation that has already been metabolized twice.

Comparison with Mechanical Carbon Capture Technologies

Here, we analyzed some biological capture and storage technologies that help reduce CO_2 levels (Hochman & Appasamy, 2024). The biological processes for scavenging atmospheric CO_2 are found to be effective in 1) removing CO_2 from fossil fuel exhaust, 2) generating O_2 for highly populated cities, 3) converting atmospheric CO_2 to useful chemicals or polymers, 4) restoring desert ecologies, increasing food crops, and/or 5) increasing the profitability and land values of waste treatment plants (Poblete et al., 2022). A variety of process biotechnologies are available for this work. Microalgal panels and photobioreactors are the most popular and have been studied for their suitability in various configurations to remove CO_2 from different emissions across a broad range of CO_2 levels (Chanquia et al., 2021). Algal processes are not yet used to treat high-temperature emissions that are near-absolutely free of contaminants. They must be filtered, sterilized, and/or integrated with additional biological and electronic processes to protect the photoreactive organisms from toxic materials and high heat (Shareefdeen et al., 2023). For example, a strain of the cyanobacteria Spirulina has demonstrated tolerance to the heat on the hot side of a TE cooler (Dębowski et al., 2021). Many photophysical technologies developed by chemical engineers and chemists could also be adapted to such systems. These chemocatalytic and nanophotonic systems are only half-commercial and are meant to prevent acid rain associated with burning coal. Consequently, they do not use CO_2 like the photo- and chemoautotrophic approaches. Thus, not only are these mechanical processes more expensive than algal processes, but they are also not as profitable.

Case Studies of Successful Biological Carbon Dioxide Removal Projects

This section aims to determine whether projects designed to capture and store CO_2 using Biological Carbon Dioxide Removal (BCDR) strategies have, at a minimum, proved that capturing and storing carbon is technically feasible. The paragraphs below explore the outcomes of real-world projects that grew biomass and used the profit to finance the recapture of the CO_2 byproduct and, in some cases, to store it or produce carbon offsets for the international market. To learn from these real-world carbon capture projects, we have drawn our data primarily from written case studies in scientific, industry, and governmental publications that provide details of the projects (Sarwer et al., 2022).

The BCDR strategies implemented in these case study projects varied in biological method (afforestation and reforestation, as well as anaerobic digestion of manure, charcoal sequestration, and carbonation of silicates/biocarbonate), size (from less than 1 hectare of growing trees to the manure from herds of more than 160,000 domesticated animals), and capture outcome (from less than 100 metric tons of CO_2 to more than 70,000 metric tons) (Ramachandran Nair et al., 2009). BCDR strategies that seek to store carbon in living organisms have limited temporal horizons, as

the carbon can be released over time in many ways (Zaks et al., 2011). Carbon stored in afforestation or reforestation campaigns can be released due to declining tree density or death, whether by natural causes, disease, or logging. Charcoal is less likely to be rapidly mineralized or decomposed, but instead, it might be used as biofuel or pyrolyzed before decomposition occurs. In the end, or even as an intermediate step, the tons of CO_2 captured in the produced carbon could eventually be re-emitted to the atmosphere (Sidi Habib et al., 2024; Žalys et al., 2023). One of the projects is the Bonn Challenge **(**afforestation/reforestation), a global effort restoring over 210 million hectares of degraded land, sequestering significant amounts of CO_2. The Biochar Initiative (charcoal sequestration) determines if applications in agriculture have resulted in long-term carbon storage with improved soil fertility. The Anaerobic Digestion Project in Denmark used processed manure from over 200,000 cattle to generate biogas while capturing CO_2 emissions, removing over 50,000 metric tons of CO_2 annually.

Future Directions and Innovation in Biological Carbon Dioxide Removal

Looking to the future, biological carbon dioxide mitigation processes and reduced dependence on carbon provide a cost-effective approach based on nature to increase the rates at which the Earth's excess carbon can be absorbed (Singh et al., 2024). Production of new systems that can reduce or be independent of water use by photorespiration is one of the significant areas of development. Using new non-rubisco strategies to provide bicarbonate for microbial substrates or storage of velvet alga products or double encapsulation as R. T. Hillman (terrestrial), C3-H: dicoma mode (black), molluscum (finger calcareous), Yuzhenka (yellow marine algae), Haliphyma with free formaldehyde production, or purple fungi Spirulina spp, *Chromocantus purpurea*, or formulations of algae with flow-based entities as active fillings such as *Microtrix rubra* algal coolers will benefit from carbon supply under anoxic conditions (Machín et al., 2023; Ray et al., 2022).

For the biotic cultivation of cassava grown under perennial conditions, new varieties and cultivation practices suitable for periodic biological cultivation are required and can be expanded or effectively grown to be grown for more abundant crops (Walker et al., 2021). Research is ongoing, but the first demonstration at a field scale is experimental. Therefore, the practical limitations of the theory behind this proposed industry have not yet been explored by any major power grid with local, regional, or panel distribution. Data enriched with unconventional methodologies and climate simulations will be used to analyze the life cycle analysis of new crops (or use combinations of elements) and networks that do not necessarily depend on the use of oceanic sources.

Policy Implications and Regulation of Biological Carbon Capture

Adopting and scaling biological carbon removal technologies introduce a suite of opportunities and challenges related to regulation and policy at local, regional, and international scales (Gupta et al., 2023). The promise of new, low-carbon bio-based materials with carbon benefits beyond only the atmosphere is likely to enhance the market value of bio-carbon and develop even more complex inter-commodity markets, potentially introducing extensive regulatory challenges beyond those outlined already. Here, we briefly explore some key implications of using biological

carbon-based materials for carbon removal in the context of EU policy and regulation. We gesture towards challenges and questions that are more relevant globally (Singh et al., 2024). These build from the current work on biotechnologies and biomaterials' regulatory challenges and opportunities and the broader integration of ecosystem services and bio-sequestration within evolving policy frameworks and financial systems approaches.

The broader challenge of incorporating these systems within larger decarbonization and ecological protection initiatives may enhance their governance costs while further diverting scarce resources from alternative technologies and innovations. Ultimately, in examining the 'improvement of nature' in an ascribed arena of 'climate governance' and against a baseline of intervention, we are concerned not just with advancing specific techniques and materials but with the nature and policing of the 'bounds' themselves (Liu et al., 2024).

Economic Considerations and Cost-Effectiveness

Potential financial aspects and impacts in developing biological strategies for CO_2 sequestration are being considered for roll-out on a larger scale. CDR costs are defined as initial research and development and demonstration costs, costs for implementing and running a technology at the deployment stage, and total economic or social costs, including incentives and subsidy requirements for a full-scale roll-out. The accuracy of these costs is difficult to verify, and direct comparisons among processes should not be regarded as irrefutable.

Biological CDR is relatively competitive compared to non-biological CDR, assuming the required benchmarked volumes of biomass production and processing per unit area are met. Several biomasses are particularly effective in terms of productivity. Our analysis indicates that two of the seven biomasses considered to be most promising show net carbon payback within less than 12 months from deployment. Thus, the sink feature must be cost-effective and show a significant positive return regarding reduced kWh costs, not as a more comprehensive network interconnection at a grid level. Companies and policymakers must avoid following purely interdisciplinary models, which could lead to the unequal sharing of co-benefits in the event of competitive constraints included in these technologies.

Environmental and Ecological Impacts of Biological Carbon Capture

To counter global warming, methods are being developed to capture CO_2 by photosynthetic organisms. These biological methods are grouped under Biological Carbon Capture and Storage. However, one could also look at the possible negative effects on the ecosystems that would carry out these biological CO_2 removal (BCD) measures. We have argued that the outcome of the BCD measures would disproportionately negatively affect ecosystems because organisms also adapt. Therefore, an adverse outcome may occur due to a significant cumulative impact from individual effects on the BCD ecosystems.

Public Perception and Acceptance of Biological Carbon Dioxide Removal Technologies

Biological CO_2 removal technologies are increasingly prominent in discussions around climate solutions. However, it is unclear how bioenergy with carbon capture and storage will integrate with anthropogenic greenhouse gas (GHG) emissions reduction measurements. Similarly, will bioenergy crops be used for CO_2 removal in a renewable economy, and is this acceptable to the public? These observations suggest that a combination of technical, ethical, and socio-cultural approaches can help articulate how potential solutions combining harmful emissions can provide sustainable and effective feedback on a regional basis regarding future scenarios and land use practices.

Acceptance of climate change mitigation infrastructure such as nuclear power, large-scale wind or solar technology, and carbon capture and storage are all limited by technology's symbolic meaning (in combination with social, economic, and material constraints). Conceptually, this understanding is built into theories of socio-technology, where even smaller-scale decisions to use environmentally sustainable energy (for home heating or variable inputs into the electricity grid) are informed by adherence to sets of values, social practices, and economic constraints. Attitude is an umbrella term that can help describe and predict behavior. It covers how much an individual knows and endorses a technology, believes that they can control it, is not concerned about risks, and finds the helpful technology. Values are also a significant predictor of environment and technology.

Challenges and Potential Solutions in Scaling Up Biological Carbon Capture

Biological strategies for carbon dioxide removal, such as the pyrolysis-bioenergy with carbon capture and storage (BECCS), have an order-of-magnitude greater effective land use than natural solutions like afforestation and reforestation. However, many challenges are associated with large-scale biological approaches, such as improving the efficiency of oil-producing algal photobioreactors, minimizing evaporative losses in large-scale phyto-desalination systems, or unintended environmental effects. To a serious scientist in 2022, efforts to scale up carbon-negative agriculture and BECCS that incorporate thousands beyond what can be explored in experiments tend to invoke combinations of derision, disbelief, and tender condescension. However, the cooking-with-gas spatial derivatives needed for scaling exist (just about!) if we can co-locate many megacities on the order of 100-km^2 semi-circular earth-buffered plots. This conceptual rebranding has implications for the evolution of land use in the Anthropocene, and the possibility of multiple pathways to "grow" carbon-negative land for various reasons - and on a scale relevant to geoengineering - is explored here. It is a common refrain that "we can, therefore, infer almost nothing about the behavior of the system" from the few studies of data-informed experimental systems in biology. Here, I track implications at each stage for the conditions to incrementally integrate systems into complex ecosystems. We are left with an order-of-magnitude disenchantment from projects that integrate with local systems. Our ability to work with regional players to incorporate a regular mega-scale BECCS (that sequesters carbon and subsidizes a homeland security nation) likely starts and ends with a top-10 rich northeastern US city basin. We

have some traction with moving large-scale quantitative work to the global grid-scale, though with complex, evolving challenges.'

Integration of Biological Carbon Capture with Other Climate Change Mitigation Strategies

Biological carbon capture, in addition to reducing CO_2 emissions, can absorb 48% of the CO_2 emissions by terrestrial, ocean, and hydrological systems. These systems contribute to CO_2 removal and the fight against global warming. Reforestation, afforestation, land restoration, conservation agriculture, and bioenergy are some of the land-based carbon sequestration strategies made by the United Nations to mitigate climate change. 2021 has defined six priority ecosystem-based initiatives in an integrated climate change solution framework to keep global warming below 1.5°C, increasing afforestation, reforestation, and agroforestry, improving forest and land management, climate change mitigation, and land-based carbon removal. Promoting the conservation and restoration of ecosystems, sustainable management of marine and terrestrial ecosystems, and investing in NBS deployment, research, and monitoring.

Research on the concepts and quantification of the synergistic impacts of combining biological removal with other explored climate change mitigation options identified synergy between plant-based carbon removal and direct air capture (DAC), bioenergy, and land use change. Research on oleaginous crops that combine biological removal with direct air carbon capture. Research by Zhao et al., (2024) shows that combining BECCS with land-based carbon sequestration would be more profitable than alone. Special emission reduction targets are needed so that non-CO2 emissions and carbon removal through biological processes are competitive. Furthermore, our aspirations to limit global warming to 1.5°C to 2°C show that negative carbon technologies (NETs) are inevitable. Evaluating the potential synergistic benefits of combining biological removal strategies with other technological processes is essential. In the future, we aim to explore further "the emergence of synergetic CO_2 reduction by combining biological strategies with other approaches in climate change mitigation with demonstrable methods."

Conclusion and Key Findings

This review has attempted to discuss the possibilities of biological carbon dioxide removal that could be quicker and cheaper than climate engineering. It has focused on increasing the efficiency of existing biological processes and allowing waste to be reused for this purpose, thus making the treatment process even more effective. Additionally, the review has attempted to explore low-cost and effective technologies that might be budding or unfamiliar worldwide.

CONCLUSION

We conclude with a concrete recommendation to expand the discussion toward defining more effective measures to safeguard contemporary ecosystems. We have identified an essential munition of tools and approaches covering various responses and needs. In all cases, the challenge now is to bring them to the desired level of tempo and size. It is also vital to admit that as such measures involve rapid and widespread action, there are no guarantees of success; this can seem somewhat daunting to our mindset. Running these activities in controlled ecosystems will allow

assessment and optimization. Aspects concerning prevention measures in living systems depend significantly on our understanding and ability to implement these globally. The appropriate infrastructure might take a few years for a global assembly.

Data availability: Data supporting the findings of this study are available from the corresponding author upon request.

Conflicts of Interest: The authors declare no conflict of interest.

REFERENCES

Alfaleh, F., Alyousif, M., & Elhaig, M. (2020). The emergence of Caryospora neofalconis in falcons in Central Saudi Arabia. *Journal of Advanced Veterinary and Animal Research*, 7(3), 530. https://doi.org/10.5455/JAVAR.2020.G450

Agarwal, P., Soni, R., Kaur, P., Madan, A., Mishra, R., Pandey, J., Singh, S., & Singh, G. (2022). Cyanobacteria as a Promising Alternative for Sustainable Environment: Synthesis of Biofuel and Biodegradable Plastics. *Frontiers in Microbiology*, *13*, 939347. https://doi.org/10.3389/fmicb.2022.939347

Asare, M. O., Száková, J., & Tlustoš, P. (2023). Mechanisms of As, Cd, Pb, and Zn hyperaccumulation by plants and their effects on soil microbiome in the rhizosphere. *Frontiers in Environmental Science*, *11*. https://doi.org/10.3389/fenvs.2023.1157415

Barati, B., Fazeli Zafar, F., Amani Babadi, A., Hao, C., Qian, L., Wang, S., & El-Fatah Abomohra, A. (2022). Microalgae as a Natural CO2 Sequester: A Study on Effect of Tobacco Smoke on Two Microalgae Biochemical Responses. *Frontiers in Energy Research*, *10*. https://doi.org/10.3389/fenrg.2022.881758

Chanquia, S. N., Vernet, G., & Kara, S. (2021). Photobioreactors for cultivation and synthesis: Specifications, challenges, and perspectives. *Engineering in Life Sciences*, *22*(12), 712–724. https://doi.org/10.1002/elsc.202100070

Chiellini, E., & Galli, G. (2002). Structural characterization and transport properties of organically modified montmorillonite/polyurethane nanocomposites. *Polymer*. https://www.academia.edu/12717668/Structural_characterization_and_transport_properties_of_organically_modified_montmorillonite_polyurethane_nanocomposites

Cooley, S. R., Klinsky, S., Morrow, D. R., & Satterfield, T. (2023). Sociotechnical Considerations About Ocean Carbon Dioxide Removal. *Annual Review of Marine Science*, *15*, 41–66. https://doi.org/10.1146/annurev-marine-032122-113850

Daneshvar, E., Wicker, R. J., Show, P.-L., & Bhatnagar, A. (2022). Biologically-mediated carbon capture and utilization by microalgae towards sustainable CO2 biofixation and biomass valorization – A review. *Chemical Engineering Journal*, *427*, 130884. https://doi.org/10.1016/j.cej.2021.130884

Dębowski, M., Krzemieniewski, M., Zieliński, M., & Kazimierowicz, J. (2021). Immobilized Microalgae-Based Photobioreactor for CO2 Capture (IMC-CO2PBR): Efficiency Estimation, Technological Parameters, and Prototype Concept. *Atmosphere*, *12*(8), Article 8. https://doi.org/10.3390/atmos12081031

Ezhumalai, G., Arun, M., Manavalan, A., Rajkumar, R., & Heese, K. (2024). A Holistic Approach to Circular Bioeconomy Through the Sustainable Utilization of Microalgal Biomass for Biofuel and Other Value-Added Products. *Microbial Ecology*, *87*(1), 61. https://doi.org/10.1007/s00248-024-02376-1

Fawzy, S., Osman, A. I., Doran, J., & Rooney, D. W. (2020). Strategies for mitigation of climate change: A review. *Environmental Chemistry Letters*, *18*(6), 2069–2094. https://doi.org/10.1007/s10311-020-01059-w

Gupta, A., Paul, A. R., & Saha, S. C. (2023). Decarbonizing the Atmosphere Using Carbon Capture, Utilization, and Sequestration: Challenges, Opportunities, and Policy Implications in India. *Atmosphere*, *14*(10), Article 10. https://doi.org/10.3390/atmos14101546

Hochman, G., & Appasamy, V. (2024). The Case for Carbon Capture and Storage Technologies. *Environments*, *11*(3), Article 3. https://doi.org/10.3390/environments11030052

Janssen, P. J. D., Lambreva, M. D., Plumeré, N., Bartolucci, C., Antonacci, A., Buonasera, K., Frese, R. N., Scognamiglio, V., & Rea, G. (2014). Photosynthesis at the forefront of a sustainable life. *Frontiers in Chemistry*, *2*, 36. https://doi.org/10.3389/fchem.2014.00036

Johnson, M. P. (2016). Photosynthesis. *Essays in Biochemistry*, *60*(3), 255–273. https://doi.org/10.1042/EBC20160016

Kumar, K., Mella-Herrera, R. A., & Golden, J. W. (2010). Cyanobacterial Heterocysts. *Cold Spring Harbor Perspectives in Biology*, *2*(4), a000315. https://doi.org/10.1101/cshperspect.a000315

Li, G., Xiao, W., Yang, T., & Lyu, T. (2023). Optimization and Process Effect for Microalgae Carbon Dioxide Fixation Technology Applications Based on Carbon Capture: A Comprehensive Review. *C*, *9*(1), Article 1. https://doi.org/10.3390/c9010035

Lin, J.-Y., Garcia, E. A., Ballesteros, F. C., Garcia-Segura, S., & Lu, M.-C. (2022). A review on chemical precipitation in carbon capture, utilization and storage. *Sustainable Environment Research*, *32*(1), 45. https://doi.org/10.1186/s42834-022-00155-6

Liu, Y., Xing, Y., Vendrell-Herrero, F., & Bustinza, O. F. (2024). Setting contextual conditions to resolve grand challenges through responsible innovation: A comparative patent analysis in the circular economy. *Journal of Product Innovation Management*, *41*(2), 449–472. https://doi.org/10.1111/jpim.12659

Machín, A., Cotto, M., Ducongé, J., & Márquez, F. (2023). Artificial Photosynthesis: Current Advancements and Future Prospects. *Biomimetics*, *8*(3), 298. https://doi.org/10.3390/biomimetics8030298

Murphy, D. J. (2024). Biological Carbon Sequestration: From Deep History to the Present Day. *Earth*, *5*(2), Article 2. https://doi.org/10.3390/earth5020010

National Academies of Sciences, E., Studies, D. on E. and L., Board, O. S., Technology, B. on C. S. and, Resources, B. on E. S. and, Resources, B. on A. and N., Systems, B. on E. and E., Climate, B. on A. S. and, & Sequestration, C. on D. a R. A. for C. D. R. and R. (2018). Terrestrial Carbon Removal and Sequestration. In *Negative Emissions Technologies and Reliable Sequestration: A Research Agenda*. National Academies Press (US). https://www.ncbi.nlm.nih.gov/books/NBK541439/

Nunes, L. J. R. (2023). The Rising Threat of Atmospheric CO2: A Review on the Causes, Impacts, and Mitigation Strategies. *Environments*, *10*(4), Article 4. https://doi.org/10.3390/environments10040066

Omotoso, A. B., & Omotayo, A. O. (2023). The interplay between agriculture, greenhouse gases, and climate change in Sub-Saharan Africa. *Regional Environmental Change*, *24*(1), 1. https://doi.org/10.1007/s10113-023-02159-3

Palmer, J., & Carton, W. (2021). Carbon Removal as Carbon Revival? Bioenergy, Negative Emissions, and the Politics of Alternative Energy Futures. *Frontiers in Climate*, *3*. https://doi.org/10.3389/fclim.2021.678031

Perera, F. (2018). Pollution from Fossil-Fuel Combustion is the Leading Environmental Threat to Global Pediatric Health and Equity: Solutions Exist. *International Journal of Environmental Research and Public Health*, *15*(1), 16. https://doi.org/10.3390/ijerph15010016

Poblete, I. B. S., Araújo, O. de Q. F., & de Medeiros, J. L. (2022). Sewage-water treatment with bio-energy production and carbon capture and storage. *Chemosphere*, *286*(Pt 2), 131763. https://doi.org/10.1016/j.chemosphere.2021.131763

Politaeva, N., Ilin, I., Velmozhina, K., & Shinkevich, P. (2023). Carbon Dioxide Utilization Using Chlorella Microalgae. *Environments*, *10*(7), https://doi.org/10.3390/environments10070109

Ramachandran Nair, P. K., Mohan Kumar, B., & Nair, V. D. (2009). Agroforestry as a strategy for carbon sequestration. *Journal of Plant Nutrition and Soil Science*, *172*(1), 10–23. https://doi.org/10.1002/jpln.200800030

Rascio, N., & Navari-Izzo, F. (2011). Heavy metal hyperaccumulating plants: How and why do they do it? And what makes them so interesting? *Plant Science: An International Journal of Experimental Plant Biology*, *180*(2), 169–181. https://doi.org/10.1016/j.plantsci.2010.08.016

Ray, S., Abraham, J., Jordan, N., Lindsay, M., & Chauhan, N. (2022). Synthetic, Photosynthetic, and Chemical Strategies to Enhance Carbon Dioxide Fixation. *C*, *8*(1), Article 1. https://doi.org/10.3390/c8010018

Rodrigues, C. I. D., Brito, L. M., & Nunes, L. J. R. (2023). Soil Carbon Sequestration in the Context of Climate Change Mitigation: A Review. *Soil Systems*, *7*(3), Article 3. https://doi.org/10.3390/soilsystems7030064

Santos Correa, S., Schultz, J., Lauersen, K. J., & Soares Rosado, A. (2022). Natural carbon fixation and advances in synthetic engineering for redesigning and creating new fixation pathways. *Journal of Advanced Research*, *47*, 75–92. https://doi.org/10.1016/j.jare.2022.07.011

Sarwer, A., Hamed, S. M., Osman, A. I., Jamil, F., Al-Muhtaseb, A. H., Alhajeri, N. S., & Rooney, D. W. (2022). Algal biomass valorization for biofuel production and carbon sequestration: A review. *Environmental Chemistry Letters*, *20*(5), 2797–2851. https://doi.org/10.1007/s10311-022-01458-1

Sethi, D., Butler, T. O., Shuhaili, F., & Vaidyanathan, S. (2020). Diatoms for Carbon Sequestration and Bio-Based Manufacturing. *Biology*, *9*(8), 217. https://doi.org/10.3390/biology9080217

Shareefdeen, Z., Elkamel, A., & Babar, Z. B. (2023). Recent Developments on the Performance of Algal Bioreactors for CO2 Removal: Focusing on the Light Intensity and Photoperiods. *BioTech*, *12*(1), 10. https://doi.org/10.3390/biotech12010010

Shukla, S. K., Khokarale, S. G., Bui, T. Q., & Mikkola, J.-P. T. (2019). Ionic Liquids: Potential Materials for Carbon Dioxide Capture and Utilization. *Frontiers in Materials*, *6*. https://doi.org/10.3389/fmats.2019.00042

Sidi Habib, S., Torii, S., S., K. M., & Charivuparampil Achuthan Nair, A. (2024). Optimization of the Factors Affecting Biogas Production Using the Taguchi Design of Experiment Method. *Biomass*, *4*(3), Article 3. https://doi.org/10.3390/biomass4030038

Singh, S., Ravi Kiran, B., & Venkata Mohan, S. (2024). Carbon farming: A circular framework to augment CO 2 sinks and to combat climate change. *Environmental Science: Advances*, *3*(4), 522–542. https://doi.org/10.1039/D3VA00296A

Siyar, R., Doulati Ardejani, F., Norouzi, P., Maghsoudy, S., Yavarzadeh, M., Taherdangkoo, R., & Butscher, C. (2022). Phytoremediation Potential of Native Hyperaccumulator Plants Growing on Heavy Metal-Contaminated Soil of Khatunabad Copper Smelter and Refinery, Iran. *Water*, *14*(22), Article 22. https://doi.org/10.3390/w14223597

Skuza, L., Szućko-Kociuba, I., Filip, E., & Bożek, I. (2022). Natural Molecular Mechanisms of Plant Hyperaccumulation and Hypertolerance towards Heavy Metals. *International Journal of Molecular Sciences*, *23*(16), 9335. https://doi.org/10.3390/ijms23169335

Thompson, M., Gamage, D., Hirotsu, N., Martin, A., & Seneweera, S. (2017). Effects of Elevated Carbon Dioxide on Photosynthesis and Carbon Partitioning: A Perspective on Root Sugar Sensing and Hormonal Crosstalk. *Frontiers in Physiology*, *8*, 578. https://doi.org/10.3389/fphys.2017.00578

Turek, T., Dziembek, D., & Hernes, M. (2021). The Use of IT Solutions Offered in the Public Cloud to Reduce the City's Carbon Footprint. *Energies*, *14*(19), Article 19. https://doi.org/10.3390/en14196389

Udawatta, R. P., Walter, D., & Jose, S. (2022). Carbon sequestration by forests and agroforests: A reality check for the United States. *Carbon Footprints*, *2*(1), N/A-N/A. https://doi.org/10.20517/cf.2022.06

Walker, A. P., De Kauwe, M. G., Bastos, A., Belmecheri, S., Georgiou, K., Keeling, R. F., McMahon, S. M., Medlyn, B. E., Moore, D. J. P., Norby, R. J., Zaehle, S., Anderson-Teixeira, K. J., Battipaglia, G., Brienen, R. J. W., Cabugao, K. G., Cailleret, M., Campbell, E., Canadell, J. G., Ciais, P., … Zuidema, P. A. (2021). Integrating the evidence for a terrestrial carbon sink caused by increasing atmospheric CO2. *New Phytologist*, *229*(5), 2413–2445. https://doi.org/10.1111/nph.16866

Wang, F., Harindintwali, J. D., Yuan, Z., Wang, M., Wang, F., Li, S., Yin, Z., Huang, L., Fu, Y., Li, L., Chang, S. X., Zhang, L., Rinklebe, J., Yuan, Z., Zhu, Q., Xiang, L., Tsang, D. C. W., Xu, L., Jiang, X., … Chen, J. M. (2021). Technologies and perspectives for achieving carbon neutrality. *Innovation (Cambridge (Mass.))*, *2*(4), 100180. https://doi.org/10.1016/j.xinn.2021.100180

Wongsodiharjo, D., & Masjud, Y. I. (2024). Utlize microalgae in order to lowering green house emission by using carbon capture. *Sustainable Urban Development and Environmental Impact Journal*, *1*(1), Article 1.

Yu King Hing, N., Aryal, U. K., & Morgan, J. A. (2021). Probing Light-Dependent Regulation of the Calvin Cycle Using a Multi-Omics Approach. *Frontiers in Plant Science*, *12*, 733122.https://doi.org/10.3389/fpls.2021.733122

Zaks, D. P. M., Winchester, N., Kucharik, C. J., Barford, C. C., Paltsev, S., & Reilly, J. M. (2011). Contribution of Anaerobic Digesters to Emissions Mitigation and Electricity Generation Under U.S. Climate Policy. *Environmental Science & Technology*, *45*(16), 6735–6742. https://doi.org/10.1021/es104227y

Žalys, B., Venslauskas, K., Navickas, K., Buivydas, E., & Rubežius, M. (2023). The Influence of CO2 Injection into Manure as a Pretreatment Method for Increased Biogas Production. *Sustainability*, *15*(4), Article 4. https://doi.org/10.3390/su15043670

SCREENING, ISOLATION, AND BIOCHEMICAL CHARACTERIZATION OF AMYLASE PRODUCED BY *BACILLUS* SPECIES FROM SUDANESE SOIL SAMPLES

Author name and information

Sundos A. Khidir1 and Elhadi A. I. Elkhalil[2*]

[1]Department of Food Science and Technology, Faculty of Agriculture, University of Alzaiem Alazhari, 13311, Khartoum North, Sudan
[2] Department of Botany and Agric. Biotechnology, Faculty of Agriculture, University of Khartoum, 13314 Shambat, Khartoum North, Sudan

* **Correspondence**: eaikhalil@yahoo.com

Keywords

Amylase; *B. megaterium; B. velezensis; B. subtilis; B. licheniformis.*

Abstract

Many microorganisms, including *Bacillus* spp., can produce amylases. The search for new promising strains is a continuous process for producing amylase for industrial use. The present study aimed to isolate amylase-producing bacteria in the Sudanese soil and characterize the produced amylase. Six isolates of *Bacillus* species with the highest amylase activity were selected for further investigations out of 32 isolates obtained from the first screening of soil samples for amylase-producing bacteria. The isolates were identified by conventional bacteriological methods followed by PCR amplification and partial sequencing of the 16S rRNA gene, and their amylase was characterized and quantified. These six isolates were 2 strains of each of *B. megaterium* and *B. subtilis*, and one strain of each of *B. velezensis* and *B. licheniformis*; their average amylase activities ranged from 4.77 to 6.10 U/ml. The produced amylases were thermo-stable at 60 °C for 70 min, with Vmax values ranging between 1.08 and 45.66 µmole/min.mg and Km values reaching up to 530.45 mM. The strains of *Bacillus* species isolated in this study represent promising candidates for amylase production on an industrial scale.

INTRODUCTION

Amylases can be isolated from different sources, such as animals, plants, and microorganisms. However, microbial amylases are more thermostable and produce greater yields (Kango *et al*. 2019). Many fungi produce amylase, both intracellularly and extracellularly, depending on the fermentation process (Patil *et al*. 2021); despite this, bacteria are the preferred source, not only because of the maximum amount of enzyme generated within a very short time but also due to its extracellular production attribute, which is, indeed, easy to isolate (Abbas, 2009). Hence, using bacterial amylases presents a viable and attractive alternative to chemical hydrolysis in starch

degradation (Samanta, 2022). Bacterial amylase has emerged as a vital enzyme in various industries, including biotechnology, textiles, food processing, and pharmaceuticals. (Farooq *et al*., 2021). To date, two main types of amylases have been identified in microorganisms: α-amylase and glucoamylase. α-Amylases are extracellular enzymes that catalyze the random hydrolysis of 1,4-α-D-glucosidic linkages in the linear amylose chain. Glucoamylase (exo-1,4-a-D-glucan glucanohydrolase) hydrolyses single glucose units from the non-reducing ends of amylose and amylopectin in a stepwise manner (Castro *et al*., 2010; Rameshkumar and Sivasudha, 2011).
Amylase production has captured around 30% of the worldwide enzyme market and is experiencing sustained growth (Tiwari *et al*. 2015). Microorganisms have emerged as preferred sources for amylase production due to their abundance, rapid growth, simple cultivation, and ability to secrete proteins extracellularly, resulting in high yields and safe handling (Singh *et al*. 2022). The thermostability of amylase is a desirable trait for industrial applications. Thermophilic organisms, especially thermophilic bacteria like *Bacillus* species, are particularly interesting due to their potential to produce novel, heat-stable enzymes (Jaiswal and Jaiswal, 2024). Thermostable amylases provide distinct advantages in industrial applications, notably minimizing the risk of contamination and facilitating faster diffusion (Patil *et al*. 2021). Thermophilic organisms are typically found in environments characterized by high temperatures, such as geothermal and volcanic regions, hydrothermal systems, submarine hot vents, and hot springs, as well as in warm soils and waters, such as Sudanese soil (Bajpai, 2023). There is a growing interest in discovering enzymes with enhanced properties, particularly thermostable raw starch-degrading amylases, which can be effectively utilized in industrial applications and produced through cost-efficient methods (Bilal and Iqbal, 2020).

Therefore, this study aimed to identify bacteria that produce amylase and characterize the properties of the enzyme produced.

MATERIALS AND METHODS

Sampling

A total of 32 soil samples (100g each) were collected from a depth of 10-20 cm from agricultural areas in Shambat (Khartoum North) and Soba (Khartoum), Khartoum State, Sudan. The soil had neutral to alkaline pH (6.8- 8.0) and was silty clay. Ten sub-samples were taken randomly to obtain a representative sample. The samples were collected using clean rubber gloves, placed into sterile containers, and transported in iceboxes to the laboratory.

Isolation of *Bacillus* spp.

Isolation of *Bacillus* was carried out according to Harrigan (1998). Ten grams of the soil sample were added to 90 ml of distilled water. The soil suspension was heated at 80 °C for 15 min. Then, five 10-fold dilutions of soil suspension were made (10^{-1}, 10^{-2}, 10^{-3}, 10^{-4} and 10^{-5}). On plates of nutrient agar, 0.1 ml of three heated dilutions (10^{-3}, 10^{-4}, 10^{-5}) of each sample were inoculated by spreading and incubated aerobically at 37 °C for 24 h. Sub-cultures were made thereafter to obtain pure colonies. Identification of the isolates as *Bacillus* species was made by conventional

bacteriological tests. Further identification was made through molecular biology methods, as detailed later.

Primary screening of amylase-producing *Bacillus*

Bacterial cultures were screened for amylolytic activity by starch hydrolysis test on a starch agar plate according to the method of Qadeer *et al*. (1989). Pure colonies were streaked onto starch agar plates, where starch served as the sole carbon source, and incubated at 37 °C for 24 h. The plates were then flooded with Gram's iodine solution (containing 250 mg iodine crystals, 2.5 g potassium iodide, and 125 ml water) to form a deep blue starch-iodine complex. A zone of no blue color around colonies (clear zone, i.e., zone of starch degradation) indicated amylase activity. This method serves as the foundation for detecting and screening amylolytic strains. Amylase-producing strains exhibiting the largest clearance zone diameter were selected for further analysis. The amylolytic activity index was calculated according to the following equation:

$$Amylolytic\ activity\ index\ of microorganism = \frac{Average\ diameter\ of\ clear\ zone - Average\ diameter\ of\ colony}{Average\ diameter\ of\ clear\ colony}$$

Secondary screening of amylase

Each isolate with a positive result for starch hydrolyses in the primary test was used for amylase production in production media (containing per liter, 6.0 g bacteriological peptone; 0.5 g $MgSO_4$ $.7H_2O$; 0.5 g KCl; 1.0 g Starch, pH 7). To prepare the inoculum for amylase production, a loopful of amylase-producing bacteria was transferred to 250 ml Erlenmeyer flasks containing 50 ml production media, after inoculation the mixture was incubated under shaking (120 rpm) at 50 °C for 24 h, and then the amylase was partially extracted by cold centrifugation (4 °C) at 5000 rpm for 20 min. After that, 1 ml of the supernatant was taken as crude enzyme added to 10 ml of 1% soluble starch in a test tube followed by addition of 0.5 ml of iodine. The disappearance of the color was followed by spectrophotometry at 2 min intervals. The point at which there was no change in the iodine color was referred to as the achromic point.

Identification of *Bacillus* species by molecular biology methods

Bacillus species isolates that showed amylolytic activity were subjected to further identification by PCR followed by sequencing as follows:

DNA Extraction

The DNA was extracted from pure cultures of *Bacillus* spp. grown on nutrient agar plates by boiling. Briefly, a few colonies were picked from the agar plate using a wire loop and suspended in 100 µl of nuclease-free water. The colony suspension was incubated at 95 °C for 15 min in a heat block, followed by centrifugation at 13.000 rpm for 5 min. The supernatant was transferred to a clean Eppendorf tube and stored at – 20 °C until used as a DNA template in PCR.

Polymerase Chain Reaction

The PCR was performed in 20 µl reaction volume containing 5 µl of the DNA template, 1 µl (10 pM) of each primer, and 13 µl nuclease-free water in Maxime PCR PreMix kit (Intron Biotechnology, Inc, Korea). This premix contained 2.5 U of *i-Taq* DNA polymerase, 2.5 mM of each dNTP, 1x reaction buffer (100 mM Tris HCl, pH 8.3, 500 mM KCl, 20 mM $MgCl_2$), and 1x gel loading buffer.

The universal primers (341F: 5′ CCTACGGGNGGCWGCAG 3′ and 802R 5′ GACTACHVGGGTATCTAATCC 3′), were used to amplify about 460 bp of the V3 and V4 regions of the 16S rRNA gene (Klindwoeth *et al*., 2013).

DNA amplification was carried out as follows: an initial 2-minute denaturation at 94 °C, followed by 35 cycles of 45-second denaturation at 94 °C, 1-minute annealing at 57 °C, 1-minute extension at 72 °C, and a final 5-minute extension at 72 °C. The PCR products were visualized by a UV trans-illuminator after electrophoresis in a 1% agarose gel and staining with SYBR-safe DNA gel stain (Invitrogen, Carlsbad, CA, USA).

Sequencing

The PCR amplification products were sent for sequencing to a commercial sequencing company (Macrogen Europe, Amsterdam, The Netherlands). Sequencing was performed using the amplification primers. The obtained sequences were edited using the BioEdit sequence alignment editor (Hall, 1999) and then aligned to the nucleotide database in GenBank using the Basic Alignment Search Tool (BLAST) of the National Centre of Biotechnology Information (NCBI) of the United States.

Amylase production

The enzyme was produced from purified isolates that exhibited a positive reaction on the starch plate test. Amylase production was done according to Pushpendra *et al*. (2012). Each isolate was cultured in nutrient broth by inoculating a fresh colony and incubating for 24 hs at 37 °C with agitation at 100 rpm as a pre-culture. The pre-culture was then inoculated into 100 ml sterile broth medium (contained per liter 6.0 g bacteriological peptone, 0.5 g $MgSO_4$.$7H_2O$, 0.5 g KCl, 1.0 g starch, maintained at pH 7) in conical 250 ml- flask and incubated for 24 h, at 50 °C with continuous agitation at 120 rpm. After incubation, the bacterial cells were separated by centrifugation at 5000 rpm for 20 min at 4 ℃. The supernatant containing the crude enzyme was used in further steps.

Amylase assay

Amylase activity was assessed by quantifying the amount of reducing sugar released from soluble starch as follows: an enzyme reaction mixture containing 0.5 ml of the crude enzyme and 0.5 ml water was allowed to incubate at room temperature for 3 to 4 min, then 0.5 ml of 1.0% soluble starch solution was added. The mixture was incubated at 30 ºC for 3 min exactly, 1.0 ml of dinitrosalicylic acid (DNSA) reagent was added, the tubes were submerged in boiling water for 5 min, then cooled at room temperature. The tube contents were diluted to a final volume of 10 ml using deionized water. The absorbance at 540 nm was measured using a spectrophotometer and

then converted to maltose concentration in mg. One unit is equivalent to the amount of enzyme which hydrolyses soluble starch into 1.0 mg maltose hydrate per minute under standard assay conditions (Miller, 1959). The enzyme activity was determined using the following equation:

$$Enzyme\ activity\ (\mathrm{IU/ml}) = \frac{Amount\ of\ reducing\ sugar \times 1000 \times dilution\ factor}{Molecular\ weight\ of\ maltose \times time \times enzymevolume}$$

Biochemical characteristics of amylases

Determination of the optimum pH

Buffers were prepared as follows: 0.1 M sodium citrate buffer pH 4, 5, and 0.1 M phosphate buffer pH 6, 7, 8, 9, and 10; the pH was adjusted using NaOH and HCl. The substrate solution containing 1% soluble starch at each different pH was prepared as previously described; 0.5 ml of the enzyme was placed in a a test tube, and then 0.5 ml of the substrate was added. The mixture was incubated at 30 °C for 10 min. The incubation was terminated by adding 1 ml DNSA and boiled at 100 °C for 5 min to stop the reaction.

Determination of the optimum temperature

To determine the optimum temperature, the reaction mixture of enzymes and substrate solutions at the respective enzyme's optimum pH was incubated for 10 min at each of the following temperatures: 30, 35, 40, 45, 50, 55, 60, 65, 70, 75, and 80 °C. Then, the amylase activity was measured as described before.

Determination of thermostability

Thermostability was assessed in aqueous solutions by pre-incubating amylase preparations at various temperatures: 40, 50, 60, 70, 80, and 90 °C for different time intervals: 10, 20, 30, 40, 50, 60, 70, 80, and 90 min. After pre-incubation, samples were cooled and incubated at their optimal temperatures. Residual enzyme activities were then estimated as previously described.

Enzyme Kinetics

Enzyme kinetics were characterized using a Lineweaver-Burk plot, which yielded the Michaelis constant (Km) and maximum reaction rate (Vmax). These parameters were determined by measuring catalytic rates at various starch concentrations under optimal pH and temperature conditions for each amylase. A specific amount of amylase was mixed with varying concentrations of starch substrate [S]: 1.0, 2.0, 3.0, 4.0, 5.0, 6.0, and 7.0 mM for 30 min.

The reaction velocity (V), expressed as moles of product formed per second, was determined using an Excel computer program. A Lineweaver-Burk plot of 1/V versus 1/[S] resulted in a linear relationship, where the y-intercept corresponds to 1/Vmax and the slope represents Km/Vmax.

RESULTS AND DISCUSSION

Identity of the *Bacillus* isolates

A total of 32 *Bacillus* species isolates were identified by conventional bacteriological methods. All isolates were positive for amplification with 16S rRNA gene primers. Sequencing results for the 6 selected isolates confirmed their identification by conventional bacteriological methods. The identities of the isolates based on the BLAST results are presented in Table 1.

Table 1. Identity of the *Bacillus* Sudanese soil isolates with amylolytic activity based on BLAST results of partial 16S rRNA gene sequence

Sudanese soil *Bacillus* isolate code	BLAST Results			
	Species	Strain	Identity %	Accession no.
SE25	*B. megaterium*	SRLS New2	98.6	KF048872
SE26	*B. velezensis*	B157	100	OP555715.1
SE27	*B. megaterium*	A-11	98.64	MT588719.1
SE28	*B. subtilis*	MK007	99	AF199464.1
SE29	*B. subtilis*	Km 2-2	100	Mn065454.1
SE32	*B. licheniformis*	BLS	100	OP537020.1

Screening of amylase-producing *Bacillus*

Primary screening

A clear zone of starch hydrolysis indicated the presence of amylase-producing bacteria, visible after iodine addition. The efficiency of these bacteria was evaluated based on the size of the hydrolysis zone. From the isolated bacteria, 32 *Bacillus* isolates produced clear zones around the colonies after adding iodine solution on starch agar plates, indicating a positive starch hydrolysis test (Table 4). Six isolates were selected because they showed the widest clear zones. The amylolytic activity index for the six isolates ranged from 0.32 to 1.40 (Table 2 and Fig 1). The highest amylolytic activity index (1.40) was recorded for *B. licheniformis* SE32. The isolates with the wide zones of hydrolysis were selected for further identification. The use of starch nutrient agar and iodine for detecting amylase (hydrolytic enzyme) producing microorganisms was reported by Yassin et al. (2021). The clear zones surrounding the colonies resulted from the amylase activity produced during microbial growth, which hydrolyzed the starch in the surrounding area. Consequently, these areas remained colorless when treated with iodine. The non-hydrolyzed part of the plate tested positive due to the presence of starch (amylose), hence the blue-black appearance, according to Akpan *et al*. (1999).

Table 2. Amylolytic activity index of *Bacillus* species isolated from Sudanese soil samples

Isolate code	Isolates	Amylolytic activity index
SE25	*B. megaterium*	0. 5
SE26	*B. velezensis*	0.81
SE27	*B. megaterium*	0.38
SE28	*B. subtilis*	0.77
SE29	*B. subtilis*	0.92
SE32	*B. licheniformis*	1.40

Figure 1. Primary screening for *Bacillus* species- producing amylase

Secondary screening of amylase by achromic point

The results of the secondary screening of amylase by achromic point revealed the qualitative efficiency of the enzyme produced by the isolates (Fig. 2), in which the gradual disappearance of the blue color developed due to the interaction of iodine with soluble starch is plotted against time. The color disappeared at 21 min (achromic point) for *B. megaterium* SE25 and *B. licheniformis* SE32, while the chromic point of isolates *B. subtilis* SE28 was reached after more than 21 min. According to these results, isolates *B. megaterium* SE25 and *B. subtilis* SE28 were promising strains for large-scale amylase production.

Amylase production

The amylase activity of the isolates ranged from 6.10 U/ml (for *B. megaterium* SE25) to 4.77 U/ml (for *B. velezensis* SE26). Table 3 demonstrates the amylolytic activity of *Bacillus* isolates inoculated in the production medium and incubated at 50 °C. Bacteria that produce thermostable amylase in extreme environments are vital in addressing various industrial challenges.

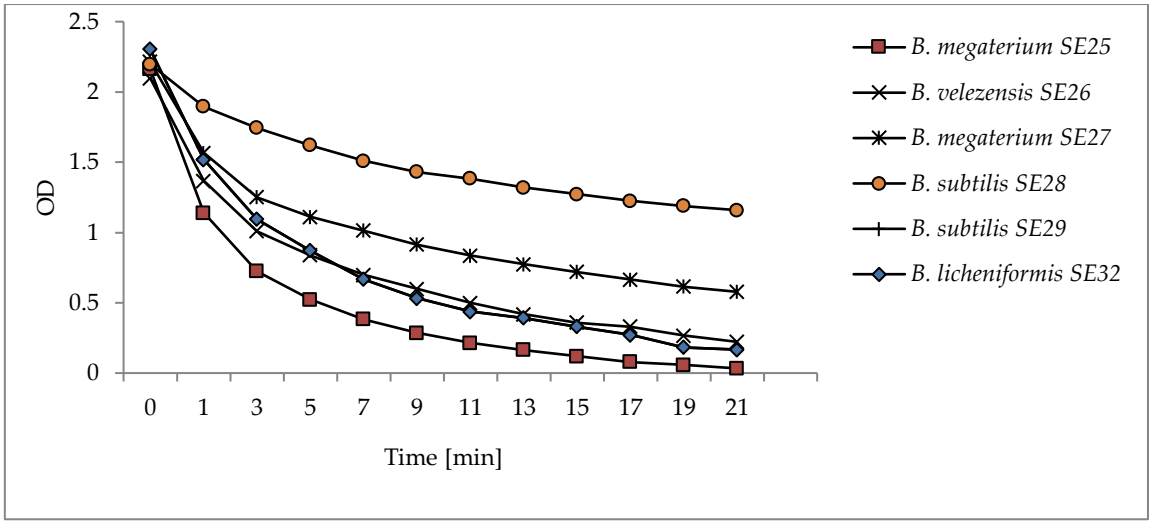

Figure 2. The achromic point of the different *Bacillus* species with amylolytic activity isolated from Sudanese soil samples

Table 3. Amylolytic activity of different *Bacillus* species isolated from Sudanese soil samples

Isolate	Amylase Activity (U/ml)
B. megaterium SE25	6.10
B. velezensis SE26	4.77
B. megaterium SE27	5.38
B. subtilis SE28	5.40
B. subtilis SE29	5.40
B. licheniformis SE32	5.10

Characterization of amylase from Bacillus species: biochemical and biophysical properties

pH profile

The optimum pH of each amylase preparation from each bacterial isolate and the pH value of different amylase preparations are presented in Fig 3. The optimal pH ranges for amylases from various *Bacillus* isolates were identified by testing their activity across a pH spectrum of 4 – 10. The pH optima of amylase from the isolates ranged between 6 and 7, while the α-amylase from *B. licheniformis* SE 32 exhibited optimal activity at pH 8. This observation agrees with what was reported earlier by Sani *et al*. (2014) and Suhartati and Hadi (2010). The relative activity of α-amylase was highest at pH 6.0 for amylase produced from *B. subtilis* SE29, a slightly acidic condition, where it exhibited 100% relative activity. A sharp decline in activity to 10% was observed when the pH was increased from 7.0 to 9.0. These findings are supported by the results from Dash *et al*. (2015). Wu et al. (2018) stated that α-amylase is the best industrial catalyst that remains stable for long durations under extreme conditions. The organisms that can tolerate

temperatures up to 40 °C and pH 6 – 8 are good enough to make them applicable for industrial purposes (Amalesh *et al*., 2013).

The pH values of the activities of amylase preparations used in this study are shown in Fig. 3. For *B. subtilis* SE29, the pH optima was acidic (pH 6). Due to the acidity tolerance of the enzyme of this strain, it has a good potential for industrial use in the hydrolysis of soluble starch as well as activity on other sources of polysaccharides (Wang *et al*., 2008).

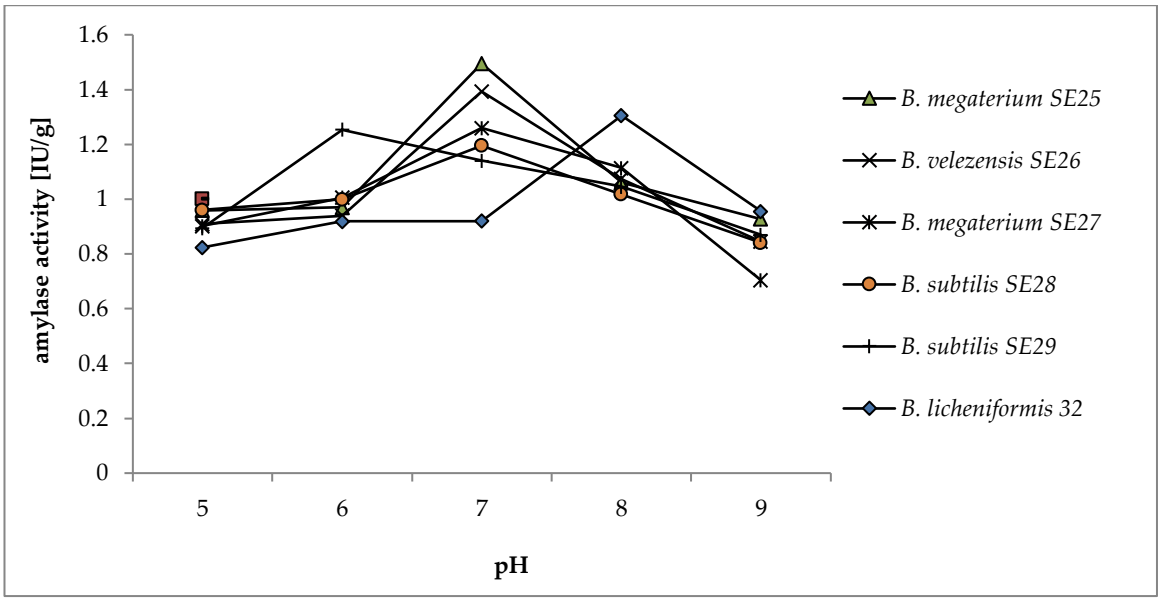

Figure 3. Optimum pH profile for amylases produced by different *Bacillus* species isolated from Sudanese soil.

Thermal behavior

Optimum temperature

Figure 4 illustrates the temperature optima for amylases activity. The enzyme's activity, measured after a 10-minute incubation with a starch solution at various temperatures, showed variations. For *B. megaterium* SE25, *B.* velezensis SE26, and *B. megaterium* SE27, the amylase displayed the highest activity at 50 °C, while for *B. licheniformis* SE32 it the highest activity at 65 °C. On the other hand, the highest activity was at 75 °C for *B. subtilis* SE29, while for *B. subtilis* SE28, the highest activity was at 70 °C. The optimum temperatures at which α-amylase activity reaches maximum, as reported by many researchers, were reviewed based on microbial sources by Gupta *et al*. (2003). The current production of amylases faces several significant challenges, including the limited availability of biocatalysts that can operate efficiently and cost-effectively under the high-temperature and low-pH conditions required to convert complex carbohydrates into simple sugars. Moreover, there is a great need for cost-effective fermentation of derived sugars from starch and other polysaccharides (Wyman *et al*., 2005). This process is costly and inefficient, highlighting the need for stable and active enzymes across various temperatures and pH levels. Among the *Bacillus* isolates in this study, *B. subtilis* SE29 obtained the highest temperature optima of 75 °C; this makes it more suitable for producing simple sugars from polysaccharides of different products, such as sugar cane, confectionery, bakeries, and other relevant industries.

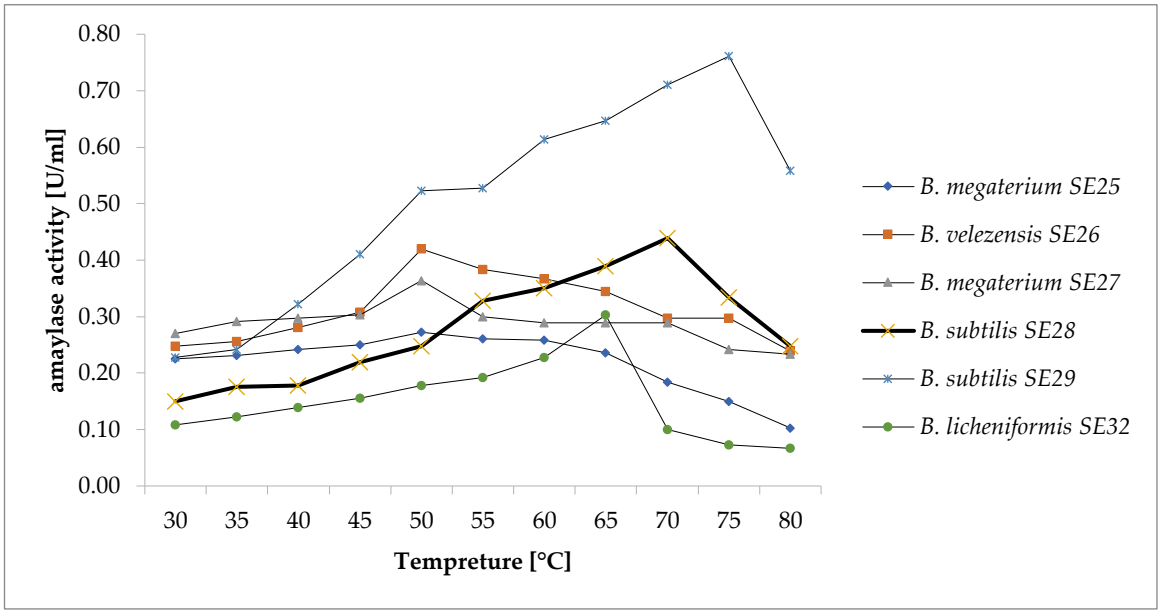

Figure 4. Temperature profile of amylase preparations produced from different *Bacillus* species isolated from Sudanese soil

Thermostability of amylases

One of the key factors in characterizing an enzyme is its thermostability. The thermal stability of the enzyme was assessed by incubating the enzyme without the substrate fractions at various temperatures ranging from 40 to 90 °C (Elkhalil and Gafar, 2013; Varalakshmi *et al*., 2008). The thermostability of amylase was evaluated by measuring its residual activity in aqueous solutions at optimal temperatures, following exposure to various temperatures (40 – 90 °C) for different time periods (10 – 90 min), as shown in Figures 5-10. The crude amylase extracted from *Bacillus* spp. remained stable for 90 min at temperatures up to 60 °C. In comparison, amylases isolated from *B. megaterium* SE25 and *B. velezensis* SE26 retained their initial activity after being incubated for 10 min at 40 °C (Fig. 5 & 6).

Amylase from *B. megaterium* SE25 completely lost its activity within 10 min when incubated at 80 °C and 90 °C. After 40 min of incubation at 70°C, amylase from *B. megaterium* SE27 maintained 50% of its original activity (Fig.7). Notably, *B. subtilis* SE28 and *B. subtilis* SE29 amylases retained 50% of their original activity when incubated at 70 °C for 60 and 90 min, respectively (Fig. 8 and 9). On the other hand, amylase from *B. licheniformis* SE32 retained 50% of its initial activity at 80 °C when incubated for 20 min (Fig. 10). It seems that *B. licheniformis* SE32 retained 100% of its amylase activity when exposed to 90 °C for 20 min (Fig. 10). Sudan's extremely hot climate creates an ideal environment for the growth and survival of extremophilic microorganisms. Amylase production has reached up to 30% of the global enzyme market and is continuously increasing (Yassin *et al.* 2021). The findings of this study recovered six thermophilic *Bacillus* isolates that could overcome the shortcomings of current amylase in the enzyme markets.

Enzyme kinetics

The enzyme kinetics of amylases from *Bacillus* isolates were determined under optimal pH and temperature conditions in 0.05 M sodium phosphate buffer, using various starch concentrations (2.0, 4.0, 6.0, 8.0, 10.0, 12.0, 14.0 and 50.0 mM) as substrates. The present study determined the maximum velocity (Vmax) and Michaelis constant (Km) of α-amylase using a Lineweaver-Burk plot analysis. Table 4 shows the Km and Vmax of different amylases. Low Km values indicate high enzyme affinity for the substrate (Hamilton *et al*., 1998).

Table 4. Enzyme kinetics of amylase produced by some *Bacillus* species measure by V_{MAX} and K_m values

Source of amylase	V_{max} m mole min-1 mg-1	K_m [Mm]
B. megaterium SE25	3.35	23.39
B. velezensis SE26	1.08	2.28
B. megaterium SE27	45.66	530.45
B. subtilis SE28	4.99	24.58
B. subtilis SE29	4.66	15.53
B. licheniformis SE32	3.55	19.76

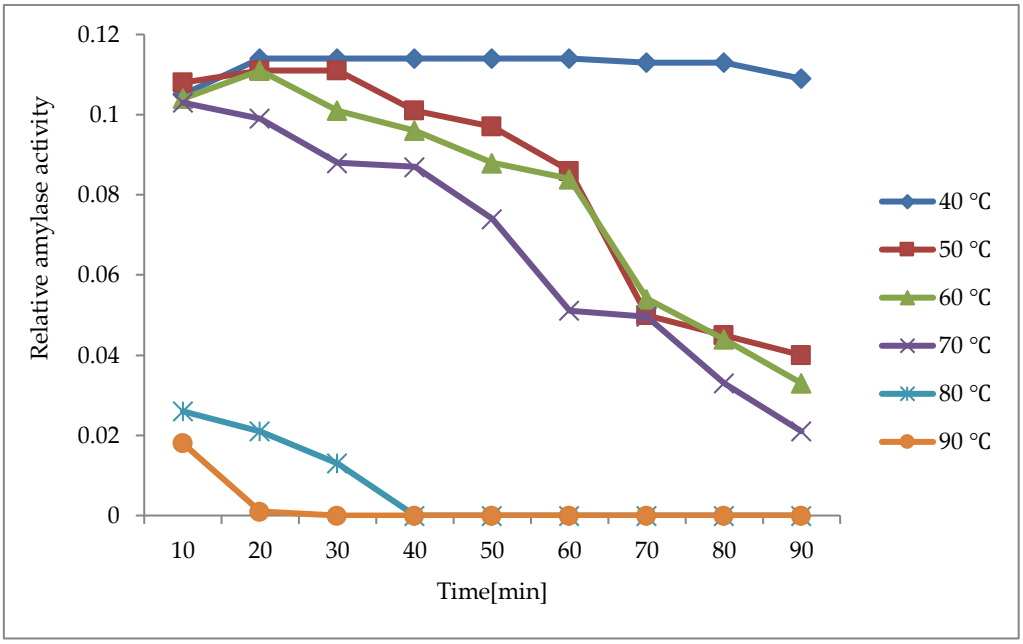

Figure 5. Residual enzymatic activity of amylase preparation from *B. megaterium* SE25 after being exposed for different lengths of time at various temperatures. Results are presented as a percentage of initial activity measured before heat treatment at the optimum temperature for 10 min.

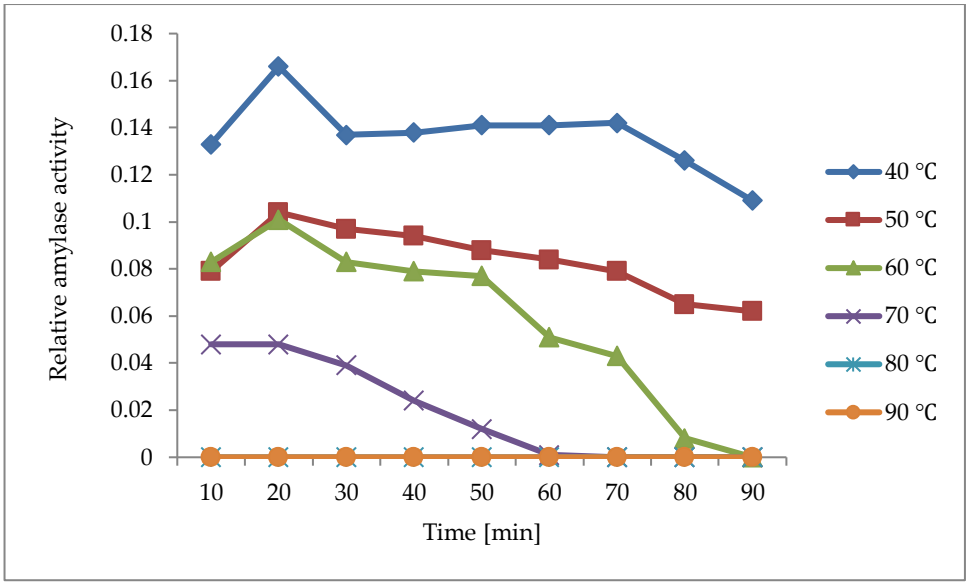

Figure 6. Residual enzymatic activity of amylase preparation from *B. velezensis* after exposure for different lengths of time at various temperatures. Results are presented as a percentage of initial activity measured before heat treatment at the optimum temperature for 10 min.

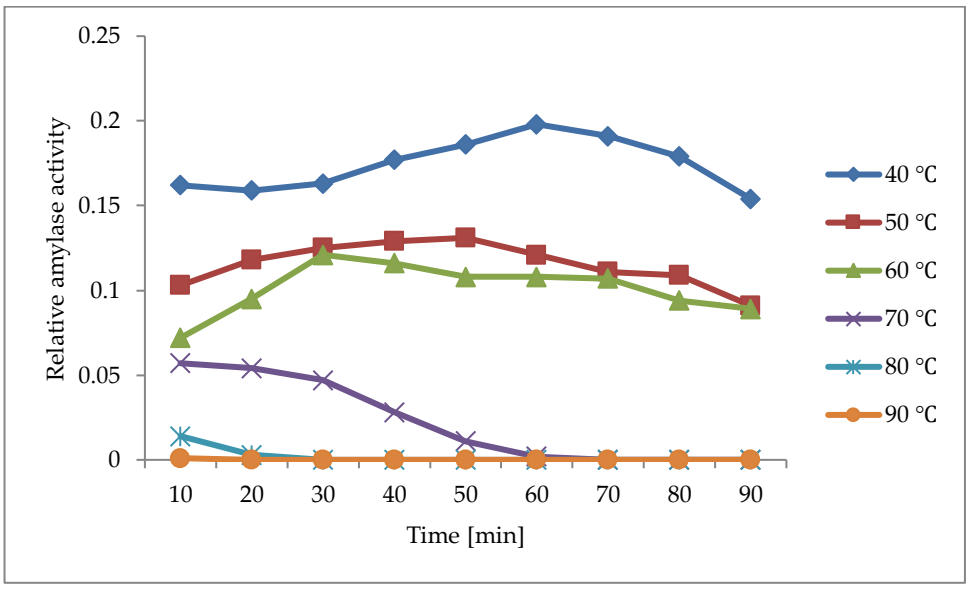

Figure 7. Residual enzymatic activity of amylase preparation from *B. megaterium* SE27 after being exposed for different lengths of time at various temperatures. Results are presented as a percentage of initial activity measured before heat treatment at the optimum temperature for 10 min.

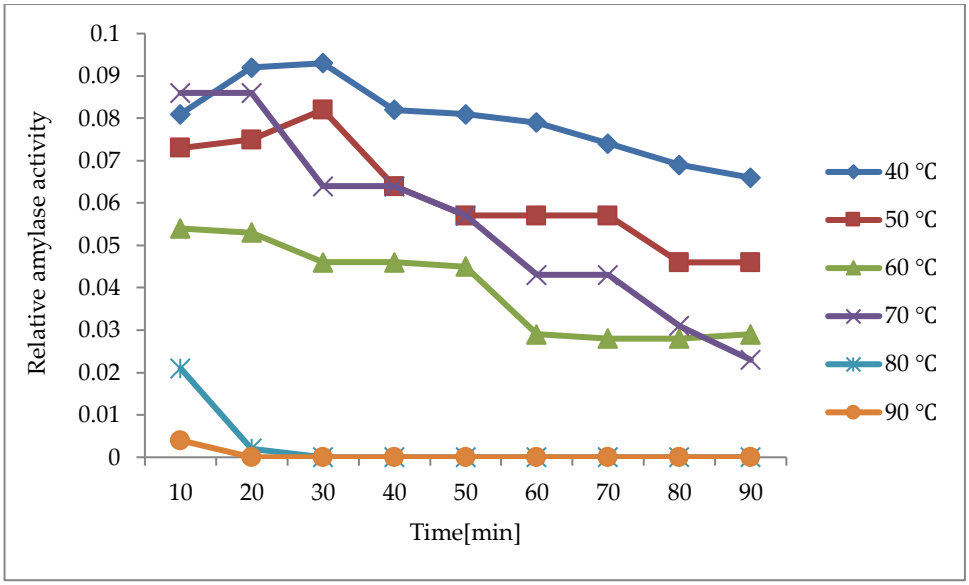

Figure 8. Residual enzymatic activity of amylase preparation from *B. subtilis* SE28 after being exposed for different lengths of time at various temperatures. Results are presented as a percentage of initial activity measured before heat treatment at the optimum temperature for 10 min.

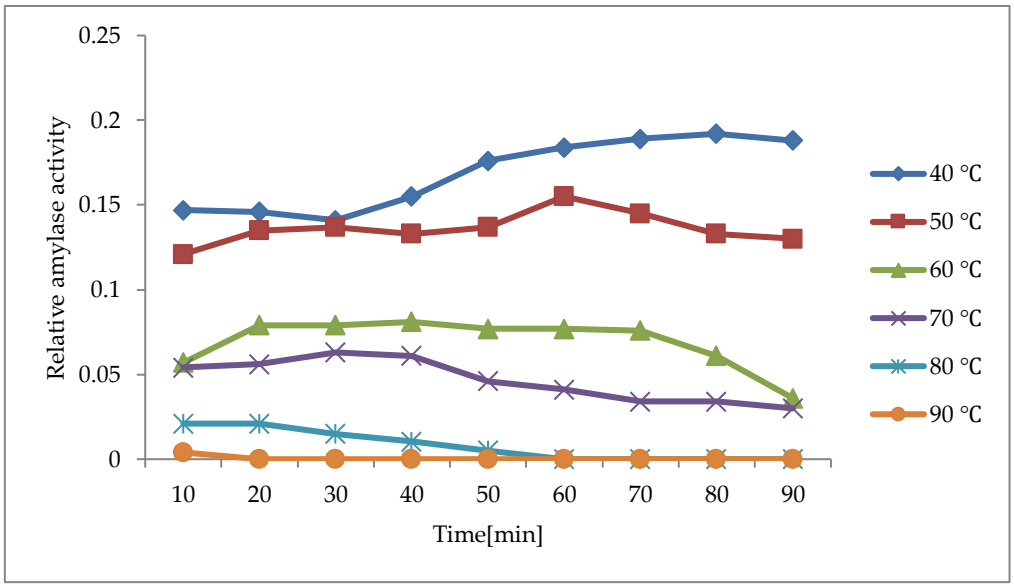

Figure 9. Residual enzymatic activity of amylase preparation from *B. subtilis* SE29 after being exposed for different lengths of time at various temperatures. Results are presented as a percentage of initial activity measured before heat treatment at the optimum temperature for 10 min.

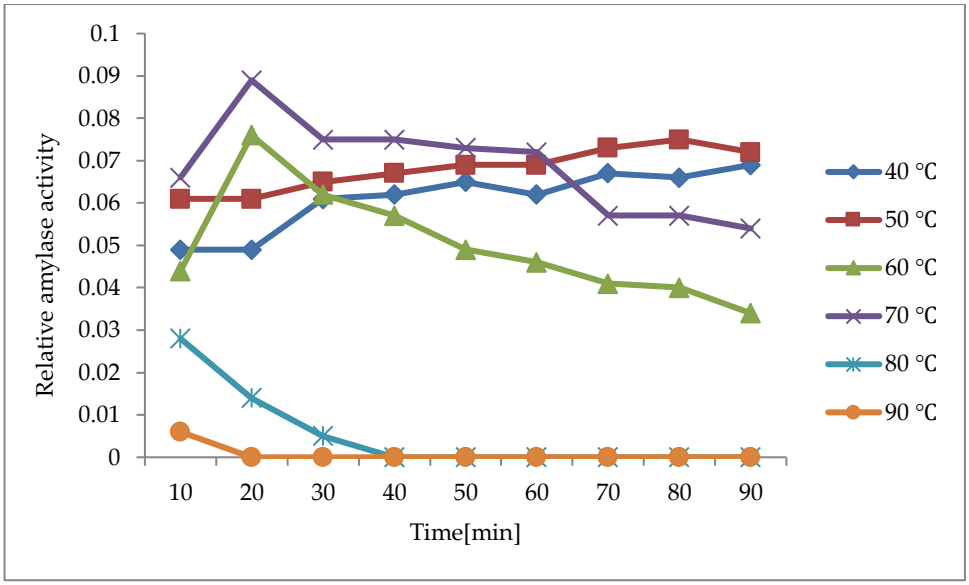

Figure 10. Residual enzymatic activity of amylase preparation from *B. licheniformis* SE32 after exposure for different lengths of time at various temperatures. Results are presented as a percentage of initial activity measured before heat treatment at the optimum temperature for 10 min.

CONCLUSION

In conclusion, the optimal conditions for amylase production differed among the various bacterial strains. The optimum pH of the extracellular enzyme for *B. subtilis* SE29 was 6. *B. subtilis* SE29 recorded the highest optimum temperature of 75 °C, consequently, the amylase produced from *B. subtilis* SE29 demonstrated exceptional characteristics, rendering it an ideal candidate for industrial application. *B. megaterium* SE25 produced the highest amylase activity among the others. The amylase enzyme produced in this study could be the beginning of its production on an industrial scale.

Declaration of competing interests

The authors declare that no conflict of interest does exist.

Ethics approval

This article does not require approval because there are no human or animal participants.

REFERENCES

Abbas, N. (2009). Isolation and Identification of α-Amylase Producing Bacteria from Soil at NWFP (Pakistan). *New Biotechnology*. 25, (1): 2009.

Akpan, I.; Bankole, M. and Adesemowo, A. (1999). A rapid plate culture method for screening of amylase producing microorganisms. *Biotechnology Techniques* 13: 411-413.

Amalesh, S.; Debmalya, M.; Sudipendra Nath, R.; Chandrima, S. and Pinaki, P. (2013). Characterization and Optimization of Amylase Producing Bacteria Isolated from Solid Waste. *Journal of Environmental Protection*, 4(6): 647-652.

Bajpai, P. (2023). Developments and applications of enzymes from thermophilic microorganisms. Elsevier.

Bilal, M., and Iqbal, H. M. (2020). State-of-the-art strategies and applied perspectives of enzyme biocatalysis in food sector—current status and future trends. *Critical Reviews in Food Science* and Nutrition, 60(12), 2052-2066.

Castro, A. M.; Carvalho, D.F.; Freire, D.M.G. and Castilho, L.R. (2010). Economic analysis of the production of amylases and other hydrolases by Aspergillus awamori in solid state fermentation of babassu cake. *Enzyme Research*, 23: 2010:576872.

Dash, B.K.; Rahman, M.M. and Sarker, P.K. (2015). Molecular identification of a newly isolated *Bacillus subtilis* BI19 and optimization of production conditions for enhanced production of extracellular amylase. *Biomedical Research International*, 2015:1-9.

Elkhalil, E. A. I. and Gafar, F.Y. (2013). Production and characterization of cellulose enzyme produce by *Bacillus* isolates from different source. *University of Khartoum Journal of Agricultural Science*, 21(1):61-82.

Farooq, M. A., Ali, S., Hassan, A., Tahir, H. M., Mumtaz, S., & Mumtaz, S. (2021). Biosynthesis and industrial applications of α-amylase: a review. *Archives of Microbiology*, 203: 1281-1292.

Gupta, R.; Gigras, P.; Mohapatra, H.; Goswami, V.K. and Chauhan, B. (2003). Microbial α-amylases: a biotechnological perspective. *Process Biochemistry*, 38(11):1599 - 1616.

Hall, T.A. (1999). BioEdit: a user-friendly biological sequence alignment editor and analysis program for Windows 95/98/NT. *Nucleic Acids Symposium Series* 41(41): 95 - 98.

Hamilton, LM.; Kelly, CT. and Fogarty, WM. (1998). Raw starch degradation by the non-raw starch absorbing bacterial alpha amylase of *Bacillus* sp. IMD. 434. *Carbohydrate Research*. 314(3): 251-257.

Harrigan, W. F. (1998). Laboratory Methods in Food Microbiology. Gulf Professional Publishing, 3rd ed. Academic Press Inc. (London) Ltd.

Jaiswal, N., and Jaiswal, P. (2024). Thermostable α-Amylases and Laccases: Paving the Way for Sustainable Industrial Applications. *Processes*, 12(7), 1341.

Kango, N., Jana, U. K., and Choukade, R. (2019). Fungal enzymes: sources and biotechnological applications. In Advancing Frontiers in Mycology and Mycotechnology: *Basic and Applied Aspects of Fungi*, Springer, 515-538.

Miller, G.L. (1959). Use of dinitrosalicylic acid reagent for determination of reducing sugar. *Analytical Chemistry*, 31(3): 426-428.

Patil, A. G., Khan, K., Aishwarya, S., Padyana, S., Huchegowda, R., Reddy, K. R., ... and Zameer, F. (2021). Fungal amylases and their industrial applications. Industrially Important Fungi for Sustainable Development: *Bioprospecting for Biomolecules*, (2) 407-434.

Pushpendra, S.; Paras, G.; Ravindra, S. and Rajesh, S. (2012). Factors affecting alfa Amylase Production on Submerged Fermentation by *Bacillus* sp. *International Journal of Pharmacy and Life Sciences*, 3(12): 2243-2246.

Qadeer, M.A.; Aurangzeb, M. and Igbal, J. (1989). Production of raw starch hydrolyzing enzymes by mould cultures. In: Malik KA, Nagvi SHM, Aleem MIH (eds) Proceeding of the international symposium on biotechnology for energy, Dec 16–21. Faisalabad, Pakistan, pp 119–128.

Rameshkumar A..and Sivasudha T. (2011). Optimization of nutritional constitute for enhanced *α*-amylase production by solid state fermentation technology. *International Journal of Micro- Biological Research*, 2(2) :148- 2011.

Samanta, S. (2022). Structural and Catalytical Features of Different Amylases and their Potential Applications. *Jordan Journal* of *Biological Sciences*, 15(2).

Sani, I.; Abdulhamid, A.; Bello, F.; Yahaya, M. and Bagudo, A. I.(2014). Isolation, partial purification and characterization of α-amylase from *Bacillus subtilis*. *Journal of Microbiology and Biotechnology Research*, 4(1):49-54.

Singh, R., Kim, S. W., Kumari, A., and Mehta, P. K. (2022). An overview of microbial α-amylase and recent biotechnological developments. *Current Biotechnology*, 11(1), 11-26.

Suhartati, T. and Hadi, S. (2010). Purification and characterization of extracellular α-amilase enzyme from locale bacteria isolate *Bacillus subtilis ITBCCB148*. *European Journal of Scientific Research*. 39(1): 64-74.

Tiwari, S. P., Srivastava, R., Singh, C. S., Shukla, K., Singh, R. K., Singh, P., ... and Sharma, R. (2015). Amylases: an overview with special reference to alpha amylase. *Jornal of Global Biosciences*, 4(1), 1886-1901.

Varalakshmi, K.N.; Kumudini, B.S.; Nandini, B.N.; Solomon, J.D.; Mahesh, B.; Suhas, R. and Kavitha, A.P. (2008). Characterization of Alpha Amylase from *Bacillus* sp.1 isolated from paddy seeds. *Journal of Applied Biosciences*, 1(2): 46 – 53.

Wang, C.M.; Shyu, C.L.; Ho, S.P. and Chiou, S. H. (2008). characterization of novel thermophilic, cellulose-

degrading bacterium *Paenibacillus* sp. Strain B 39. *Letters in Applied Microbiology*, 47(1): 46- 53.

Wu, X.; Wang, Y.; Tong, B.; Chen, X. and Chen, J. (2018). Purification and bio-chemical characterization of a thermostable and acid-stable alpha-amylase from *Bacillus licheniformis* B4–423. *International Journal of Biological Macromolecules*, 109:329–337.

Wyman, C.E.; Dale, B.E.; Elander, R.T.; Hotzapple, M.; ladisch, M.R.; and Lee, Y.Y. (2005). Coordinated development of leading biomass pretreatment technologies. *Bioresource Technology*, 96(18):1959- 1966.

Yassin, S.N., Jiru, T.M. and Indracanti, M. (2021). Screening and Characterization of Thermostable Amylase-Producing Bacteria Isolated from Soil Samples of Afdera, Afar Region, and Molecular Detection of Amylase-Coding Gene. *International Journal of Microbiology*, 5592885.

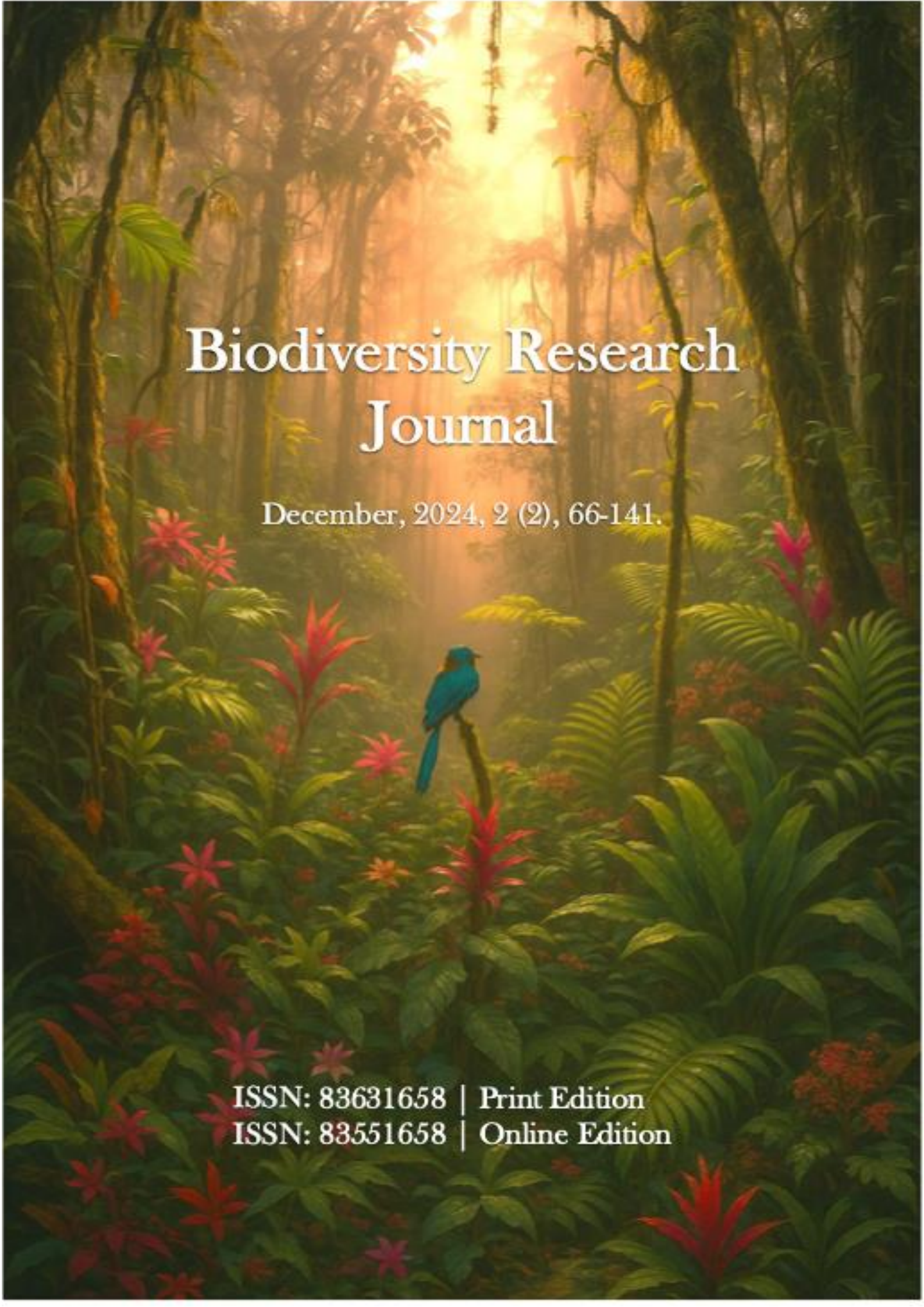

Biodiversity Research Journal

December, 2024, 2 (2), 66-141.

ISSN: 83631658 | Print Edition
ISSN: 83551658 | Online Edition